Cellular and molecular response to mechanical articular cartilage injury

Eltawil, Noha

Cellular and Molecular response to mechanical articular cartilage injury

Noha Eltawil

Thesis submitted for the degree of doctor of philosophy in Medical Sciences from University of London

Queen Mary University of London
Barts and The London School of Medicine

2010

ACKNOWLEDGEMENTS

I owe special thanks to Professor Costantino Pitzalis not only for giving me the opportunity to be part of his group and undertake this project, but also for his continuous help and support throughout the whole work.

I am very grateful to Dr Francesco Dell'Accio for his invaluable supervision, scientific guidance, enthusiastic help and constant feedback.

Thanks also must be extended to Professor Cosimo De Bari for being such a great help especially in the first two years of my PhD.

I would like also to acknowledge Professor Bruce Caterson and Dr Debbie Tudor, Cardiff University for kindly providing anti-TEGE^{373} and anti-VDIPEN antibodies; Dr Lindsay King from IBEX, Canada for kindly providing the CP II antibody.

I must thank all my colleagues in the department of Experimental Medicine and Rheumatology for their friendship, cooperation, and constructive remarks.

My sincere thanks are due to my family for their love, care and understanding. Without their support, I would have not been able to accomplish this work.

Finally, I would like to thank the Egyptian government for giving me the opportunity to have this experience in the UK and for funding my PhD studentship (grant MM45/05) and the Arthritis Research Campaign for financially supporting this project (grant 16290).

DECLARATION

The work presented in this thesis is less than 100,000 words and was performed and analyzed by the candidate except for the surgical procedures, the in vitro culture and injury of human cartilage explants, RNA extraction and quantitative real time PCR done on these explants and the microarray analysis which were all performed by Dr Francesco Dell'accio.

Prof. Costantino Pitzalis and Dr Francesco Dell'accio closely supervised the project providing scientific guidance and advice regarding experimental design and planning as well as interpretation of the results and critical revision of the manuscript.

Candidate:

Noha Eltawil

Supervisors

Dr. Francesco Dell'Accio

Prof. Costantino Pitzalis

ABSTRACT

Joint injures frequently involve structural damage to articular cartilage and the underlying subchondral bone. The outcome of acute joint surface defects (JSD) varies from spontaneous healing to the development of post-traumatic osteoarthritis (PTOA). The cellular and molecular mechanisms regulating joint surface repair are still unknown and failure of these reparative mechanisms could be a contributing factor for PTOA development. The absence of animal models suitable for molecular functional studies in cartilage regeneration has so far represented a bottleneck for the research in this field.

In this study we have generated a mouse model of joint surface injury which, in a strain- and age-dependent manner results either in spontaneous healing in the DBA/1 strain or in PTOA in C57BL/6 strain. The healing outcome in DBA/1 mice was associated with progressive decline of chondrocyte apoptosis, cell proliferation within the repair tissue, persistent type II collagen neo-deposition, less type II collagen degradation, and aggrecan degradation predominantly driven by metalloproteinases, with minor aggrecanase activity. Furthermore, we have demonstrated that mechanical injury to articular cartilage in vitro and in vivo results in activation of a signalling response with reactivation of morphogenetic pathways such as BMP and Wnt. Notably, we have observed a striking up-regulation of Wnt16 following cartilage injury and in osteoarthritis and showed that this molecule might have a chondro-protective role in murine osteoarthritis. The in vivo model of JSD, being amenable to genetic manipulation, offers the opportunity to investigate the function of different candidate molecules modulated in response to injury which is an essential prerequisite to develop novel molecular therapeutics to support joint surface healing and to prevent possible evolution of PTOA.

TABLE OF CONTENTS

LIST OF FIGURES

LIST OF TABLES

ABBREVIATIONS

ACI	Autologous chondrocyte implantation
ADAMTSs	A disintegrin and metalloproteinase with thrombospondin motifs
ALK1	Activin-like receptor kinase 1
APC	Adenomatous polyposis coli
BMP	Bone Morphogenetic protein
CK1α	Casein kinase 1 α
COL2A1	Collagen type II alpha 1 chain
COMP	Cartilage oligomeric matrix protein
CRD	Cysteine-rich domain
CSW	Cross-sectional width
CSA	Cross-sectional area
DKK	Dickkopf
DMM	Destabilization of medial meniscus
Dsh	Dishevelled
ECM	Extracellular matrix
ERK	Extracellulary regulated kinase
FGF	Fibroblast growth factor
FGFR3	Fibroblast growth factor receptor 3
Fzd	Frizzled receptors
GAG	Glycosaminoglycans
Gdf5/CDMP1 1	Growth and differentiation factor 5/ cartilage-derived morphogenetic protein
Gdf6/CDMP2 2	Growth and differentiation factor 6/ cartilage-derived morphogenetic protein
Gsk3 β	Glycogen synthase kinase 3 β
HS	Heparan sulfate
IGD	Inter-globular domain
IGF	Insulin growth factor
Ihh	Indian hedgehog
IL1	Interleukin-1
JNK	C-jun-terminal kinase
JSD	Joint surface defect

JSI	Joint surface injury
KO	Knock-out
LRP	LDL-receptor-related protein
MMPs	Matrix metalloproteinases
MSCs	Mesenchymal stem cells
OA	Osteoarthritis
PHH3	Phospho-Histone H3
PTHrP	Parathyroid hormone-related protein
PTOA	Post-traumatic osteoarthritis
Runx 2/cbfa1	Runt related transcription factor 2/core binding factor alpha 1
sFRP	Secreted Frizzled-related protein
SOX9	Sry-related HMG-box gene 9
STAT1	Signal transducer and activator of transcription 1
TCF/LEF	T cell factor / lymphoid enhancer factor
TGF-β	Transforming growth factor- β
TIMPs	Tissue inhibitors of metalloproteinase
TNF-α	Tumor necrosis factor-α
WIF	Wnt inhibitory factor
WISP	Wnt-induced signaling protein
WNT	Wingless-type MMTV integration site family
WT	Wild-type

CHAPTER 1

INTRODUCTION

1.1 Synovial joints

The synovial joint (Figure 1.1) is a complex organ that allows frictionless motion of the skeletal elements. The joint is composed of several tissues of mesenchymal origin including the fibrous capsule, the synovial membrane, bone, ligaments and the articular cartilage. The capsule, which surrounds the joint and seals the articular cavity, is lined with synovial membrane which is composed mainly of macrophage-like synoviocytes (type B synoviocytes) and fibroblast-like cells (type A synoviocytes) responsible for synovial fluid secretion. The synovial fluid has a high concentration of hyaluronic acid and lubricin providing nutrients to the avascular articular cartilage and lubricating the joint. The articulating ends of the bones are covered with smooth hyaline articular cartilage that functions as a weight-bearing and gliding surface. The articular cartilage is supported by a plate of subchondral bone that transmits the load from the cartilage to the underlying trabecular bone. The joint is further stabilized by the surrounding tendons, ligaments and muscles (1).

Figure 1.1: Diagrammatic view of the synovial joint structure

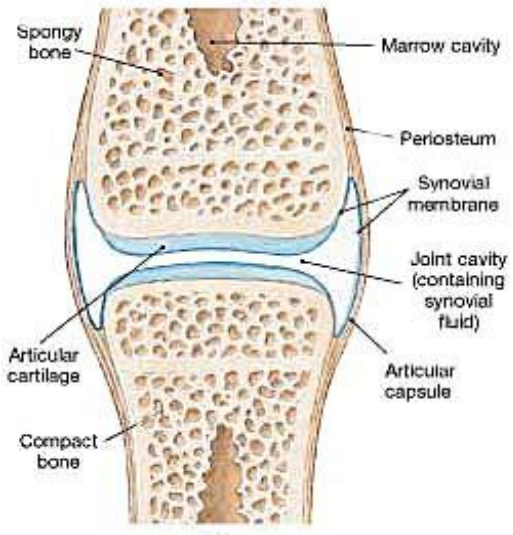

1.1.1. Structure and Function of articular cartilage

The articular cartilage is an avascular, aneural and alymphatic tissue covering the articulating surfaces of synovial joints. It plays a vital role in the function of the musculoskeletal system by allowing smooth frictionless motion between articular surfaces. Furthermore, it acts as shock absorber and distributes mechanical loads over a large contact area, thereby minimizing the focal stress on the subchondral bone. This tissue is composed of highly specialized cells, chondrocytes, embedded within a dense extracellular matrix (ECM) that consists of (i) fluid, mostly water (70-80% of the wet weight), gases and metabolites (ii) a framework of structural macromolecules that include mainly type II collagen, the highly sulfated proteoglycans predominantly aggrecan, other fibrillar (IX and XI) and non-fibrillar (type VI and X) collagens and additional non-collagenous protein molecules such as fibronectin and cartilage oligomeric protein (2).

Articular cartilage, however, is not a homogeneous tissue with morphological and biochemical differences existing from the surface zone to the deeper layers (Figure 1.2) (3). The superficial zone is characterized by the presence of flattened cells that secrete lubricin (4) and a layer of tightly packed collagen fibers parallel to articular surface called lamina splendens. This structure maintains the tensile properties of cartilage and enables it to resist shear forces during normal joint function and loading. The middle or transitional zone contains randomly distributed spherical chondrocytes, proteoglycans and arcade like collagen fibers (5). In the deep zone, chondrocytes are spheroidal in shape and arranged in columns perpendicular to the surface. This zone has the highest concentration of proteoglycans and the largest diameter of collagen fibrils that are

perpendicular to the surface. Below the deep zone, is the calcified zone where chondrocytes express alkaline phosphatase and type X collagen (6) and therefore their phenotype resemble that of the hypertrophic chondrocytes in the epiphyseal cartilage. Collagen fibers originating within the deep zone cross the tide mark to be inserted into the underlying layers providing a strong anchoring system for the tissue on the subchondral bone (3).

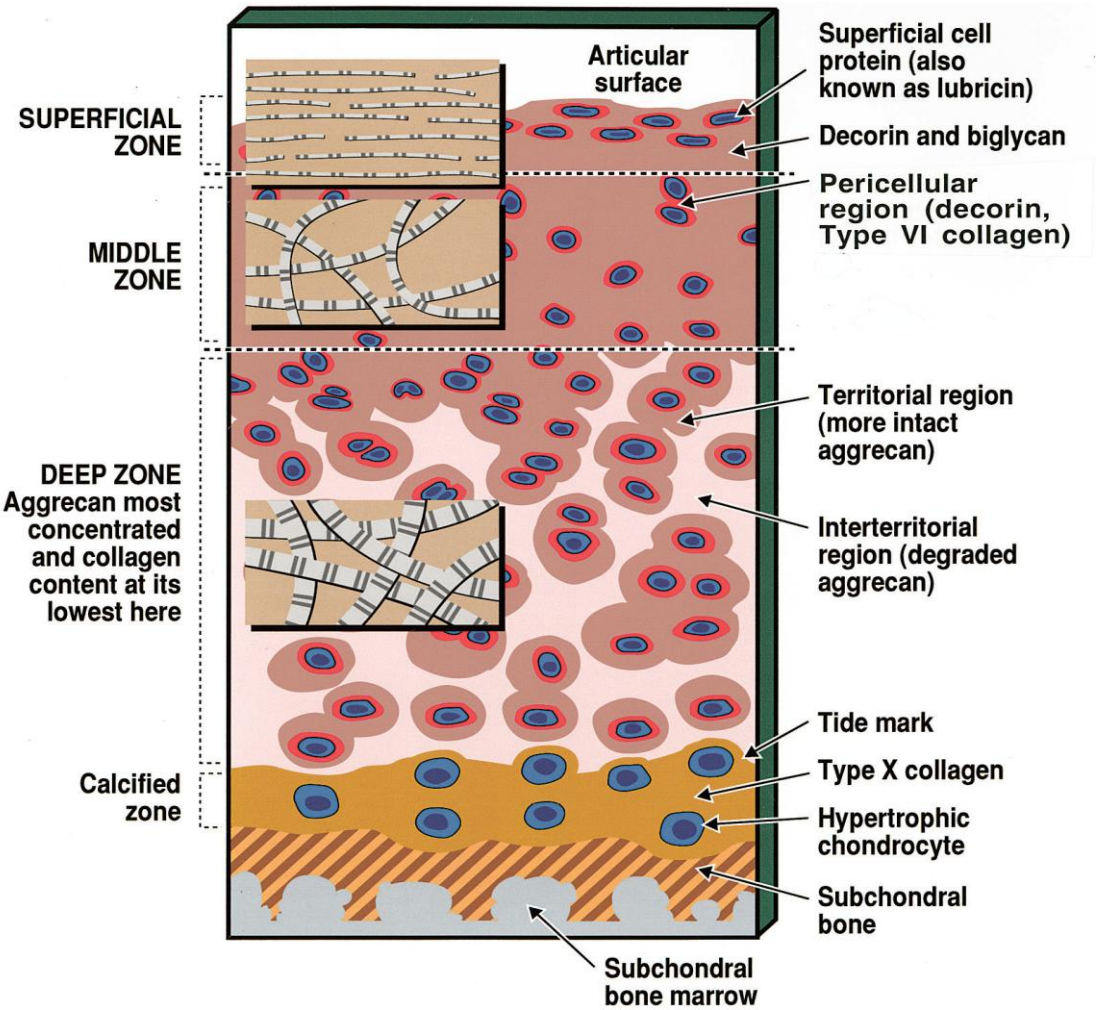

Figure 1.2: A schematic diagram of the cellular and fibrillar organization in the different zones of articular cartilage (Figure from (3)).

Articular chondrocytes

Chondrocytes are highly specialized cells that form 1-5% of the cartilage volume. They are responsible for the synthesis and the maintenance of the ECM. Because cartilage is avascular, chondrocytes receive nutrients through diffusion and therefore survive on low oxygen tension and depend on anaerobic metabolism (7). In the normal articular cartilage, tracks interconnecting chondrocytes' lacunae and cytoplasmic projections were observed and proposed to be involved in tissue signaling and nutrition (8-10). The ability of chondrocytes to synthesize and maintain ECM gradually decreases with aging due to cell senescence and decreased responsiveness to anabolic growth factors (11).

Extracellular matrix

The ECM provides the cartilage with its characteristic biomechanical properties and plays a vital role in regulating the transmission of different chemical and physical signals to the chondrocytes thereby acting as a signal transducer for these cells (12).

According to the distance from the chondrocytes, the cartilage ECM is organized into three different regions (3):

1) Pericellular matrix: It is a thin (2μm) rim of matrix surrounding chondrocytes together forming the chondron. This region is rich in the heparan sulphate proteoglycan perlecan (13), type VI collagen and cell membrane associated molecules such as fibronectin and chondronectin.

2) Territorial matrix: This region of the matrix encloses cluster of chondrocytes including their pericellular matrix. The ECM in this area is rich in chondroitin sulfate and the collagen fibrils are arranged in criss-cross manner forming a fibril basket that surround clustered chondrocytes and protect them from mechanical impacts (2).

3) Inter-territorial matrix: It accounts for most of the matrix volume in cartilage. The composition and the orientation of the fibers in that region are different depending on the functional requirement and cellular organization of each zone as descried earlier.

Collagens

Collagens account for 15-20% of cartilage tissue. Type II collagen is the most abundant component (90-95%) in the fibrillar framework that gives the articular cartilage its tensile strength. Cartilage also contains other types of collagens such as type VI collagen which is mainly located in the pericellular matrix to help in the attachment of the chondrocytes to the surrounding matrix, type IX collagen and type XI collagen (fibril-associated collagens) that are cross-linked to Type II collagen reinforcing the inter-fibrillar connections. Type X collagen is only expressed by the hypertrophied chondrocytes in the calcified layer (14).

The basic molecular unit of collagen is tropocollagen which is a fibrillar molecule forming rod-like structures measuring 280nm in length and 1.5nm in diameter. Tropocollagen consists of three α-polypeptide chain subunits arranged in a tripe helix configuration. A distinctive feature of collagen is the regular arrangement of amino acids in each of the three α chains. The amino acid sequence often follows the pattern Glycine-proline-Y or Glycine-X-hydroxyproline. Therefore, glycine accounts for 33.5% of the amino acid sequence while proline and hydroxyl-proline form 12% and 10% respectively. Differences in the chemical structure of the α-polypeptide chains are responsible for the various types of collagen. For example, type II collagen has three identical α1 chains while type VI collagen is formed of three different α chains (α1, α2, α3). During collagen biosynthesis, each α chain is synthesized intracellulary with an additional peptide (telopeptide) on both the amino- and carboxyl-terminal ends to form

the procollagen molecule. This peptide prevents premature intra-cellular precipitation and assembly of the procollagen molecule. When procollagen is transported out of the cell, the procollagen peptidase enzyme removes the telopeptides and thus allows the resulting protein (tropocollagen) to assemble into polymeric collagen fibrils (15).

Proteoglycans

This family of macromolecules consists of a core protein attached covalently to one or more glycosaminoglycans (GAG). GAGs are long linear chains of repeated disaccharides that are negatively charged due to the presence of sulfate and carboxyl groups. The negative charge attracts cations such as Na_2 that in turn increases osmolarity of the articular cartilage and thus contributes to the compressive strength and resilience to that tissue (5). Mechanical compression forces associated with joint motion expel the water out of the cartilage ECM and when pressure is released water is attracted back by GAG negative charge. Such water movement is essential for the nutrition of cartilage facilitating the interchange of O_2, CO_2 and other molecules between the synovial fluid and articular cartilage (2).

The most abundant proteoglycan in cartilage is aggrecan. The protein core of aggrecan (Figure 1.3) consists of three globular structural domains (G1 & G2 at the N-terminal end and G3 at the C-terminal end) separated by two extended inter-globular domains (E1 &E2). The G1 domain is linked to hyaluronic acid thus forming larger aggregates containing up to 100 aggrecan molecules. GAGs (Chondroitin sulfate and keratin sulfate) are attached to the E2 inter-globular domain (Figure 1.3) (16).

Less abundant small proteoglycans are also present in cartilage including decorin, biglycan, fibromodulin and perlecan. Such small proteoglycans bind to other matrix macromolecules and thus play a role in stabilizing the matrix (17). In addition, small

cartilage proteoglycans also bind several growth factors including TGFβ (18) and FGFs (13) thereby on one hand regulating their actions and contributing to the formation of gradients, and on the other hand acting as storage for signaling molecules.

Other non-collagenous proteins

Several non-collagenous proteins and glycoproteins have been found in cartilage ECM and have been proposed to play a role in cell/matrix interaction and in binding different components of ECM. Cartilage oligomeric matrix protein (COMP), a pentameric glycoprotein, can bind to collagen through zinc-dependent interactions and therefore facilitate collagen cross-linking (19). Chondronectin is a glycoprotein macromolecule that binds to chondroitin sulfate, hyaluronic acid and type II collagen mediating the adherence of the chondrocytes to the surrounding ECM. Fibronectin, a large dimer localized in pericellular matrix, is composed of 2 similar polypeptide subunits attached together by disulfide bonds. Each arm of this V shaped macromolecule has binding sites for various extra-cellular matrix components and integrins at the cell membrane (3).

Matrix turnover

Throughout life, articular cartilage undergoes continuous remodeling as chondrocytes can detect changes in ECM compositions and respond accordingly to maintain the integrity of the matrix. Normally, there is a balance between anabolic and catabolic activities as chondrocytes replace matrix macromolecules lost through degradation. This remodeling is accelerated in pathological conditions such as osteoarthritis (OA) (20) and during cartilage repair, for instance following autologous chondrocyte implantation (ACI) (21). The main proteinases responsible for cartilage matrix degradation are matrix metalloproteinases (MMPs) and the A disintegrin and metalloproteinase with

thrombospondin motifs (ADAMTSs). The catalytic action of these enzymes is inhibited by the tissue inhibitors of metalloproteinases (TIMPs) (22).

MMPs are a family of 23 zinc-containing proteinases that are capable of degrading ECM proteins. They share a conserved domain structure that consists of a pro-peptide domain with Cysteine switch that interact with the zinc-dependent active site to prevent binding and cleavage of the substrate and keeping the enzyme in an inactive form, a catalytic domain with the Zinc binding motif and a haemopexin-like C-terminal domain that is responsible for protein-protein interaction and therefore determine the substrate specificity. The hinge (linker) region connects the catalytic and C-terminal domains. MMPs are traditionally classified according to their substrates into collagenases (MMP-1, 8 and 13), gelatinases (MMP-2 & MMP-9), stromelysins (MMP-3, 10 and 11) and membrane-type MT-MMPs (MMP-14, 15, 16, 17, 24 and 25). Some members of MMPs such as MMP-7, 12 and 19, however, do not easily fit into any of these classes as they are capable of degrading many substrates (reviewed in (22). In addition to their role in the continuous matrix remodeling, the degradation of ECM by MMPs has been postulated to create space for cells to migrate, regulate tissue architecture, release growth factors bound to ECM molecules and activate or inactivate signaling molecules. Thus they have important roles in morphogenesis, remodeling, angiogenesis and wound healing (23). Dysregulated or excessive MMP activity has been proposed as a pathogenic mechanism associated with different diseases including the destruction of cartilage in arthritis. In OA cartilage, elevated levels of several MMPs were observed (24;25). Mice expressing constitutively active MMP13 under the control of the cartilage-specific type II collagen promoter showed increased OA lesions compared to their wild-type (WT) littermates when challenged in an OA model induced by

destabilization of the medial meniscus (DMM) (26) and significant protection against OA was achieved when treating STR/Ort mice with Ro-32-3555 (collagenase selective inhibitor of MMP-1, 8and 13) (27). When evaluating the MMP-3 KO mice in the DMM model, no difference was seen in comparison to their WT mice. MMP-9 null mutant mice, however, developed three fold higher OA score than WT mice when challenged in the same model (26). These data, together with the failure of clinical trials of compounds inhibiting MMP activity due to occurrence of musculoskeletal side effect, suggest that MMP activity may be required for remodeling and homeostatic responses in joint tissue.

ADAMTSs are 19 members that comprise a related family to MMPs as they also contain a zinc atom at their catalytic domain. ADAMTSs have been shown to cleave aggrecan specifically at four different sites in the chondroitin sulfate CS -2 domain at the C terminus and at the $TEGE^{373}\downarrow^{374}ALGS$ inter-globular domain (IGD) near the N terminus (Figure 1.3). The aggrecan fragment ($TEGE^{373}$) resulting from the cleavage at the $TEGE^{373}\downarrow^{374}ALGS$ inter-globular domain was identified in the synovial fluid of patients with osteoarthritis and inflammatory joint disease (28;29) and was used to raise antibodies that specifically detect aggrecanase-cleaved aggrecan. The first ADAMTS to be identified was ADAMTS-4 (aggrecanase-1) (30) followed by ADAMTS-5 (aggrecanase-2) (31). Recently, ADAMTS-5 has been shown as the main aggrecanase in mouse and human cartilage (32;33). Indeed, deletion of ADAMTS-5, but not ADAMTS-4, resulted in cartilage protection from degradation after surgical induction of joint instability leading to OA (32;34). Although MMPs can also cleave aggrecan in the inter-globular domain at the $DIPEN^{341}\downarrow^{342}FFGVG$ site, it is believed that ADAMTS-mediated activity is crucial for aggrecan breakdown during OA as mice resistant to aggrecanase cleavage in the IGD (Jaffa mice) were protected from cartilage erosion in

experimental arthritis whereas mice resistant to IGD cleavage at the MMP cleavage site (Chloe mice) developed severe OA like features (16).

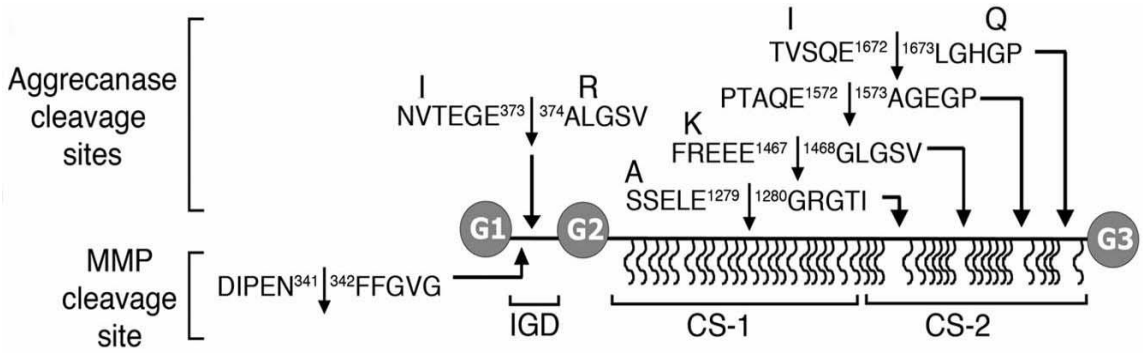

Figure 1.3: The aggrecan core protein is composed of two N-terminal (G1 and G2) and one C-terminal (G3) globular domains that are connected by the inter-globular domain E1&E2. The E2 domain between G2 and G3 is loaded with CS chains (wavy lines). Arrows indicate the aggrecanase and MMP cleavage site sequences in the mouse IGD and CS-2 domains and the amino acids that are different in human aggrecan are shown above. Numbering corresponds with the mouse sequence (Figure from (16))

TIMPs are natural inhibitors of MMPs. In humans, there are four TIMPs that limit the degrading activity of MMPs with different effectiveness. TIMP activity was higher than MMP activity in normal non-arthritic human cartilage but the balance between MMP and TIMP was shifted towards MMPs in OA cartilage (35). In addition, TIMP-3 KO mice developed spontaneous OA at 6 months of age whereas their WT controls did not, thereby supporting the protective role of TIMP-3 against OA development (36). Interestingly, TIMP-3 was reported as an inhibitor for both ADAMTS-4 and ADAMTS-5 (37).

Different cytokines released into cartilage matrix in response to various stimuli can modify chondrocyte anabolic and catabolic activities. For example, inflammatory molecules such as interleukin1 (IL1) and tumor necrosis factors (TNFα) can induce

matrix degradation through the production and activation of MMPs and ADAMTSs (38;39). On the other hand, anabolic effects can be induced by other signaling molecules such as fibroblast growth factor (FGF), insulin growth factor (IGF) and transforming growth factor-β (TGF-β) superfamily including BMPs that can stimulate ECM synthesis and oppose catabolic activities (40) by down-regulating MMPs and inducing TIMP-1&3 expression in chondrocyte (41). These mechanisms ensure a lifelong balanced remodeling of the cartilage ECM.

1.1.2. Embryonic development of the skeleton and synovial joints

During embryonic limb development, mesenchymal cells within the limb bud condensate into uninterrupted elements that prefigure the future skeleton. Mesenchymal condensations are initiated and patterned by a coordinated morphogenetic signaling involving FGF, hedgehog, BMP and Wnt signaling that regulate the distribution and the proliferation of mesenchymal cells (42). The cells located in the periphery of these condensations give rise to perichondrial cells which subsequently differentiate into osteoblasts forming the bone collar whereas, the cells in the center differentiate under the control of Sox9 into chondrocytes expressing proteoglycans and collagen type II (43). The skeletal elements then ossify through endochondral bone formation. In this process, chondrocytes further differentiate to become post-mitotic, prehypertrophic and then hypertrophic chondrocytes which express type X collagen and alkaline phosphatase. Hypertrophic chondrocytes calcify their surrounding ECM and eventually die through apoptosis. Following vascular invasion of the calcified cartilage, several cell types populate the cartilage anlagen including osteoclasts, which degrade the matrix, and osteoblasts, which form bone at the expense of cartilage (Figure 1.4). These events are controlled by several signaling pathways including BMP, Wnt, FGF and Indian hedgehog (reviewed in (44)).

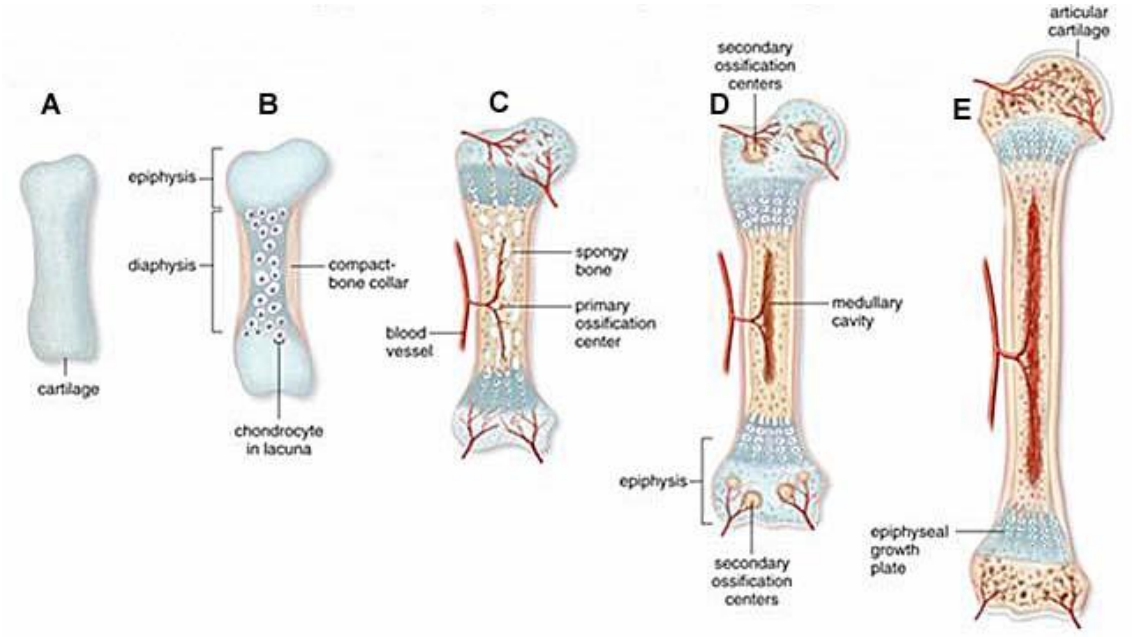

Figure 1.4: Diagrammatic representation for endochondral bone formation: a) cartilaginous model for future bone develops. b) Chondrocytes become hypertrophic and peripheral cells differentiate into osteoblast to form the bone collar. c) Hypertrophic chondrocytes induce ECM mineralization and cells die through apoptosis, the calcified matrix is then invaded by blood vessels that deliver osteoblasts and osteoclast precursors initiating endochondral ossification and forming the primary ossification center d) The medullary cavity is then formed and secondary ossification center appear in the epiphysis. e) Longitudinal growth continues from growth plate.

Joint formation

The synovial joints form through segmentation of the pre-existing continuous mesenchymal anlagen (Figure 1.5). This process begins at the site of future articulation with the appearance of a high cell density region, called interzone, formed of flattened cells interconnected with gap junctions and expressing joint specific markers such as Gdf5/CDMP1 (45), Wnt-4, -9a,-16 (46;47), Noggin (48), Gli3 (49), CD44 (50) and Erg (51). The interzone cells differentiate into three layers. The cells of the central layer of the interzone (the central intermediate lamina) will eventually disappear to form the joint cavity. Cavitation takes place through a combined action of programmed cell death,

embryonic limb movements and Hyaluronan synthesis (52). Hyaluronan binds to specific cell surface receptors (CD44) inhibiting their aggregation and facilitating the formation of a fluid filled cavity separating the skeletal elements (53). Meanwhile, cells on either side of the central intermediate lamina will give rise to articular chondrocytes, synovial lining and inner joint ligaments (54). In contrast to the epiphyseal chondrocytes, the articular cartilage is resistant to vascular invasion, mineralization and endochondral bone formation (reviewed in (55)).

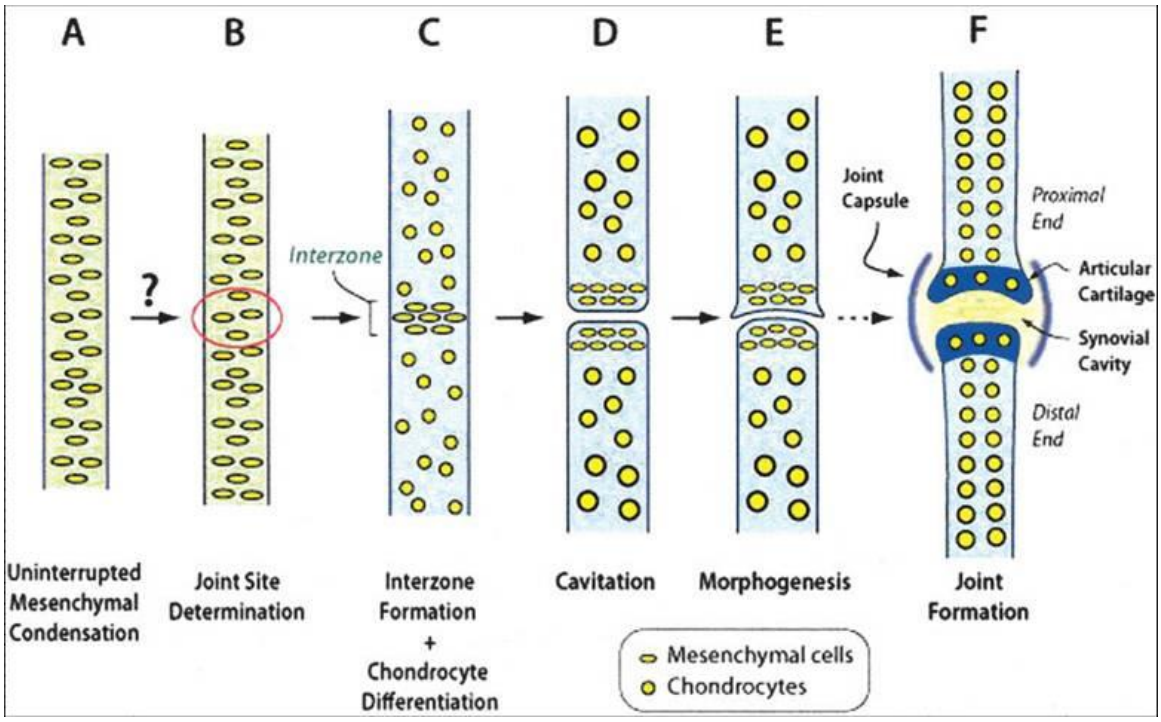

Figure 1.5: Diagrammatic representation for synovial joint formation. **A:** uninterrupted Mesenchymal condensations appear in the early limb bud. **B:** Unknown upstream patterning mechanisms determine the exact location for joint initiation. **C:** The interzone forms at the joint site by further gathering and condensation of mesenchymal cells. The rest of the mesenchymal cells constituting the condensations differentiate into chondrocytes to establish the cartilaginous skeleton. **D:** The cavitation process starts to form the synovial cavity separating the adjacent skeletal anlagen. **E:** Morphogenesis takes place to shape the opposing sides of the joint **F:** The different tissues within the joint, including the opposing end of the bone, articular cartilage, capsule, synovial cavity ligaments, and menisci undergo the final maturation and differentiation leading to a mature joint. (Figure from (55)).

1.1.3. Signaling pathways involved in embryonic joint development

The process of joint formation is regulated by a large number of signaling factors and morphogens including members of Wnt family and bone morphogenetic proteins BMPs.

1.1.3.1. Wnt signaling

An outline of the Wnt pathway

Wnt proteins constitute a family of 19 secreted, cysteine-rich glycoproteins. They share 35%-83% amino-acid sequence identity with a conserved pattern of 23 cysteine residues and an N-terminal signal sequence (56). Wnt proteins are synthesized in the endoplasmic reticulum where they undergo a number of post-translational modifications including gylcosylation and palmitoylation that are required for secretion and signaling activity (57). Once secreted, Wnt proteins associate with Heparan sulphate proteoglycans in the ECM and bind to cell surface (58). It has been recently shown that glycosaminoglycans not only modulate Wnt signaling by concentrating Wnt proteins at the cell surface and presenting wnt ligands to cell surface receptors (59;60) but also can maintain the solubility of Wnt proteins, thus stabilizing their signaling activity (61).

Wnts exert their actions through binding to Frizzled (Fzd) receptors and LDL-receptor-related-protein (LRP) co-receptors. Fzd receptors, of which 10 members have been identified in humans and mice, have an extracellular amino-terminal cysteine-rich domain (CRD) that binds Wnts, seven transmembrane domains and a short cytoplasmic tail at the carboxyl terminus. Two members of LRP family (LRP-5 & LRP-6) can bind Wnts to form a complex with Wnts and Fzd. Wnt signals can be transduced through the Canonical β-catenin-dependent pathway or the non-canonical β-catenin-independent

pathways that include the planar cell polarity pathway and the Ca^{2+} dependant pathway (62). Different sets of Wnts and Fzd can activate each of these pathways leading to unique cellular responses.

The Canonical Wnt/β-catenin pathway (shown in Figure 1.6) is the most studied and the best characterized. Signaling through this pathway depends on the levels of β-catenin in the cell. In the absence of Wnt ligands, β-catenin is constitutively phosphorylated by a destruction complex that contains adenomatous polyposis coli (APC), Axin, glycogen synthase kinase 3β (Gsk3β) and casein kinase 1α (CK1α). Phosphorylated β-catenin is recognized by E3 ubiquitin ligase and targeted for proteosomal degradation. The binding of Wnt ligands to Fzd/LRP recruits a complex formed of Dishevelled (Dsh), Axin, Gsk3β to Fzd receptors at the cell membrane. Gsk3β then phosphorylates LRP5/6 receptor allowing Axin to dock onto the phosphorylated residues removing it from the destruction complex which is thereby inactivated. Non-phosphorylated β-catenin will then accumulate in the cytoplasm, translocate into the nucleus and form complexes with transcription factors, such as members of T cell factor / lymphoid enhancer factor (TCF-LEF) modulating the expression of Wnt responsive genes. These target genes include OPG, Myc and CyclinD as well as members of the Wnt pathway itself like axin2 which provide a feedback control during Wnt signaling (reviewed in (63)).

Planar cell polarity pathway PCP (shown in Figure 1.6) regulates the polarity of the cells through organizing their cytoskeleton. For instance, it is required for the proper orientation of cilia in epithelial sheets and for the control of polarized cell movement during gastrulation and neurulation. In the non-canonical planer cell polarity pathway, Wnt signaling is mediated through Fzd receptors leading to recruitment of Dsh and activation of two parallel pathways involving the small GTPases Rho and Rac. For

activation of the Rho branch of the signaling, Dsh forms a complex with dishevelled associated activator of morphogenesis (Daam1). The activation of Rho GTPase results in activation of Rho-associated kinase (ROCK) and myosin leading to actin polymerization and cytoskeletal rearrangement. The second branch of the signaling activates Rac GTPase independent of Daam1. The activated Rac stimulates c-JUN N-terminal domain kinase (JNK) activity and cytoskeletal modulation. The downstream factors for planar cell polarity pathway are poorly defined and it is still unclear whether this pathway has any role in transcriptional regulation or it functions only through cytoskeletal modulation (reviewed in (62).

Wnt/Ca^{2+} pathway (shown in Figure 1.6) involves activation of G–protein that will lead to an increase in intracellular Ca^{2+} release from sarcoplasmic reticulum and the subsequent stimulation of Ca^{2+} sensitive proteins such as Ca^{2+}/calmodulin-dependent kinase II (CamKII) and protein kinase C (PKC) (64).

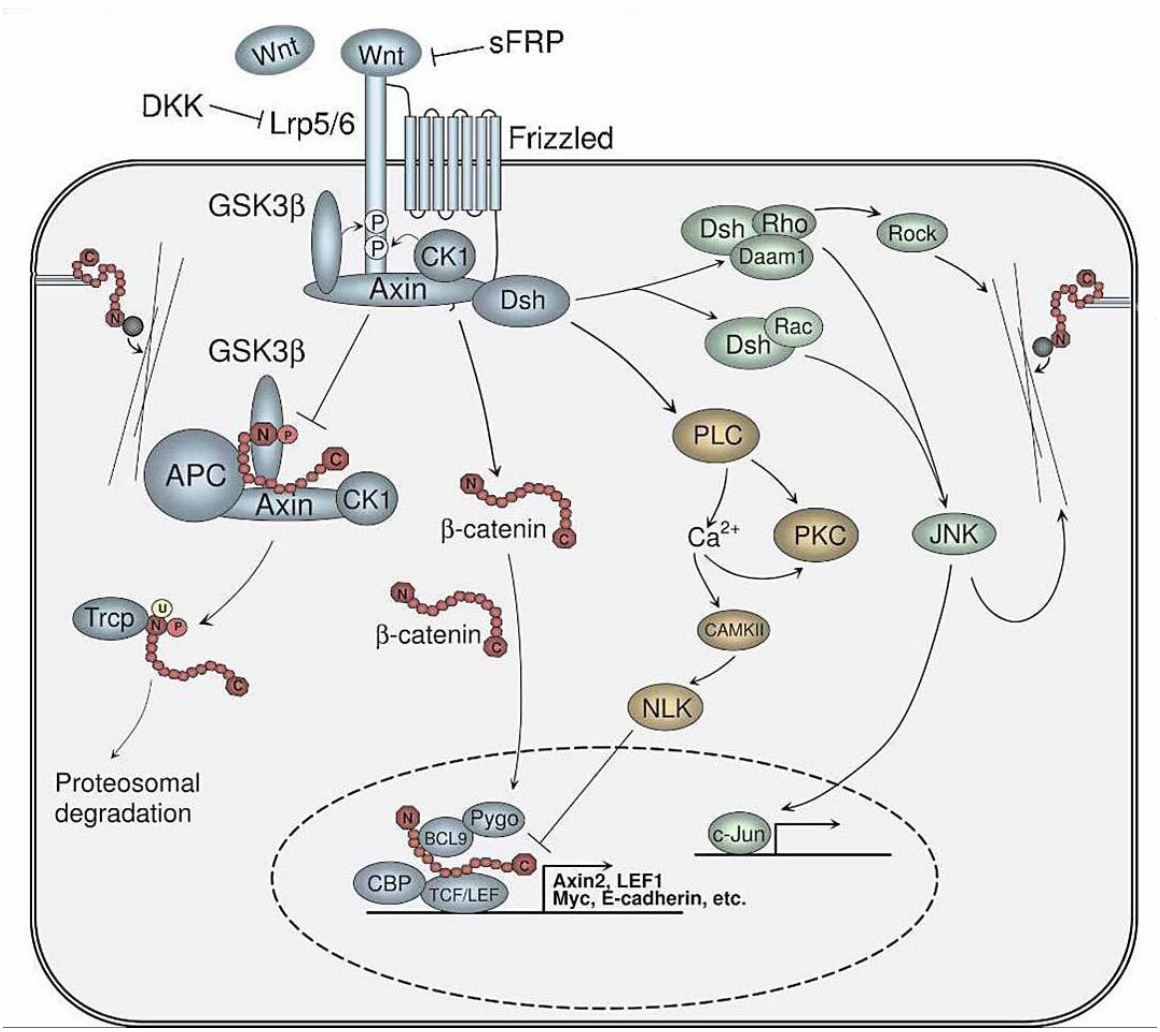

Figure 1.6: Wnt signaling pathways: Diagram exemplifying the three main signal transduction pathways. The canonical Wnt/β-catenin pathway (in blue and red): the degradation complex is disassembled resulting in β-catenin accumulation and translocation into the nucleus. The planar cell polarity pathway (green): the signal is transduced through small GTPases Rho and Rac to JNK regulating the cytoskeleton. The Wnt/ Ca^{2+} pathway (orange): stimulates the release of intra-cellular Ca^{2+} activating protein kinase C (PKC) and Ca^{2+} /calmodulin-dependent kinase II (camKII). Figure from (65)

.

Wnt signaling can be modulated extracellulary by several secreted proteins such as Wnt-inhibitory factors (WIF), Cerberus, sclerostin, Dickkopf (DKK) and a family of 5 secreted Frizzled-related proteins (sFRP) including sFRP3 (Frzb). sFRPs display homology to the extracellular cysteine-rich domain (CRD) of Fzd molecules but lack the transmembrane segment therefore they can interact directly with Wnt proteins antagonizing their functions through preventing their binding to Fzd receptor. DKK molecules bind to LRP5/6 with high affinity promoting its internalization through Clathrin-mediated endocytosis (66) and thus making it unavailable for Wnt interaction.

In the cytoplasm, Nkd protein encoded by the Naked gene can bind directly to Dsh to inhibit Wnt signaling (67). Axins, GSK-3 and APC are repressors of Wnt signaling as they participate in regulating β-catenin degradation in the cytoplasm (68). The nuclear localization of β-catenin upon Wnt stimulation is regulated by Rac1-JNK2 that phosphorylates the stabilized β-catenin at Ser191 and Ser605 and directs it to the nucleus (69). Recently, Smad7 has been shown to interact with Axin dissociating β-catenin from the degradation complex and stabilizing it. However, rather than being translocated to the nucleus, Smad7-stabilized- β-catenin binds to E-cadherin complex to promote cell-cell adhesion (70). The levels of cadherin-bound and signaling pool of β-catenin are tightly regulated in the cell to coordinate changes in gene expression with cellular adhesions and migration (71).

Within the nucleus, the transcriptional activation of target genes by β-catenin/TCF complex is regulated by a number of transcriptional co-activators and co-repressors. For instance, CBP (72) and Brg-1 (73) are co-activators that induce chromatin remodeling favoring gene transcription. Further interaction between β-catenin/TCF complex and chromatin can be mediated by BCL/Legless and pygopos (74). On the other hand,

Wnt-dependent gene expression can be suppressed by a number of transcriptional inhibitors such as Groucho that makes DNA refractory to transcriptional activation through the interaction with Histone deacetylase (HDAC) (75). The β-catenin binding proteins Chibby and ICAT block the interaction between β-catenin and TCF leading to the dissociation of β-catenin/TCF complex (76;77). Nemo-like kinase (NLK) phosphorylates TCF/LEF factors and thus inhibits the interaction of the beta-catenin-TCF complex with DNA and negatively regulates the Wnt signaling pathway (78).

Role of Wnt signaling in embryonic joint development

Wnt signaling has a crucial role in regulating cell fate determination, proliferation, migration and patterning during embryonic developmental. Wnt/β-catenin signaling has been shown to be active during early and late stages of joint formation in all joints (54). Wnt 4, Wnt9a (known previously as Wnt14) and Wnt16 were found to be expressed in the joint interzones (46;47). Expression of these Wnt genes in the prospective joint region is one of the earliest markers of joint determination that is followed by induction of growth and differentiation factor-5 (Gdf5) expression (46) and the formation of the joint interzone (47). Activation of Wnt/β-catenin signaling is required and sufficient for joint formation as genetic deletion of β-catenin in early mesenchymal condensations in *β-cat$^{fl/fl}$; Dermo1-Cre* (47) and *β-cat$^{fl/fl}$; Prx1-Cre* (79) mice resulted in joint fusion/ablation whereas, ectopic expression of constitutively active β-catenin induced ectopic joint formation and expression of joint markers including GDF5 (47). Furthermore, experiments overexpressing Wnt9a signaling in chick and mouse limbs resulted in morphological and molecular changes characteristic of the joint interzone region including the up-regulation of Gdf5, CD44 and down-regulation of Sox9 and

Col2a suggesting that Wnt9a is involved in joint induction (46;47). Wnt signaling is not only needed for initiation of joint formation but also required to suppress chondrogenesis of cells in presumptive joint region thereby, enabling joint formation and maintaining the fate of the joint interzone cells and the integrity of joints at later stages (79). The individual loss of either Wnt4 (80) or Wnt 16 (unpublished data) did not lead to joint abnormality and deletion of Wnt9a resulted only in partial fusion of carpal and tarsal joints that was augmented in Wnt9a/Wnt4 double mutants. This indicates that Wnt4, wnt14 and Wnt16 may play partially redundant roles in the process of joint formation (79). Conditional mutants deficient in Wnt/β-catenin signaling created using Col2-Cre or Gdf5-Cre had anatomically normal joints with some fusion observed in the wrist or ankle area only (47;54). Histologically, these grossly normal joints displayed a defective flattened superficial cell layer that expressed markedly reduced levels of lubricin and Col2a indicating that Wnt/β-catenin signaling plays an important role in generation and maintenance of the superficial zone of articular cartilage (54).

Role of Wnt signaling in joint homeostasis

Different lines of evidence suggest that molecular pathways involved in embryonic joint development including Wnt signaling play a role in postnatal joint homeostasis.

Differential expression studies have reported regulation of several molecules involved in Wnt signaling in OA cartilage, bone, and synovial membrane. These include up-regulation of Frzb2 (sFRP4) (81), Wnt7b (82), Fz-6, DKK-3, and Wnt-induced signaling protein 1 (WISP-1) (83;84), Wnt5b, Fz3, sFRP5, APC and Axin2 (85), and downregulation of frzb (82).

.

More importantly, an association between the development of hip OA and polymorphism in the Wnt antagonist Frzb gene substituting Arg324Gly has been demonstrated (86). This mutation reduces the antagonistic activity of Frzb without affecting its interaction with Wnt ligands (86;87). Furthermore, functional deletion of Frzb in different murine models of OA results in exacerbation of the disease. Cartilage breakdown in Frzb-/- mice was associated with increased Wnt signaling in the articular cartilage and with increased expression levels and activity of MMP3 (88). This study also demonstrated an interaction between Frzb and MMP3, probably through Frzb netrin domain, leading to dose dependent inhibition of MMP3 activity. Polymorphism in LRP5 or WISP1 gene were found to be associated with spinal osteoarthritis in postmenopausal Japanese women (89;90) strongly indicating the involvement of wnt signaling in OA.

Wnt/β-catenin pathway was found to be involved in cartilage matrix catabolism by activating the expression of MMPs and ADAMTSs (91). It has been reported that Wnt3a and Wnt7a can induce articular cartilage de-differentiation through transcriptional activation of β-catenin and c-Jun N-terminal kinase (JNK) pathway (92;93). It has been also demonstrated that Wnt/β-catenin signaling inhibits apoptosis in articular chondrocytes by activating cell survival signaling such as phosphatidylinositol 3-kinase/Akt which block apoptotic signaling cascades (92).

The Wnt pathway was identified as a key regulator of joint remodelling as blocking the activity of DKK-1 reversed bone destruction in mouse models of inflammatory arthritis (94). In this important paper, it was shown that joint inflammation up-regulates the levels of DKK-1 in a TNFα-dependent manner, which in turn inhibited bone formation in an OPG-dependent manner. Administration of a blocking antibody to DKK-1 restored bone formation, blocked the formation of joint erosions and transformed the rheumatoid

arthritis-like phenotype of collagen induced arthritis in mice into an OA like phenotype characterized by osteophyte formation. The critical role of Wnt signaling in postnatal joint homeostasis was further highlighted by recent studies inhibiting or activating β-catenin signaling in articular chondrocytes. Both gain and loss of function experiments resulted in articular cartilage destruction and development of a spontaneous OA like phenotype but through different mechanisms (95;96). Increased cell apoptosis contributed to articular cartilage damage in Col2a1-ICAT transgenic mice where Wnt/ β-catenin signaling was blocked in chondrocytes (96) whereas, premature chondrocyte differentiation caused OA development in mice with conditional activation of β-catenin in adult articular chondrocytes (95). This indicate that Wnt signaling needs to be tightly controlled in articular chondrocytes to maintain a functional, stable phenotype thus supporting joint function throughout life.

1.1.3.2. BMP signaling

An outline of the BMP pathway

Bone morphogenetic proteins (BMPs), originally identified as proteins that induce ectopic bone and cartilage formation, are multifunctional growth factors and morphogens that belong to the transforming growth factor β superfamily that also include TGF-βs, activins/inhibins, nodal and anti-mullerian hormone. More than 20 proteins have been identified and subdivided into several groups based on their structure similarities (97):

- BMP2/4: BMP-2 and BMP-4
- BMP-5,-6, -7 (Osteogenic protein-1 OP1), -8 (OP2) and BMP-8b (OP3)
- BMP3: BMP-3 (osteogenin) and BMP-3b (GDF-10)
- BMP9/10: BMP-9 (GDF-2), BMP-10
- Growth and differentiation factors GDF: GDF-5 (Cartilage derived morphogenetic protein-1 CDMP-1), GDF-6 (CDMP-2, BMP13), GDF-7 (BMP12)
- GDF1: GDF1, GDF3
- GDF8: GDF-8 (myostatin), GDF-11(BMP-11)
- GDF9: GDF-9, GDF-9b (BMP15), GDF15

BMPs are synthesized as large precursor molecules that are then cleaved at a consensus Arg-X-X-Arg site to generate mature dimers held together by disulfide bonds (98). BMPs can bind to three distinct type II serine/ threonine kinase receptors (BMP type II receptor BMPR-II, activin type II receptor ActR-II and activin type IIB receptor ActR-IIB) which in turn recruit and phosphorylate type I serine/ threonine kinase receptors (activin receptor like kinase ALK-2, 3 and 6) at Gly-Ser domains forming BMP-receptor II- receptor I complex. On receptor activation, type I receptors

phosphorylate receptor regulated Smads (R-Smads) which are Smads 1, 5 and 8. The phosphorylated R-Smads form a complex with Co-Smad (Smad-4) and translocate into the nucleus where, in complex with several co-activators and co-repressors, they participate in the transcriptional regulation of target genes (Figure 1.7) (99)

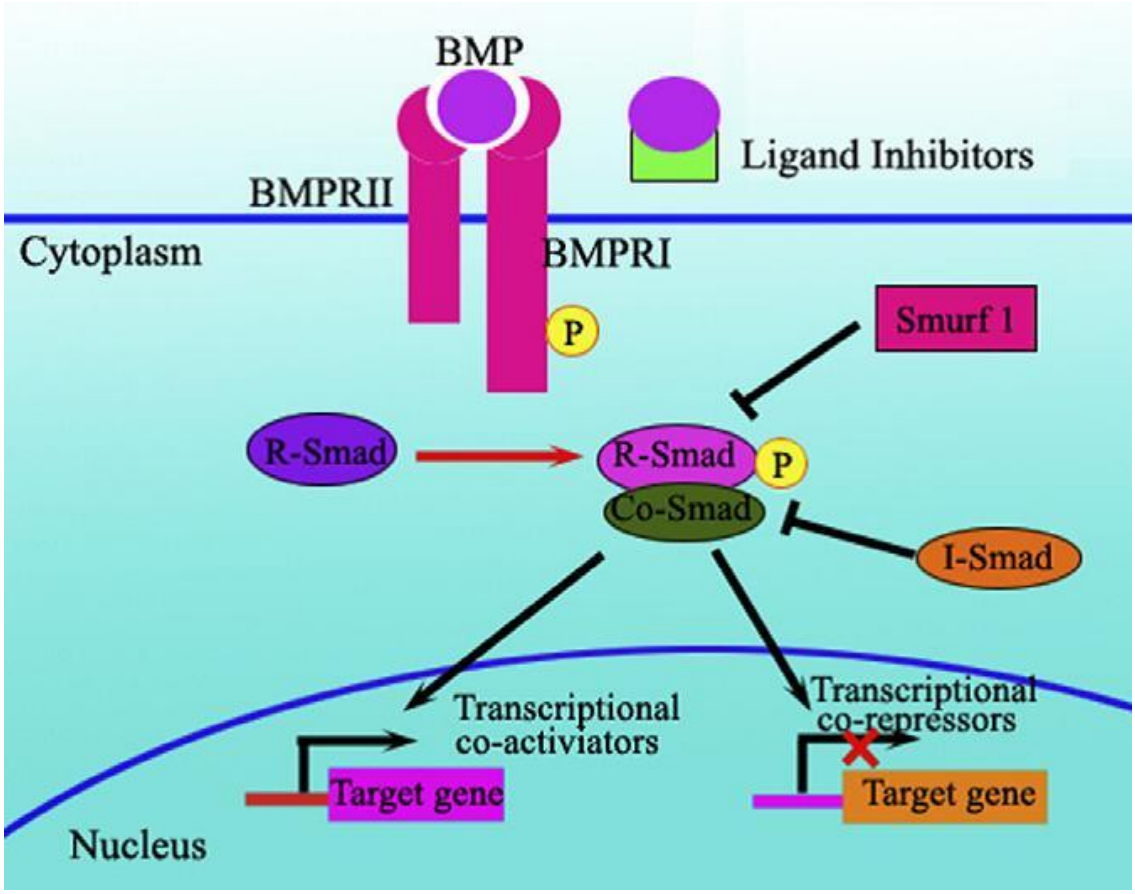

Figure 1.7: BMP signaling pathway: BMPs bind to type II receptor phosphorylating type I receptor which in turn phosphorylates R Smads (Smad1/5/8). The R-Smads form a complex with Co-Smad (Smad4) and translocate into the nucleus where they regulate transcription of target genes. The signaling is modulated extracellulary by BMP antagonist (including noggin, chordin and follistatin), intracellulary by I-Smads and Smurfs and in the nucleus by transcriptional co-activators and co-repressor. (Figure from (99))

BMP signaling is regulated by different mechanisms on all levels of its pathway (Figure 1.7). Extracellulary, the activity of BMPs is inhibited by soluble BMP antagonists such as Noggin, Chordin, Germilin, Dan, Cerberus and Follistatin which bind to the ligands preventing their interaction with the receptors. Intracellulary, Smad signaling is antagonized by inhibitory Smads (I-Smad) such as Smad6 and Smad7 which can compete with R-Smads for activation by type I receptors and interact with R-Smads to prevent the complex formation between R-Smads and Co-Smads. In addition, E3 ubiquitin-protein ligase Smurf1 and Smurf2 facilitate R-Smads ubiquitination and degradation thus regulating their intracellular pool. In the nucleus, transcriptional co-activators such p300 and CBP and co-repressors such as c-Ski and SnoN regulate the transcription of target genes by controlling the accessibility of the Smad complex to the transcription machinery (100).

Role of BMP signaling in embryonic joint development

Many members of BMP family have been implicated in skeletal and joint development. BMPs including GDF-5/CDMP1 (101), GDF-6 (45), BMP-2 and BMP-4 (102) along with BMP antagonists Noggin and Chordin (103) are among the earliest factors to be expressed during the process of joint formation.

At the early stages of limb development, GDF-5 is expressed throughout the mesenchymal condensations promoting the recruitment and the differentiation of cells into chondrogenesis (45). At later stages, GDF-5 expression is restricted to joint interzones where positive cells form distinct progenitor cells responsible for articular cartilage and synovial joint formation (54). Mutations in GDF-5/CDMP1 cause the brachypodism phenotype in mice and chondrodyplasia in humans. These phenotypes are

mainly characterized by short limbs, loss of proximal inter-phalangeal joints and fusion of bones in the wrist and ankle joints (101;104;105). Exogenous GDF-5 protein could rescue the abnormalities present in the digits of brachypodism mice. However, in spite of its early appearance in joint formation, GDF-5 is not sufficient for joint specification as its overexpression in mouse wild type limbs resulted in joint fusions probably by causing cartilage overgrowth but did not lead to morphological or molecular changes characteristic of the formation of a new joint (106). GDF-6 and GDF-7 are also expressed in developing joints and mice lacking GDF-6 displayed fusions between bones in the wrist and ankles and compound ablation of GDF-5 and 6 genes caused additional widespread joints defects (107).

BMPs play a key role in mediating inter-digital apoptosis (108) and BMP-7 up-regulates HA and CD44 expression in chondrocytes (109). Therefore these molecules might be involved in regulating the process of joint cavitation. Over-expression of BMP-2 or BMP-4 led to a dramatic increase in the volume of cartilage elements, altered their shape and led to joint fusion. This increase in volume appeared to result from an increase in the amount of matrix and in the number of precursors recruited to chondrogenic fate (102).

BMP antagonists (Noggin and chordin) are expressed in the developing skeletal elements. Noggin is expressed in the limb mesenchyme and in the cartilage condensation including the developing joint (45;48). In noggin knockout mice, the mesenchymal condensations and the cartilage anlagens became larger and the joints failed to form indicating the importance of noggin in the normal development of both long bones and joints (48). In humans, several skeletal phenotypes such as multiple synostoses syndrome in which multiple joint fusions is a principal feature (110) and Tarsal-Carpal Coalition Syndrome (111) have been reported as a result of different noggin mutations.

Chordin is also expressed in developing joints (45) and chordin-null mice develop normal joints with minor craniofacial skeletal defects (112). BMP antagonists are thus required to regulate the extent of chondrogenesis preventing premature rapid conversion of mesenchymal condensation into chondrocytes (55).

Role of BMP signaling in adult joint homeostasis

Several studies have linked the regulation of BMP signaling with adult joint homeostasis. Different BMP ligands, receptors, intra-cellular mediators and antagonists are expressed in normal adult cartilage with some alteration in the expression levels in arthritic conditions. For example, BMP-2 was expressed at low levels in normal cartilage but highly expressed during osteoarthritis (113;114). BMP-7/OP-1 was found in the superficial and middle layers of healthy cartilage but markedly reduced with increasing age or progression of OA (115). CDMP-1 and CDMP-2 expression were also reported in normal articular cartilage predominantly in the superficial layer but further extended to all damaged areas in osteoarthritic cartilage (116). Expression of BMP antagonists such as Chordin, Follistatin and Gremlin was upregulated in osteoarthritis compared to normal cartilage (117;118).

In vitro studies demonstrated that different BMPs have anabolic effects on cartilage stimulating proteoglycan and collagen type II synthesis (109;119;120) and genetic studies in humans showed that polymorphisms in either GDF-5 or BMP-2 genes were associated with increased susceptibility to OA development (121;122).

The role of BMPs in cartilage homeostasis has been extensively studied in vivo. Intra-articular injection of BMP-2 in the mouse knee increased proteoglycan and collagen type II synthesis in the articular cartilage (123;124) and resulted in osteophyte

formation (125). Intra-articular treatment with BMP-7 had a chondroprotective effect in different animal models of OA (126;127). A tissue specific conditional knock-out mouse lacking BMPRIa receptor in articular region ($GDF5^{+/cre}$; $BMPRIa^{-/floxP}$ mice) showed progressive damage to articular cartilage postnatally compared to their wild type littermates (128). Noggin haploinsufficiency provided protection for articular cartilage in methylated bovine serum albumin (mBSA) induced arthritis and noggin overexpression by adenovirus administration made cartilage more vulnerable to destruction in the same model of arthritis (129). Taken together, these data support the critical function of BMP signaling and the importance of its critical control in maintaining cartilage homeostasis.

1.2. Joint surface injury and repair

1.2.1. Epidemiology and Natural history

Joint surface defects (JSD) are common lesions involving the loss of articular cartilage with or without the underlying subchondral bone. In a retrospective study reviewing 31,516 knee arthroscopies, chondral lesions were observed in 63% of patients. 74% of these patients had a single chondral lesions and 36.6% had no associated ligamentous or meniscal pathology (130). In a Prospective study evaluating 1.000 knee arthroscopies; Hjelle et al (131) reported the presence of chondral defects in 61% of the patients. The patellar articular surface (43.3%) and the medial femoral condyle (39.6%) were the most common locations of lesions reported in two recent studies analyzing 5114 and 25,124 knee arthroscopies (132;133).

JSD are often symptomatic and disabling (134), associated with progressive cartilage loss and may predispose to post-traumatic secondary osteoarthritis (PTOA) which was estimated to account for 13% of knee OA and 73% of ankle OA (135). Joint trauma in young age was reported to double the risk of developing OA (136) and joint surface defects were an independent risk factor for the need of prosthetic joint replacement within 4 years if occurring in patients with already established OA (137;138). Cartilage breakdown is the inevitable outcome of most rheumatic conditions causing pain and disability for millions of people worldwide. Therefore, joint surface restoration is a major priority in modern medicine (139).

It has been long thought that cartilage injuries never heal and lead to progressive joint degeneration and OA development (140). However, recent longitudinal studies have

showed evidence of spontaneous healing. In a long term (14 years) follow up study of 28 young athletes with isolated severe chondral damage in the weight-bearing area of the knee joint, 22 patients (78%) had excellent or good knee function and were able to return to pre-injury sport activities without any initial specific treatment (141). In another independent study, 79% of patients with chondral lesions also returned to pre-injury sports activities including jumping, twisting, and pivoting in the absence of any intervention on the cartilage lesion (142).

In prospective MRI studies, approximately 50% of asymptomatic individuals have chondral defects. Only 18.15% of individuals with a chondral defect had history of knee trauma. After 2.3 years follow up, 33% of the subjects had a worsening and 37% of the subjects had an improvement in cartilage defect score as graded by MRI and the rest remained stable. Worsening in scores was associated with age, female sex and body mass index (143). This confirms that functional as well as anatomical restoration can happen in a number of cases. In people with already established knee OA, superimposed chondral defects tended to progress in 81%, remained stable in 15% and improved only in 4% of patients over 2 years (144).

So far, it is not possible to predict the outcome of JSD as its natural history varies from spontaneous healing to secondary post-traumatic OA development (135;143). The reasons why some injured joints return to their normal function whereas other degenerate can be partially explained by the presence of risk factors related to the patient or to the nature of the injury itself that can interfere with joint surface repair.

1.2.2. Factors influencing outcome

Age is a strong risk factor for the development of PTOA (143). Articular cartilage undergoes significant age related changes in chondrocyte function, molecular composition and organization of the matrix including the production of shorter aggrecan molecules, increase in collagen cross-linking and decreased water content (145). With age, articular cartilage chondrocytes show a decrease in their mitotic and synthetic activity, become less responsive to anabolic growth factors and thus less able to maintain and repair cartilage tissue after injury (146). Clinical studies have shown that the risk of developing PTOA following articular cartilage injury in the knee joints increased 3-4 fold in patients older than 50 years (147). Animal studies in rabbits have demonstrated better reparative response in younger animals in comparison to older ones (148). However, the exact mechanisms of the age-dependent decline in the repair capacity of joint surface are unknown. It was postulated that such phenomenon might be due to age-related decrease in proliferative and synthetic activity of chondrocytes, unavailability of sufficient stem cell pool, insufficient release of growth factors or decreased sensitivity of cells to signaling molecules (149).

The Size and the depth of the defect are important factors determining the repair outcome. Defects exceeding a critical size do not achieve spontaneous repair and more likely develop secondary OA. In rabbits and goats, 3 mm diameter defects underwent complete repair whereas large (more than 5 mm) diameter defects showed progressive degeneration (150). Similarly in horses, large 9mm diameter lesion did not heal but a smaller 3mm diameter lesion was fully repaired in three months (151).

Cartilage lesions can be classified as either partial or full thickness depending on whether they extend or not to the subchondral bone. Partial thickness defects do not heal spontaneously. It has been suggested that this repair failure is due to the fact that they do not penetrate the subchondral bone and thus had no access to progenitor cells residing in bone marrow spaces. However, these lesions are asymptomatic and there is no evidence that they may evolve into osteoarthritis. Therefore, they do not represent an indication for surgical intervention (143;152). Full thickness cartilage defect extend to the underlying subchondral bone causing hemorrhage and fibrin clot formation. Experimental data suggest that mesenchymal stem cells (MSCs) from the underlying bone marrow migrate into the injury site and subsequently differentiate and assume a chondrocyte phenotype and start to synthesize collagen type II and proteoglycans. The subchondral bone plate is restored through the process of endochondral bone formation with the preservation of the articular cartilage surface (5;153). Although full thickness defects heal better than partial thickness lesions, they are clinically relevant because sometimes they persist and become symptomatic and disabling and therefore represent an indication for chondral surgery (154).

Associated joint instability and Malalignment is poor prognostic factor as it alters the joint biomechanics. Traumatic lesions causing combined joint surface injury and joint instability through rupture of ligaments, menisci or joint capsule, increase the susceptibility of joints to degenerate and therefore, associated with a higher risk for PTOA development (155). Joint instability affects the normal apposition of joint surfaces during motion and thus causes excessive focal shear and compressive forces on some regions of the articular surface leading to its degeneration (156). Experimental models show that mechanical instability induced by anterior cruciate ligament (ACL)

transection (157) or menisectomy of the knee joint leads to progressive joint degeneration (158). The combination of instability and articular cartilage injury were more likely to cause rapid progressive loss of cartilage than either condition alone (159). In humans, meniscal lesions and meniscal instability are well known risk factors of OA (160) and poor repair of JSD (143)

1.2.3. Available treatments

Several surgical therapeutic approaches have been developed in order to relief the symptoms, reconstruct joint surface, improve joint functionality and avoid progression towards OA.

1) Bone marrow stimulation procedures

Microfracture and pridie drilling take advantage of the intrinsic repair response observed upon penetration of subchondral bone in full thickness defects. Access to the subchondral bone marrow is gained by perforating the bed of the JSD through generating micro-holes. This induces the formation of fibrin clot and the recruitment of bone marrow-derived MSCs which subsequently undergo chondrogenesis. The resulting repair tissue is variable in composition, structure and durability. Biopsy specimens obtained from patients 2 years after microfracture showed that 11.4% were predominately formed of hyaline cartilage, 17.1% were formed of a mixture of hyaline and fibrocartilage and the rest were mainly formed of fibrocartilage (161).

The durability of the repair tissue is controversial. Although favorable outcome and longevity were reported after microfracture for up to 7 years (162), an independent longitudinal study of patients treated with microfracture over 36 months showed a significant deterioration after 18 month following an initial improvement especially in

individuals older than 40 years (163). The rate of failure after microfracture (patient needing re-operation due to lack of healing of the treated defect and persistent symptoms) increased from 2.5% after 2 year follow up to 23% after 5 years (164).

2) Cartilage replacement procedure (Mosaicplasty)

Mosaicplasty is performed by implanting autologous osteochondral graft, obtained from non weight-bearing area of the joint, into the full thickness defect. This technique can be done either as an open procedure or arthroscopically (165). In a large series of more than 1.000 mosaicplasties involving different compartments in the knee joint (166), good results were reported in 92%, 87% and 74% of patients defects in femoral condyles, tibial plateau and patellofemoral joints respectively for up to 10 years post-operatively. Survival of the transplanted cartilage and acceptable fibrocartilage covering of the donor site were found in 81 of 98 second look arthroscopies (166).

The main advantage of this technique is that it immediately fills the defect with hyaline articular cartilage and thus provides a fast symptomatic relief. Nonetheless, this procedure has several disadvantages. For example, harvesting of osteochondral plug induces chondrocyte death at the margin of the plug leading to tissue degeneration and failure of the graft (167). Lateral integration of the plug with native cartilage is hindered by the loss of chondrocyte viability at the margins and the inevitable spaces left between the graft and recipient tissue. This raises the concern that synovial fluid may leak into the subchondral layer causing cyst formation (154). Moreover, the translocation of tissue from low weight bearing area to a high weight bearing area may lead to degeneration of the graft as a consequence of mechanical overloading in the new position (168). There are also technical difficulties in restoring smooth joint surface due to differences in cartilage thickness between donor site and native tissues (169). Donor

site morbidity, associated with osteochondral transfer, must also be considered as it always associated with chondrocyte death adjacent to the harvest sites leading to degeneration of the tissue overtime (152). Failure of cartilaginous repair tissue to fill the void created in the donor site has been reported and associated with increased stiffness of the joint (170).

3) Autologous chondrocyte implantation (ACI)

In this procedure, healthy cartilage is harvested from non-weight bearing area of the joint at an initial arthroscopy. Autologous chondrocytes are released by enzymatic digestion, expanded in vitro for 2-3 weeks and then injected into the chondral defect underneath a periosteal flap in a second surgical procedure (171). In 1994, Brittberg et al presented clinical results of first 23 patients (14-48 years old) with full thickness cartilage defect in the knee treated by ACI. They reported good results in 70% of all patients and 88% of cases with femoral condylar transplants 2 years after transplantation (171). Long term clinical studies showed satisfactory results in 80% of patients (92% of patients with femoral condylar defect) for up to 9 years (172) and good results were reported in 51 of 61 patients treated with ACI in a 5-11 years follow up study (173).

Three potential sources were proposed for the origin of the repair tissue in ACI procedure; the transplanted chondrocytes, precursor cells from periosteal flap or mesenchymal stem cells derived from the underlying bone marrow (152). Using a goat model of ACI and a tracking dye, it has been shown that the implanted chondrocytes persisted in the cartilage defect and constituted the majority of the repair cartilage tissue after 12 weeks (174). However, it can not be excluded that these cells may play a different role including the support of the local repair mechanisms by delivering bioactive molecules such as BMPs and FGFs (174).

It is known that the in vitro chondrocyte expansion, necessary for obtaining enough numbers of cells, cause gradual de-differentiation of chondrocytes (175) and affect their phenotypic stability potentially leading to loss of their capacity to form stable cartilage in vivo, and to resist vascular invasion and endochondral bone formation (176). This is a pivotal issue for successful cell based repair protocol. Molecular markers, such as FGFR3, BMP2, COL2A1 and ALK1, can predict the ability of expanded human articular chondrocytes to form ectopic stable cartilage in vivo and thus can be used to monitor the phenotypic stability of chondrocytes during in vitro expansion (176). Importantly, Saris et al have demonstrated that ACI performed using chondrocytes optimized by these markers for its biological potency to form stable cartilage tissue in vivo results in better structural and clinical outcome than microfracture (177;178).

Randomized control trials

Randomized control trials have been performed to identify a superior method for cartilage repair. Mosaicplasty has largely been abandoned in recent years due to the several problems listed above and to a poorer performance compared to ACI in randomized clinical trial (179). Microfracture and ACI have repeatedly shown similar efficacy in clinical trials. Knutsen et al., 2004 compared ACI with microfracture two years after surgery and there was little difference in favor of microfracture in term of clinical scores but there was no significant difference in macroscopic or histological results between the two treatment groups (161). In a follow-up study at 5 years in the same cohort, both ACI and microfracture had comparably satisfactory results in 77% of the patients with no significant difference in the clinical and radiographic outcome between the two treatment groups (164). One important finding of this study was that the histological quality of the repair tissue correlated with the clinical outcome as none of

patients with good quality cartilage (predominantly hyaline) at 2 years had a later failure at the 5 years follow up (164).

A recent randomized control trial comparing a variant of ACI where the chondrocyte are quality controlled for their cartilage forming capacity after in vitro expansion (176) versus microfracture three year after treatment, reported superior structural and clinical outcome in chondral defects treated with characterized chondrocyte implantation (178;180) thereby stressing the importance of phenotypic stability of implanted chondrocytes in achieving better structural regeneration.

Despite the presence of many different treatment methods providing symptomatic relief, each method has several limitations and no method has yet been able to regenerate a neo-cartilage similar in structure and mechanical properties to that of a native normal hyaline articular cartilage, and the best treatment for long term durability is still unknown. Most importantly, the current therapeutic options involve invasive and challenging surgeries and the cell-based technologies are extremely expensive. Therefore, intense research is still ongoing to identify novel therapeutic options that could circumvent these problems.

1.2.4. Cartilage tissue engineering

Tissue engineering is a fast developing area in medicine that combine cells, scaffolding biomaterials and signaling molecules to engineer functional replacement tissue for clinical use. There are two main approaches for tissue engineering. In the first, repair tissue is engineered completely in vitro and then implanted into the defect. The advantage of this method is that the manufacturing is well controlled and the tissue will be immediately capable of weight bearing. However, there are several problems

associated with the implantation of pre-formed mature implant including tissue integration, mechanical fixation, immune reactivity and inadequate physical properties. In addition, the clinical application of this approach is difficult because of the high costs that it implies and the regulatory hurdles that a composite product should pass before it can be approved.

In the second approach, the basic building blocks containing a matrix scaffold, cells and signaling molecules will be assembled in vitro. The desired differentiation and remodeling processes will take place in vivo following implantation under the control of the delivered signaling molecules and physiological mechanical loading. In this case, the immature engineered cartilage could be injected in a minimally invasive procedure that may reduce morbidity and it is hoped that the repair tissue will integrate with the native articular cartilage by taking the shape of the defect that it has been injected into. However, the high costs, the complex regulation that cell based product will be subjected to and the difficult control over cellular activity on the long term are all considered as disadvantages of this technique (152).

Stem cells

Although the use of autologous chondrocytes in ACI offers the advantage of using differentiated cells that are committed to the appropriate phenotype, several concerns have been raised regarding the additional injury affecting the donor site, the need for two operations, the in vitro manipulation of the cells that may affect its phenotypic stability (176) and finally the high cost associated with the in vitro chondrocyte expansion. Therefore, chondrogenic cells that are in more abundant supply and more easily obtained have been proposed as an alternative source for cartilage reconstruction. Mesenchymal stem cells (MSCs) are multipotent cells that have the capacity to differentiate into a

variety of other connective tissue cells, including chondrocytes (181) and can be isolated from several tissues such as bone marrow (181), periosteum (182), synovial membrane (183), articular cartilage (184), skeletal muscle and adipose tissue (185). These properties of MSCs would allow the generation of large quality controlled batches for allogeneic transplantation and thus overcome the limitation and variability of autologous cell protocols (186). However, the immunogenicity of MSCs must be taken into consideration as conflicting results have been obtained in different experimental conditions, tissue/organ systems or animal species (187)

The implantation of undifferentiated bone marrow MSCs has been tested in a variety of animal models with initial encouraging results (188;189;190). However, at later time points, cartilage tissue became thinner due to progressive endochondral bone formation with the advancement of the bone front at the expenses of overlying articular cartilage (191;192). This can be explained by the known characteristic of these cells to terminally differentiate into hypertrophic chondrocytes and/or the insufficiency of the in vivo environment to promote chondrogenesis (193). Thus, the implantation of a pre-committed MSCs towards chondrogenic lineage was proposed to reduce the risk of undesired tissue formation. The in vitro chondrogenic differentiation of MSCs can be induced through a large variety of different growth factors including TGF-β1, IGF-1, BMPs and FGFs (194). However, this acquired phenotype was not stable in vivo in a nude mouse assay of ectopic cartilage formation (195). During in vitro chondrogenic induction, MSCs not only up-regulate hyaline cartilage specific markers such as collagen type II and aggrecan, but also up-regulate markers for hypertrophic chondrocytes and osteogenesis such as Collagen type X, MMP13 and increase in

alkaline phosphatase activity (196). In contrast, engineered cartilage from mature chondrocytes does not express type X collagen or alkaline phosphatase (197).

At present, there are scattered studies in humans testing the potential of autologous culture expanded bone marrow MSCs transplantation to promote the repair of articular cartilage defects. One clinical trial compared autologous expanded bone marrow derived MSCs cultured on a collagen scaffold versus cell free scaffold controls. The 2-year outcome showed significantly better hyaline cartilage formation in the cell-transplanted group compared to the cell-free control group (198). In 3 case reports, cultured MSCs were placed into cartilage defects and covered with autologous periosteum. Clinical symptoms had improved significantly for up to 2 years however; the histological outcome of repair tissue was variable ranging from hyaline like cartilage to fibrocartilage (199-201). It is still unclear whether the newly formed tissue consisted of the implanted MSCs or the applied cells indirectly promote regeneration via secreted bioactive factors.

Further studies are still needed to better understand the regulatory mechanisms involved in enhancing and maintaining chondrogenic differentiation. It is crucial also to characterize the difference between MSCs derived from different tissues to determine the best source in terms of chondrogenic ability and easy accessibility. Importantly, the role and the contribution of transplanted cells to the repair tissue as well as structural and functional properties of this tissue over long term must be addressed and compared to results obtained from ACI procedure.

Scaffolds

Biomaterial science runs in parallel with the advances in tissue engineering in an attempt to develop biocompatible, biodegradable, porous, mechanically stable and supportive

scaffolds that not only can be used to keep the implanted cells in the site of damage but can also influence cell differentiation and tissue pattering through controlled delivery of bioactive molecules (202). Scaffold materials may be either natural or synthetic. Natural materials include agarose, hyaluronan, gelatin, fibrin and collagen derivatives. These materials can be produced in an injectable form which later can set to gel and fill any shape and size of cartilage defect. The use of agarose, gelatin and fibrin has been limited by their mechanical fragility and the possibility of evoking immune reactions. Collagens and hyaluronan provide a substrate that would normally be found in articular cartilage and thus have better biocompatibility (168). Synthetic scaffolds can be manufactured from polyglycolic and polylactic acids in many variants. The mechanical and biochemical properties of the synthetic materials can be modified to generate products more resistant to the friction of joint motion and easier to be fixed to the recipient site. The degradation rate can also be adjusted to be sufficient for scaffold purpose without impeding tissue regeneration (203). The scaffold architecture can be designed to mimic the depth-dependent heterogeneity of articular cartilage structure (204) or to generate biphasic scaffolds to promote the simultaneous growth of bone and cartilage with a stable interface for engineering osteochondral tissue (205). At the same time, the immune reaction problems of the natural materials are avoided (206).

Synthetic self-assembling biomaterials are being developed to generate 3D scaffolds that polymerize spontaneously in situ to support implanted cells and act as carriers systems for controlled release of bioactive molecules to achieve a coordinated process of cell differentiation and tissue repair. One example of such strategy comes from the field of neural regeneration, Silva and colleagues (207) described the generation a self-polymerizing peptide carrying the neurite-promoting laminin epitope IKVAV. This

peptide assembled itself into nanofibers encapsulating neuronal progenitor cells and presenting them to a bioactive peptide at high density. This induced rapid neuronal differentiation of the progenitor cells, while discouraging development of astrocytes. In a similar approach in bone regeneration, Lutolf et al (208) have engineered a hydrogel that can promote cell adhesion through an integrin-dependent mechanism and deliver rhBMP-2 at the site of critical size cranial defects in rats. The hydrogel was infiltrated rapidly by fibroblast-like cells and replaced with bone tissue resulting in efficient and highly localized bone regeneration.

Signaling molecules

Several growth factors and signaling molecules influence various cell activities such as proliferation, migration, differentiation and matrix synthesis and therefore could be used to specifically guide the course of differentiation in the desired direction and to maintain the chondrocyte phenotype. A number of growth factors such as TGF-β, IGF1, FGF and especially BMPs have been shown to induce chondrogenesis and stimulate the anabolic activity of chondrocytes (209) and therefore have represented for many years an attractive therapeutic target for chondro-protection and cartilage repair. These bioactive molecules have been intensively explored in vitro and in animal models (210;211;212;213;214). However, their use might result in adverse effects in the joints such as osteophyte formation, swelling and synovial hyperplasia (125;215). In addition, the delivery of these proteins to the sites of cartilage damage at therapeutic concentrations and for sustained periods of time has been difficult due to their limited half-lives in vivo (209).

Thus far, these approaches to cartilage engineering are still at the experimental stage of development and several issues must be addressed before the application in clinical

practice. These issues include the potency, safety and toxicity of the cellular product/proposed molecules, the optimal source, dose and delivery system for cells/growth factors to the lesion, anatomical and functional integration of the resulting repair tissue with the surrounding cartilage and bone, cost effectiveness, identification of proper clinical indications and management of adverse effect (186).

Another alternative or complementary approach for cartilage tissue regeneration and restoration of joint homeostasis could be the controlled delivery of bioactive molecules to the site of injury for a defined period of time and at the right dose to trigger/support repair response by recruiting joint progenitor cells to the site of damage and controlling their fate decisions and differentiation in vivo (molecular therapy). This approach would thereby avoid the limitations of the current cell-based therapies that are related to in vitro manipulation of cells, high costs, variability, disease transmission and immunogenicity. A key step for the development of such an approach is the identification of the appropriate potential molecular signal (s) that can be targeted to enhance the biological repair of joint surface defects with phenotypically stable cartilage resistant to vascular invasion and endochondral bone formation.

1.3. Models of acute cartilage injury

1.3.1. In vitro models

Many in vitro models in which cartilage injury can be induced by either explantation, re-cutting (216) or impact loading (217) have been developed to investigate the cellular and molecular response of adult articular cartilage to acute mechanical injury. Several studies have investigated the effect of cartilage injury on chondrocyte viability and demonstrated that mechanical overloading and wounding can induce cell death in cartilage tissue (218-220). The extent of chondrocyte apoptosis was positively correlated with the amount of load applied (221) and was associated with cartilage damage and degeneration suggesting a role of chondrocyte cell death in the pathogenesis of PTOA (222). Redman et al studied the cellular response of articular cartilage to sharp and blunt trauma and showed extensive cell death in response to trephine (blunt) trauma and limited cell death adjacent to lesion edge when cartilage is wounded with scalpel (sharp trauma) (223). It is not yet clear how mechanical injury triggers the apoptotic process but it was postulated that disruption of cell-matrix interaction during injury might be the stimulus for chondrocyte apoptosis (224). Activation of cellular proliferation was also reported following a single impact load (225) and in cartilage explants subjected to sharp and blunt trauma (223).

Mechanical cartilage injury has been demonstrated to cause strong up-regulation of MMPs and aggrecanases suggesting that these enzymes may be involved in the active degradation of proteoglycans after injury (226;227). Chondrocytes respond to low/moderate loading by up-regulating their biosynthetic activity to maintain the

mechanical properties and function of the tissue (228). However, impact loading was found to decrease proteoglycan synthesis correlating with increased load frequency and duration (229).

Intracellular signaling pathways such as extracellulary regulated kinase (ERK), p38, and c-jun-terminal kinase (JNK) were strongly activated by mechanical injury and were sufficient to induce expression of inflammatory mediators such as IL-1α and β (230). The activation of ERK pathway upon cutting or loading articular cartilage was dependent on fibroblast growth factor-2 (FGF-2) release from pericellular matrix (13;216;231). FGF-2 plays a pivotal role in promoting MSCs migration during the early phases of articular cartilage repair (232) and in protecting cartilage from degradation by suppressing aggrecanase activity (233). This data indicate a functional role of molecular signals activated in response to injury and validate the use of in vitro models to identify therapeutic targets to enhance cartilage repair.

1.3.2. In vivo animal models

Several animal models have been generated to study the pathophysiology of joint surface injury and to develop/evaluate different therapeutic approaches for reconstructing the damaged articular cartilage. Although none of these models reproduces the human lesions due to the physiological and anatomical differences between human joints and those of experimental animals (234), the use of animal models has played a significant role in the current advancement of joint resurfacing techniques and in our understanding of cartilage response to injury and phenomenology of repair process.

In these models, partial cartilage defects neither heal spontaneously nor evolve into OA (152). This is in line with the human data in which similar defects are asymptomatic with no evidence of OA evolution (143). In full thickness joint surface injury, however, spontaneous structural repair was reported in several large animal models such as rats (235), rabbits (153), dogs (236) and horses (151). Interestingly, this repair phenomenon involved a coordinated and polarized morphogenetic process recapitulating chondrogenesis and endochondral bone formation during embryonic skeletogenesis (153). These data thereby document the presence of cartilage repair mechanisms that involve endogenous progenitors in adult animals and suggest that mechanisms similar to those involved in skeletal development were reactivated during postnatal repair process. This was further supported by a recent study characterizing the early events of repair of full thickness defects in rats and demonstrating that morphogenetic and molecular events taking place during repair are analogous to those observed during skeletal development (237).

Although the histological features of cartilage repair process has been extensively characterized, the molecular and cellular mechanisms governing such events are not yet understood. This could be attributed to the unavailability of a suitable animal model amenable to genetic manipulation to allow functional testing of molecules involved in joint surface repair. Therefore, one of the main aims of the work presented in this thesis was to develop a reproducible and consistent adult mammalian animal model of joint surface injury/repair that is suitable for biological and biochemical quantification, detailed molecular analysis and genetic studies.

CHAPTER 2

HYPOTHESIS AND AIMS OF THE STUDY

2.1. Hypothesis:

This work tests the hypothesis that mechanical injury to adult articular cartilage can trigger a specific molecular and cellular response in this tissue leading to joint surface repair.

Previous experiments in animal models and recent clinical evidence demonstrate that the joint surface, under favorable circumstances, can heal cartilage defects. So far, the molecular and cellular program governing the repair process is unknown. We anticipate that some signalling molecules activated upon cartilage injury may regulate joint surface regeneration and therefore may represent a molecular tool to enhance/support the biological repair processes in patients with chronic joint surface defects.

2.2. Aims of the study:

The ultimate goal of this study was to investigate the cellular and molecular mechanisms regulating joint surface healing by studying the early response to mechanical articular cartilage injury.

The specific aims for this thesis were to:

1. Characterize the molecular response of articular cartilage to acute mechanical injury.

2. Generate and validate an in vivo model of joint surface injury and regeneration in adult mice as this species is amenable for genetic manipulation and thus allow functional molecular studies.

3. Characterize the cellular responses and ECM remodeling following acute mechanical injury of the joint surface in vivo

4. Investigate whether the modulation of signaling pathways in response to cartilage injury in vitro also takes place in vivo where cartilage interacts with neighbouring tissues in the joint.

5. Investigate the function of Wnt16, a morphogen expressed specifically by injured articular cartilage, in joint surface homeostasis, regeneration, and development of experimental OA.

CHAPTER 3

MATERIALS AND METHODS

3.1: Generation of the acute mechanical cartilage injury

To investigate the response of articular cartilage to mechanical injury, we used an in vivo and in vitro cartilage injury models.

3.1.1: In vivo joint surface injury model

Male C57BL/6, DBA/1 and MRL/Mpj mice strains were purchased from Jackson laboratory. BAT-GAL mice in which β-galactosidase is expressed under the transcriptional control of TCF/LEF1 responsive elements were obtained as a kind gift from Professor Stefano Piccolo (University of Padua, Italy) and Axin2 knock-in mice in which a LacZ cassette replace exon 2 of the Axin 2 gene were obtained from Dr. Boris Jerchow and Professor Walter Birchmeier (Center for Molecular Medicine, Berlin, Germany). Wnt16 null mutants were obtained through a collaboration with Professor Jing Yu and Professor Andrew McMahon (Harvard University, Boston USA).

All mice were maintained on free diet under pathogen free conditions. Mice were anesthetized using Ketamine (40 mg/kg) and Xylazine (5 mg/kg). After lateral skin incision, medial Para-patellar arthrotomy was performed under a dissection microscope (Leica), by inserting microsurgical scalpel medially and proximally to the insertion of the patellar tendon on the tibia and extending it proximally until the attachment of the quadriceps muscle. The medial margin of the quadriceps was separated from the muscles of the medial compartment (Figure 3.1.A&B). The joint was extended and the patella was dislocated laterally (Figure 3.1C). The joint was then fully flexed to expose the patellar groove. A longitudinal full thickness injury was made in the patellar groove using a custom made device in which a glass bead was placed approximately 200μm to

the tip of a 26G needle (Figure 3.1D). The tip of the needle was placed anteriorly to the intercondylar notch and gently moved along the entire length of the patellar groove (Figure 3.1D). The patellar dislocation was then reduced. The joint capsule and the skin were sutured in separate layers. The contra-lateral knee was either left non-operated or subjected to arthrotomy and patellar dislocation without cartilage injury (sham-operated controls). After recovery, the mice were allowed to walk freely in standard cages and then killed at different time points. All procedures were approved by the local Ethics committee and the UK Home Office.

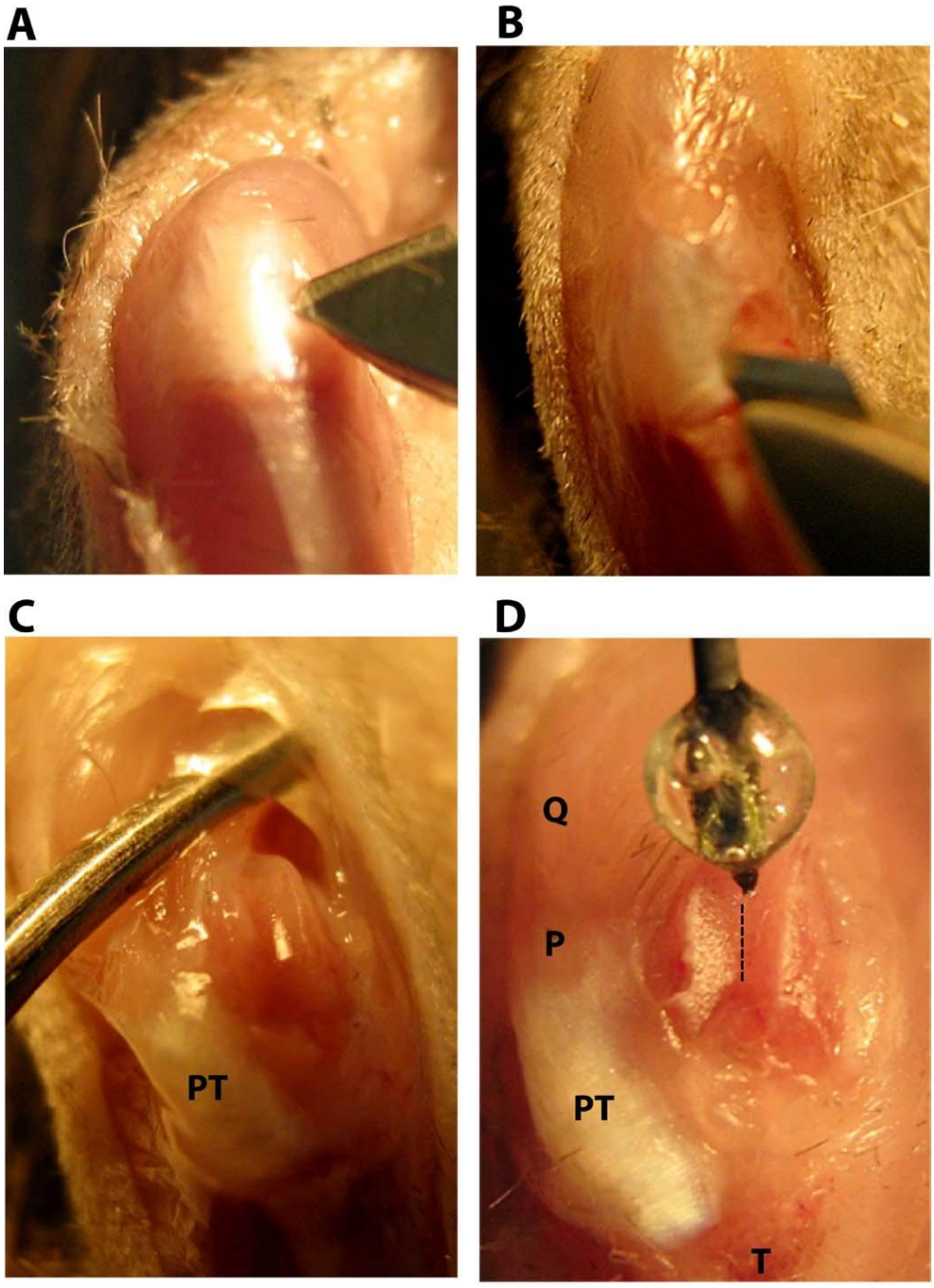

Figure 3.1: surgical induction of joint surface injury in mice: Lateral skin incision (A) and medial Para-patellar arthrotomy was performed (B). The patellar groove is exposed by lateral dislocation of the patella (C). The devise is placed with its tip just anteriorly to the intercondylar notch (lower end of dotted line) and dragged proximally in the centre of the entire length of patellar groove (dotted line) (D). P=Patella; PT=Patellar tendon; Q=quadriceps muscle and T=Tibial tuberosity.

3.1.2: In vitro cartilage injury model

Cartilage samples were obtained from patients who underwent either total knee replacement for unicompartmental OA (7 patients with a mean ± SD age of 68 ± 7 years) or limb amputation because of traffic accident (a 53-years-old man). A rectangular cartilage explant was dissected and divided into three equal parts of 6x 6 mm each. One part was immediately snap-frozen in liquid nitrogen for total RNA extraction preserving a full thickness slice for histological analysis (freshly isolated sample). The remaining 2 explants were maintained in culture in 4ml of Dulbecco's modified Eagles's medium (Invitrogen, UK) in the presence or absence of 10% FBS (Invitrogen, UK) and antibiotics/ antimycotics (Invitrogen, UK) in individual 33mm bacteriological petri dishes (BD Bioscience) to avoid spreading of the cells from the explants. After 6 days, the medium was replaced and one of each pair of adjacent samples was cut at 1 mm interval using a scalpel (injured sample). The other explant of each pair was left uninjured (uninjured sample). After 24 hours, the culture was terminated and explants were used for RNA extraction and histological analysis. The peripheral part (1mm) of each explant was discarded to eliminate the portion of cartilage that was injured during the initial dissection before the culture. The model is summarized in Figure 3.2

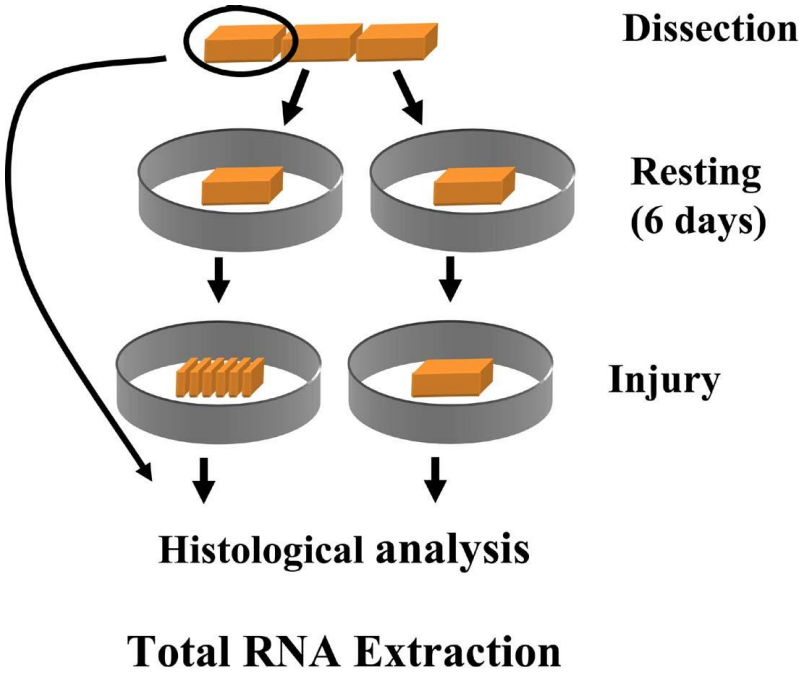

Figure 3.2: In vitro model of mechanical cartilage injury: Adult human articular cartilage explants were obtained, dissected and processed immediately or placed in culture in separate bacteriological Petri dishes. After 6 days, one explant was injured and 24 hours later the cultures were terminated for gene expression and histological analysis.

3.2: Surgical destabilization of the medial meniscus (DMM)

DMM was performed according to the previously published procedure (34). Breifly, mice were anesthetized using intra-peritoneal injection of Ketamine (40 mg/kg) and Xylazine (5 mg/kg). A longitudinal incision medial to the patellar ligament was made, the joint capsule was opened, and the meniscotibial ligament, anchoring the medial meniscus to the tibial plateau, was identified and transected, resulting in destabilization of the medial meniscus (DMM). In sham operated animals, arthrotomy was performed without any further manipulation. In both sham and DMM animals, the joint capsule and the skin were sutured separately. After recovery from anesthesia the mice were allowed to move freely and were kept under standard conditions.

3.3. Tissue processing for Histology and immunohistochemistry

3.3.1. Fixation and decalcification

Mouse knee joints were dissected immediately after killing the animals and fixed in buffered isotonic solution of 4% PFA (Paraformaldehyde) at 4°C for 24h. The joints were then washed with phosphate buffered saline (PBS) and decalcified in 4% EDTA (ethylenediaminetetra-acetic acid) for 2 weeks at room temperature with changing the solution every 3 days.

Human cartilage explants were also fixed in buffered isotonic solution of 4% Paraformaldehyde at 4°C over night immediately after the termination of the cultures and then processed for embedding

3.3.2. Embedding

Paraffin embedding

Following fixation and, when appropriate, decalcification, the tissues were washed in PBS and fitted into the embedding cassettes and processed in Leica TP 1050 tissue processor as follows:

1) 70% Ethanol, two changes, 1 hour each.

2) 80% Ethanol, two changes, 1 hour each.

3) 95% Ethanol, two changes, 1 hour each.

4) 100% Ethanol, three changes, 1 hour each.

5) Xylene or xylene substitute, three changes, 1 hour each.

6) Paraffin wax (56-58 C), two changes, 1 hour and half each.

Finally the tissue samples were embedded into paraffin blocks and placed in a cold plate to set for at least 2 hours. Cartilage explants were embedded with their lateral side facing down so that cutting would result in full thickness sections. Mouse joints were orientated in a “kneeling position” with the anterior aspect of the tibia facing down, and the femur angles at 90’ with the tibia directed upward. This orientation resulted in sections that were frontal in the tibia and coronal in the femur, as shown in figure 5.1A. Paraffin embedded samples were stored in boxes at room temperature until use.

Frozen sample embedding

Samples were washed in PBS and transferred into 5% sucrose/PBS and incubated for 2 hours at 4°C on rotating plate. The solution was then replaced with 30% sucrose/PBS for an overnight incubation at 4°C. Half of the solution was then replaced with OCT (optimal cutting temperature) mounting medium and samples were kept on the rotating plate until solution was homogeneous. A drop of OCT was placed in a shallow cylinder made of aluminum foil. The sample was embedded in the OCT and then covered completely with OCT. A 6 well plate filled with isopentane (2-methyl butane) was placed in a box filled with liquid nitrogen, bringing the isopentane at its freezing point (-160°C). The cylinder with the embedded sample was then placed within the ice-cold isopentane, until completely frozen. Blocks were then stored at -80°C in 6 well plate until needed.

3.3.3: Sample sectioning

Paraffin embedded samples

Paraffin embedded mouse knee joints and cartilage explants were placed on ice to cool down and serially sectioned at 5µm interval using Leica RM 2135 microtome

(Knowlhill, UK). The sections were then floated on a warm water bath (45^{o} C), and picked up onto Superfrost microscopic slides and allowed to dry on a 70°C hot plate. After few hours, the slides were removed from the hot plate and stored in cardboard boxes at room temperature until use.

Frozen samples

The frozen blocks were equilibrated to the cutting temperature by incubating the blocks overnight in a -20°C freezer and then placing them in the cryostat with adjusting the temperature between -21 and -24 °C. 5µm-thick sections were cut and collected onto Superfrost microscopy slides. Slides were left overnight at room temperature to dry, individually wrapped in aluminum foil, placed in boxes and stored at -80ºC until use. Each slide was allowed to adjust to room temperature before being unwrapped and used.

3.4: Histological and histochemical stainings

3.4.1: Toluidine blue staining

To determine the level reached during sample sectioning, rapid and simple Toluidine blue staining was performed. Slides were dried on a 70°C hot plate for 1 minute, deparaffinized in xylene for 1 minute, dehydrated in 100% ethanol for another minute and washed in water. The section was covered with a drop of Toluidine blue (Appendix) for few seconds, washed in water and visualized under the microscope. The slides were then left to air-dry, cleared in xylene and mounted with DEPEX.

3.4.2: Hematoxylin and Eosin (H&E) staining

To visualize the microscopic structure of the tissues, H&E staining was performed according to the standard protocols. Briefly, paraffin embedded sections were deparaffinized in xylene (2 changes, 5 minutes each), gradually rehydrated in descending grades of ethanol (100%, 70% and 50% ethanol for 5 minutes each) and rinsed with water for 5 minutes. Slides were then placed in jars containing filtered Mayer's Hematoxylin (BDH, UK) for 5 minutes, washed in water and placed in 1% Acid Alcohol for a few seconds. The slides were then washed again in water and placed in Eosin (BDH, UK) for 1 minute. Finally the slides were washed again, dehydrated in ascending grades of ethanol (50%, 70% and 100% for 5 minutes each), cleared in xylene (2 changes, 5 minutes each) and mounted in organic solvent soluble mounting medium (DEPEX).

3.4.3: Safranin O/Light green staining

To stain the highly sulfated, negatively charged glycosaminoglycans in the cartilaginous tissue, Safranin O/Fast green staining was performed on mouse knee joints and human cartilage explants. Slides were deparaffinized and rehydrated as previously described. Sections were then stained in Safranin O (Raymond A. lamb Ltd, UK) for 15 minutes, washed in water, incubated with 0.5% Light green (Raymond A. lamb Ltd, UK) and evaluated every 30 sec for the intensity of counterstain. Slides were washed again in water, hydrated, cleared and mounted in DEPEX.

3.4.4: X-GAL staining

Whole mount X-GAL staining was performed on samples obtained from BAT-GAL and Axin2 KI mice. Tissues were fixed for 1 hours in fixing solution containing 2% Paraformaldehyde and 0.02% glutaraldehyde in PBS, washed twice with PBS and incubated overnight at 30^{o}C in a freshly made staining solution (Appendix) containing the β-galactosidase substrate X-Gal (5-bromo-4-chloro-3-indolyl-beta-d-galactopyranoside). Tissues were then washed with PBS, decalcified, embedded in OCT and sectioned as previously described.

3.5: Histomorphometry

Histomorphometric analysis was done on sections obtained from animals killed one day following the injury. Non-consecutive sections from levels indicated in figure 5.1A were used to evaluate variability within the same animal and between different experimental animals. In this analysis, articular cartilage thickness, cross sectional depth, cross sectional width and cross sectional area of the injury were measured using cell-p software (Olympus, UK). The ratio between the depth of the injury and the cartilage thickness was calculated and represented as percentage value. The coefficient of variation was calculated by dividing the standard deviation by the mean. All the data are expressed as the mean ± standard error of the mean (SEM).

3.6: Histological scoring

The structural outcome of the joint surface injury in mice was assessed using well validated histological scoring systems. Cartilage repair was scored as previously described by Wakitani et al (188). This grading scale is composed of 5 categories with

total score ranging from 0 to 14. The cell morphology was graded from 0 (for repair tissue that looks normal compared to native adjacent uninjured cartilage) to 4 points when cartilaginous tissue was absent. The degree of metachromatic matrix staining was graded from 0 when the intensity of the staining was comparable to normal adjacent cartilage to 3 when metachromasia was completely absent. The surface regularity was scored 0 when more than three-quarter of the surface was smooth to 0 when less than one-quarter was smooth. The average thickness of the cartilage in the defect compared to that of the surrounding normal cartilage was graded 0 when repair cartilage was more than two-third of the surrounding cartilage to 2 when it is less than one-third. The integration of the repair tissue with the adjacent cartilage was scored 0 when no gap was seen between them to 2 when there was a complete lack of integration (Table 3.1).

The severity of OA in mouse articular cartilage and in human cartilage explants was evaluated using Modified Mankin score (238;239). This score is assessing structure giving 0 to normally looking cartilage to 6 when there is completely disorganized structure. Cellular appearance was scored 0 when it is normal to 3 when hypo-cellularity was seen. The intensity of matrix staining was scored 0 when normal to 4 when it was completely absent. Therefore, 0 points indicate normal cartilage, whereas 13 points represents sever cartilage lesions (Table 3.2).

Cartilage damage induced by destabilization of medial meniscus was scored using modified Mankin score and Chambers score (240) in which 0= Normal cartilage 0.5= loss of metachromatic staining without structural changes. 1= roughened articular surface and small fibrillations. 2= fibrillations down to the layer immediately below the superficial layer and some loss of surface lamina. 3= Loss of surface lamina and fibrillations extending down to the calcified cartilage. 4= Major fibrillations and

cartilage erosion down to the subchondral bone. 5= Major fibrillations and erosion of up to 80% of the Cartilage. 6= Severe loss involving more than 80% of cartilage. The medial tibial plateau, medial femoral condyle, lateral tibial plateau and lateral femoral condyle were scored separately. Scores of the four quadrants were then added to obtain the summed score.

Scoring was performed independently by two observers blinded to the group assignment (myself and Dr Dell'Accio). All the data are expressed as the mean ± standard error of the mean (SEM).

Table 3.1: Histological repair grading scale

Category	points
Cell Morphology	
Hyaline cartilage	**0**
Mostly Hyaline cartilage	**1**
Mostly fibrocartilage	**2**
Mostly non-cartilage	**3**
Non-cartilage only	**4**
Matrix staining (Metachromasia)	
Normal (compared with host adjacent cartilage)	**0**
Slightly reduced	**1**
Markedly reduced	**2**
No metachromatic stain	**3**
Surface regularity	
Smooth (>3/4)	**0**
Moderate (>1/2-3/4)	**1**
Irregular (1/4- 1/2)	**2**
Severely irregular (<1/4)	**3**
Thickness of cartilage	
>2/3	**0**
1/3 – 2/3	**1**
<1/3	**2**
Integration with host adjacent cartilage	
Both edges integrated	**0**
One edge integrated	**1**
Neither edge integrated	**2**
Total Maximum score	**14**

Wakitani et al., JBJS, 1994

Table 3.2: Modified Mankin Score

Category	points
Structure	
Normal	**0**
Slight disorganization (Cellular row absent, some superficial clusters	**1**
Irregular surface, including fissures into the radial layer	**2**
Pannus	**3**
Superficial cartilage layers absent	**4**
Fissures into the calcified cartilage layer	**5**
Sever disorganization (Chaotic structure)	**6**
Cellular abnormalities	
Normal	**0**
Hypercellularity	**1**
Clusters	**2**
Hypocellularity	**3**
Matrix staining (Metachromasia)	
Normal	**0**
Staining reduced in radial layer	**1**
Staining reduced in inter-territorial matrix	**2**
Only present in pericellular matrix	**3**
Absent	**4**
Total Maximum score	**13**

Mankin et al., 1971 & van der Sluijs et al., 1992

Table 3.3: Chambers Score

Category	points
No damage	**0**
Loss of metachromatic staining without structural changes	**0.5**
Roughened articular surface and small fibrillations	**1**
Fibrillations down to the layer immediately below superficial layer	**2**
Loss of surface lamina and fibrillations extending down to the calcified cartilage	**3**
Major fibrillations and cartilage erosion down to the subchondral bone	**4**
Major fibrillations and erosion of up to 80% of the cartilage	**5**
More than 80% loss of cartilage	**6**

Chambers et al., 2001

3.7: immunohistochemistry

Paraffin sections were de-paraffinized and re-hydrated by incubating the slides in xylene (2 changes, 5 minutes each), followed by passages in 100% absolute ethanol (2 changes, 5 minutes each), 70% ethanol (2 changes, 5 minutes each) and 50% ethanol (2 changes, 5 minutes each). Slides were then post-fixed with 4% buffered PFA and washed in phosphate buffered saline (PBS). For Antigen retrieval, sections were either boiled in sodium citrate buffer (PH 6) for 10 minutes and then allowed to cool down for 30 minutes at room temperature or treated by proteolytic enzymes. For proteolytic induced Antigen Retrieval, several enzymes were used depending on the antigen to be demonstrated. In pepsin digestion, sections were equilibrated in 0.02% HCL for 15 minutes at 37 °C and then digested in 0.25 mg/ml of Pepsin (sigma UK) in 0.02% HCL for 45 minutes at 37^{o}C. In Chondroitinase ABC digestion, sections were equilibrated in

0.1*M* Tris HCL, pH 8.0 for 15 minutes and then digested in Chondroitinase ABC (Sigma, UK) in 0.1*M* Tris HCL, pH 8.0 for one hour at 37ºC. In Proteinase K treatment, the solution containing the enzyme was pre-warmed at 37°C for 15 min before use and placed on the slides for 5 minutes at 37°C.

After the antigen retrieval step, slides were post-fixed in 4% buffered PFA for 10 minutes at room temperature and washed twice in 0.2% Tween-20 in phosphate buffered saline (PBST). The endogenous peroxidase activity was quenched by incubating the sections with 3% H_2O_2 for 15 minutes to avoid non specific staining if DAB substrate was used for detection. The sections were blocked in 0.5% bovine serum albumin in PBST for one hour at room temperature, blotted and incubated overnight in a humid chamber at 4 °C with a primary antibody (Table 3.4) diluted in an antibody diluent (DakoCytomation, UK). Sections were then washed twice in PBST, incubated for one hour with the appropriate secondary antibody (Table 3.4) and washed twice in PBST.

Pilot titration experiments were run to determine the optimal working dilutions for the primary and secondary antibodies. These dilutions were then used in subsequent experiments. Negative controls were treated with isotype and species matched immunoglobulins or normal serum instead of the primary antibody. The specificity of the Wnt16 antibody was further confirmed by pre-absorbing the primary antibody with a blocking peptide (697 cell lysate form human pre-B lineage leukemia cell line). The antibody was incubated with the blocking peptide at a ratio of 1: 2 for 2 hours at 37°C, centrifuged for 15 minutes at full speed and then applied to tissue sections.

If Avidin-Biotin complex (ABC) was to be used as an amplification system, sections were incubated for 30 minutes with StreptABComplex/HRP (DakoCytomation, UK) and then washed in PBST. Liquid DAB substrate Chromogen system was used as peroxidase

substrate. Slides were washed in PBS and either mounted directly in Mowiol containing 4, 6-diamindino-2-phenylidole (DAPI) for nuclear staining or counterstained with Hematoxylin, and mounted with DPX (BDH, UK). Images were captured using a Nikon digital camera linked to an Olympus BX61 microscope. Images were analyzed with Cell-P software (Olympus UK Ltd, UK). Adobe Photoshop software was used to optimize the images for best rendering.

A complete list of primary and secondary antibodies for detection of various targets used in this study as well as the antigen retrieval methods and colorimetric systems used in each immunostaining is reported in Table 3.4.

Table 3.4: A summary of the immunostainings performed in this thesis

Staining	Antigen Retrieval	Primary antibody	Secondary antibody	Colori-metric System
PHH3	Pepsin Digestion	Rabbit anti human/mouse PHH3 (Cell Signaling) 1:50	Cy™3 conjugated goat anti rabbit antibody (Jackson immunoResearch Laboratories, USA) 1:600	Florescent
CPII	Pepsin Digestion	Rabbit anti human/mouse ***CP II antibodies*** (kindly provided by Dr Lindsay King from IBEX, Canada) 1:800	Cy™3 conjugated goat anti rabbit antibody (Jackson immunoResearch Laboratories, USA) 1:600	Florescent
Col2-3/4C$_{short}$	Pepsin Digestion	Rabbit anti human/mouse C1,2C (Col2-3/4Cshort) (IBEX, Canada) 1:800	EnVision®+Dual Link system-HRP (DakoCytomation, UK)	DAB Substrate Chromogen System (DakoCytomation, UK)
TEGE^{373}	Chondroitinase ABC Digestion	anti-TEGE^{373} (kindly provided by Professor Bruce Caterson and Dr Debbie Tudor, Cardiff University). 1:10	EnVision®+Dual Link system-HRP (DakoCytomation, UK)	DAB Substrate Chromogen System (DakoCytomation, UK)
VDIPEN	Chondroitinase ABC Digestion	anti-VDIPEN (kindly provided by Professor Bruce Caterson and Dr Debbie Tudor, Cardiff University). 1:10	EnVision®+Dual Link system-HRP (DakoCytomation, UK)	DAB Substrate Chromogen System (DakoCytomation, UK)

BMP2	Pepsin Digestion	Rabbit anti human/mouse BMP2 (abcam,UK) 1:20	Biotinlyated sheep anti rabbit (Serotec,UK) 1:100	StreptABCcomplex/HRP and DAB Substrate Chromogen System (DakoCytomation, UK)
PSMAD 1, 5, 8	Boiling in Citrate Buffer	Rabbit anti human/mouse PSMAD 1,5, 8 (Cell signaling, USA) 1:100	Biotinlyated sheep anti rabbit (Serotec,UK) 1:100	StreptABCcomplex/HRP and DAB Substrate Chromogen System (DakoCytomation, UK)
FRZB	Pepsin Digestion	Goat anti human/mouse FRZB (R&D, UK) 1:100	Biotinlyated rabbit anti goat (DAKO, UK) 1:300	StreptABCcomplex/HRP and DAB Substrate Chromogen System (DakoCytomation, UK)
Wnt16	Pepsin Digestion	Mouse anti human WNt16 (BD PharMingen, UK) 1:200	Biotinlyated rabbit anti mouse (DAKO, UK) 1:200	StreptABCcomplex/HRP and DAB Substrate Chromogen System (DakoCytomation, UK)

β- Catenin	Pepsin Digestion	Rabbit anti human/mouse β-catenin (Cell signaling, USA) 1:50	Biotinlyated sheep anti rabbit (Serotec,UK) 1:100	StreptABCcomplex/HRP and DAB Substrate Chromogen System (DakoCytomation, UK)
OPG	Pepsin Digestion	Goat anti human/mouse OPG (Santa cruze, UK) 1:100	Biotinlyated rabbit anti goat (DAKO, UK) 1:200	StreptABCcomplex/HRP and DAB Substrate Chromogen System (DakoCytomation, UK)

3.8. Apoptosis Detection (TUNEL analysis)

Detection of apoptotic cells was performed by coupling the TUNEL assay and the cytological appearance of the cells. DNA fragments that are generated by the cleavage of DNA during apoptosis were detected by the terminal deoxnucleotidyl transferase-mediated dUTP nick-end labeling (TUNEL) using the TACS in situ apoptosis detection kit. In this system, Biotinlyated nucleotides are incorporated into the 3´-OH ends of the DNA fragments by terminal deoxnucleotidyl transferase (TdT). The Biotinlyated nucleotides are then detected using a streptavidin-fluorescein conjugate and positive cells are subsequently visualized using a fluorescence microscope. The TUNEL assay was performed according to the manufactures protocol (R&D systems, UK). Briefly, paraffin sections were de-paraffinized and re-hydrated as described above, washed twice in DNase-free water and then incubated in 1% phosphate- buffered saline (PBS) for 10 minutes. Enzymatic proteolysis was performed by Proteinase K digestion for 10 minutes at 37ºC. Next, sections were washed in DNase-free water and incubated for one minute in TdT Labeling buffer. DNA fragments in apoptotic cells were labeled by incubating the sections in humidity chamber for one hour at 37ºC with labeling reaction mix. The enzymatic reaction was then stopped by placing the slides in TdT Stop buffer for 5 minutes at room temperature. Sections were incubated with Streptavidin-FITC Detection Solution in the dark for 20 minutes, washed in PBS and mounted in Mowiol (Calbiochem) containing 4, 6-diamindino-2-phenylindole (DAPI) for nuclear staining. The fluorescin-stained cells were subsequently visualized using a florescence microscope equipped with a digital camera. For positive control, sections were digested

with TACS-DNase prior to TUNEL assay. For negative control, TUNEL assay was carried using labeling Reaction Mix without TdT Enzyme.

3.9. Gene expression analysis

3.9.1. Total RNA extraction

Adult human cartilage explants and mouse femoral heads were snap-frozen in liquid nitrogen immediately after termination of the culture, powdered with a mortar and pestle pre-chilled in liquid nitrogen and subsequently homogenized in TRIZOL reagent (a mono-phasic solution of phenol and guanidine isothiocyanate) (Invitrogen, UK) using a homogenizer. Articular cartilage from mouse knee joints was directly homogenized in 1ml TRIZOL reagent using a syringe and a 26G needle for 5 minutes. The suspension was then incubated on ice for 20 minutes and spun at 10.000g for 10 minutes at 4 ºC to remove insoluble debris. Chloroform (200µl/1ml TRIZOL) was added and the tubes were shaken for 30 seconds, incubated on ice for 2 minutes and centrifuged at 10.000g for 15 minutes at 4 ºC. Following centrifugation, the mixture separates into a lower red phenol-chloroform phase containing proteins, an inter-phase containing DNA, and a colorless upper aqueous phase containing RNA. The aqueous phase was removed to another sterile, RNAse free tube and 5µg RNase-free glycogen was added and tubes were incubated on ice for 5 minutes. RNA was then precipitated from the aqueous phase by mixing with an equal amount of ice-cold isopropyl alcohol, incubating on ice for 20 minutes and centrifuging at top speed for 60 minutes at 4 ºC. The RNA precipitate forms a gel-like pellet on the side and bottom of the tube. The supernatant is then removed and the RNA pellets were washed once with 1 ml of 70% ethanol, centrifuged

for 5 minutes at 4°C. As much ethanol as possible was removed carefully using a pipette without disturbing the pellet. The pellet was then dried for 15 minutes at room temperature and re-suspended in RNase-free water.

For the human cartilage explants, The aqueous phase was removed to clean tube and equal volume of phenol solution saturated with 0.1M citrate buffer (pH 4.3) (Sigma-Aldrich, UK) was added to each tube, mixed thoroughly, incubated on ice for 30 minutes. Chloroform-isoamyl alcohol 24:1 (2ml) was added to each tube, mixed thoroughly, incubated on ice for 2 minutes and centrifuged at 10.000g for 15 minutes. The aqueous phase was then removed to a clean tube and extraction with phenol and separation with Chloroform-isoamyl alcohol were repeated as prescribed above for 3 times. The aqueous phase obtained after the third separation was collected and RNA was precipitated with isopropyl alcohol (1 hour at 14.000 at 4°C), washed in 70% ethanol in water, dried and suspended in water according to the standard protocol. RNA yield was assessed by spectrophotometry using a NanoDrop spectrophotometer (Labtech, UK).

3.9.2. Reverse transcription PCR

RNA was reverse transcribed to cDNA using the Thermoscript RT-PCR System for First-Strand cDNA Synthesis (Invitrogen, UK). Briefly, 1µg of purified total RNA from each sample was mixed with 1 µl of Oligo(dT)20 Primers (50 µM) and 2 µl of 10 mM dNTP mix and brought to a 12 µl volume reaction with DEPC-treated water in a 0.5ml PCR tube. After brief spinning down in a microcentrifuge, samples were incubated for 5 min at 65°C and samples were immediately cooled on ice. For the final reaction, 8 µl of a master mix containing 1 µl of ThermoScript™ RT (15 U/µl), 1 µl of 0.1 M DTT, 1 µl of RNaseOUT™ Ribonuclease Inhibitor (40 units/µl), 1 µl of DEPC-treated water and 4

µl of 5X cDNA synthesis buffer were added. After mixing and a brief spin down of the tubes, the reverse transcription to cDNA was run in a PCR machine (Applied Biosystems 9700) for 1h at 50°C and the reverse transcriptase was inactivated at 85°C for 5 min. In order to remove the original RNA that could interfere with the quantitative real-time PCR analysis, RNA digestion was performed using 1µl of E. coli RNase H (2 units/µl) at 37°C for 20 min. Finally, the completed cDNA strand was stored at -20°C until used.

3.9.3. Quantitative real time PCR

For quantitative Taqman real-time evaluation of gene expression levels, sequence-specific primers and probes from Applied Biosystems were used (Table 3.6). When using the double-stranded DNA binding dye SYBR green, QuantiTect primer assays (Qiagen, UK) or primers designed using Vector NTI (Invitrogen, UK) were ordered (Table 3.5& 3.6). Primers were designed in parts of the sequence that were unique to the target gene as assessed by running BLAST searches. We aimed at generating amplicons between 100 and 300 base pairs, as close as possible to the poly-A sequence with primers with a GC content between 45 and 65%, a target Tm of 60^{o}C and no more than 1^{o}C of difference between them.

The real-time PCR were run in triplicate on 384-well PCR plates (Applied Biosystems using the 7900HT Taqman Instrument (Applied Biosystems). The thermal cycling conditions used comprised a 2 minutes equilibration step at 50ºC, a 95ºC Taq polymerase enzyme activation step for 10 min, and 40 cycles including a denaturation step at 95 ºC for 15 sec and one step of annealing and extension at 60ºC for 60 sec.

Results were then analyzed using the 7900HT Sequence Detection System Version 2.1 (SDS 2.1).

Relative quantification was measured using the Comparative Ct (Threshold Cycle) method and normalized for the expression of housekeeping gene beta-actin. The ΔCt (Ct of the target gene minus CT of the endogenous control) for each of the triplicate and then the average ΔCt of the triplicates were calculated. To calculate the ΔΔCt, the ΔCt of each sample was subtracted to the chosen reference sample (normal control or untreated sample). The relative quantity was then calculated following the equation $RQ= 2^{-\Delta\Delta CT}$. In order to assess the efficiency of the real-time PCR for each gene, a standard curve was prepared by serial 2^5 dilutions (i.e. 1:1, 1:32 and 1:1024) of the cDNA from a positive control sample. Dissociation curve was checked when SYBR green is used to confirm specificity.

Table 3.5: List of primers used in human articular cartilage

Gene	mRNA Accession number	Primer	Amplicon size	source
hBMP2	NM_001200	F5'CGTCAAGCCAAACACAAACAGCG-3' R 5'CACCCACAACCCTCCACAACCAT-3'	341 bp	Invitrogen
hFRZB	U24163	F 5'GGGCTATGAAGATGAGGAACGT-3' R 5'-ACCGAGTCGATCCTTCCACTT-3'	79 bp	Invitrogen
hWNT16	NM_016087	F 5'- AAAGAAATGTTTCCCTGCCC -3' R 5'-GACATTTTCCATGGGTTTGC -3	106 bp	Invitrogen
hAxin2	NM_004655	F 5'-TACCGGAGGATGCTGAAGGC-3' R 5'-CCACTGGCCGATTCTTCTT-3'	345bp	Invitrogen
hβ-actin	BC014861	F 5'-CACGGCTGCTTCCAGCTC-3' R 5'-CACAGGACTCCATGCCCAG-3'	134 bp	Invitrogen

Table 3.6: List of primers used in mouse samples

Gene	mRNA Accession number	Assay ID	Amplicon size	Source
mAxin 2	NM_015732	Mm01265782_g1	84bp	Applied Biosystems
mWNT16	NM_053116	Mm01168147_g1	107bp	Applied Biosystems
m β-actin	NM_007393	Mm02619580_g1	143bp	Applied Biosystems
mWNT4	NM_009523	QT00104622	134bp	Qiagen
mWNT9a	NM_139298	QT01062250	139bp	Qiagen
mOPG	NM_008764	QT00106757	111bp	Qiagen
mCol2a1	NM_031163	QT01055523	60bp	Qiagen
mCol10a1	NM_009925	QT00144809	148bp	Qiagen
mAggrecan	NM_007424	QT00175364	143bp	Qiagen
m β-actin	NM_007393	QT01136772	77bp	Qiagen

3.10. Tissue culture

Mouse articular cartilage was dissected from the femoral heads of 8-weeks BAT-GAL old male mice by separating the articular cartilage surface from subchondral bone using a scalpel. Samples were obtained in sterile condition and washed twice in Dulbecco's modified Eagle medium (D-MEM/F-12 1:1, high glucose; Invitrogen) containing 10% fetal bovine serum (FBS; Invitrogen), 1mM Sodium Pyruvate (Sigma-Aldrich) and 2× antibiotic-antimycotic solution (Gibco, Invitrogen). Articular cartilage samples were then incubated in sterile Dulbecco's modified Eagle medium (D-MEM/F-12 Invitrogen)

containing 10% fetal bovine serum (FBS; Invitrogen), 1mM Sodium Pyruvate (Sigma-Aldrich) and 1× antibiotic-antimycotic solution (Gibco, Invitrogen). After 6 days, the samples were treated with 100ng/ml of mouse recombinant Wnt3A (R&D, UK) or 0.1%BSA-PBS for one or two days.

3.11. Maintaining and Breeding Wnt16 KO colony

Wnt16 null mice were kindly provided by Prof. Andrew McMahon, Harvard University, USA. In these mice, exon 2 of the Wnt16 gene was excised using cre/loxP technology. They are fertile and apparently phenotypically normal.

3.11.1. Genotyping

Mouse genomic DNA was extracted using Extract-N-Amp™ Tissue PCR Kit (Sigma, UK) according to the manufacturer instructions. Briefly, tissue samples (obtained from ear marking) were incubated in Tissue Preparation Solution and Extraction Solution for 10 minutes at room temperature. The samples was heated to 95 °C for 3 minutes and then mixed with neutralizing solution prior to PCR. An aliquot of the DNA extract is then added directly to the PCR mix supplied within the kit in the presence of Forward primer: 5'-gcggaacccagggcaactggat-3' and Reverse primer 5'-gtatgtcctaccatccccgag-3'. The amplification reaction was performed using an Applied Biosystems GeneAmp PCR System 9700 thermocycler under the following conditions:

10 min at 95°C followed by 40 cycles of a three step PCR

- 30 sec at 95°C
- 30 sec at 55°C
- 30 sec at 72°C

Following amplification, DNA product was separated by 1% agarose gel electrophoresis and visualized with ethidium bromide. To prepare agarose gels, agarose powder was suspended in 1x Tris Acetic Acid EDTA (TAE) buffer (see Appendix), boiled in a microwave for 2 minutes, then 5µl of ethidium bromide was added and the solution was poured into a gel tray where a comb was inserted. After polymerization, the comb was removed and the gel was placed in the electrophoresis tank and covered with 1x TAE running buffer. Samples were loaded into the gel wells. DNA ladder (1Kb Ladder, Fermentas,UK) was used as a reference for molecular weight. Electrophoresis was carried out at 100V (voltage) for 45 minutes. DNA was visualized using a UV light trans-illuminator and examined for the size of bands. Wild-type mice will have 500bp band, Knock-out mice will have 250bp band and heterozygous mice will have both (Fig. 3.3).

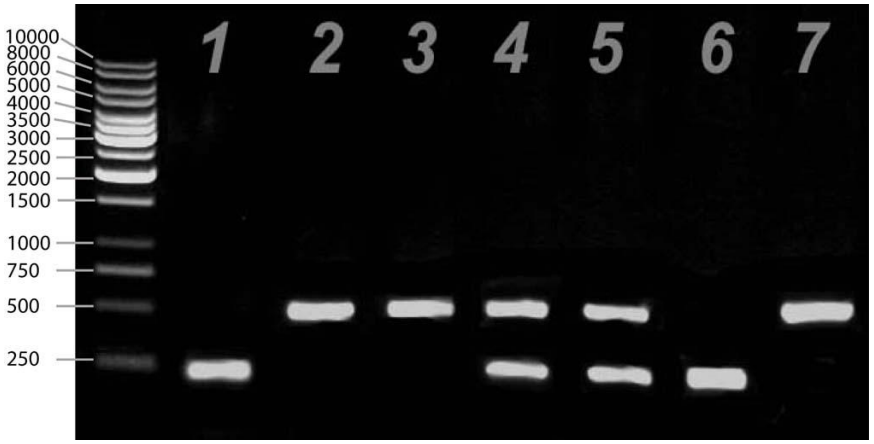

Figure 3.3: Wnt16 mice genotyping: Representative Agarose gel showing different genotypes for WNT16 gene in 7 mice. Mice number 1 & 6 are knock-outs, Mice 2, 3 & 7 are wild-types and Mice number 4 & 5 are heterozygous.

3.11.2. Backcrossing into DBA/1 strain

We originally obtained 2 female wnt16 deficient mutants on a mixed C57/BL6 / 129EvSv background. To transfer the Wnt16 null trait into the DBA/1 background, the mutant mice were backcrossed into the DBA/1 strain. To this end, the female $Wnt16^{-/-}$ mutants were mated with wild-type male DBA/1 mice. From each generation 2 heterozygous females were selected for mating with the wild-type male DBA/1 mouse and the rest of the mice were discarded. With each successive backcross, there is an increase in the percentage of DBA/1 DNA that constitutes to the genome of the offspring as shown in Table 3.7. We aimed at backcrossing 10 times when 99.9% of the DNA will be of DBA/1 origin for the final experiments.

Table 3.7: The residual percentage of 129 DNA remaining after each backcrossing

Generation	129%	DBA/1%
F1	50.00	50.00
N2	25.00	75.00
N3	12.50	87.50
N4	6.25	93.750
N5	3.13	96.875
N6	1.58	98.438
N7	0.78	99..219
N8	0.39	99..609
N9	0.20	99..805
N10	0.098	99..902
N11	0.049	99..951
N12	0.024	99..976
N13	0.012	99..988
N14	0.0061	99.994
N15	0.0031	99..997
N16	0.0015	99.998
N17	0.00078	99..999
N18	0.00038	99..99962
N19	0.00019	99..99981
N20	0.00010	99..99990

3.13. Statistical analysis

The mean histological scores were compared using the Mann-Whitney U test for unpaired non-parametric data. Student's unpaired *t*-test was used for the other comparisons between the two strains. Differences were considered statistically significant when P *was* < 0.05.

CHAPTER 4: RESULTS

Molecular response of articular cartilage to injury

4.1. Genes modulated by mechanical cartilage injury

To explore the early molecular response of adult human articular cartilage to acute mechanical injury at the whole genome level, Dr Dell'Accio, in our Laboratory, performed a microarray analysis on freshly isolated, uninjured and injured cartilage explants in a well validated in vitro model of cartilage injury (Described in Materials and Methods chapter and summarized in Figure 3.2) (241). Using a functional gene clustering algorithm on the differentially modulated genes, we revealed statistically significant clustering of genes encoding signalling molecules, or known to play a role in wound healing, or involved in cell communication, morphogenesis and development including skeletal development (Figure 4.1) (241). This finding suggests that the adult articular cartilage, following injury, deploys a molecular response that involves the release of signalling molecules and morphogens which might have the potential to activate the repair process. Therapeutic targeting of these pathways may improve current protocols of joint surface repair and/or prevent the evolution of post-traumatic OA.

Therefore, we further focused on molecular pathways known to play a crucial role in embryonic skeletogenesis, joint morphogenesis and post-natal homeostasis as well as repair process.

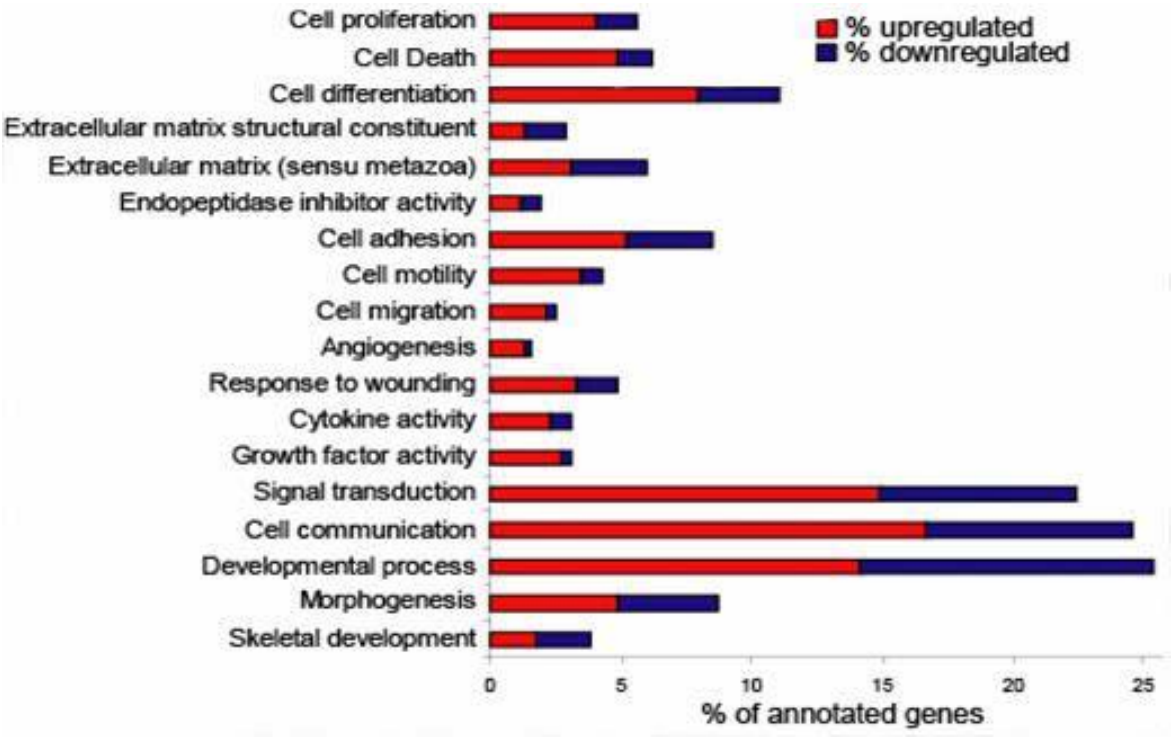

Figure 4.1: Representative clusters of genes differentially expressed following injury to human articular cartilage. Figure from Dell'accio et al., 2008 (241)

4.2. BMP pathway is activated upon cartilage injury in vitro

BMPs are secreted molecules that belong to TGF-β superfamily of morphogens. Upon binding to their ligands, BMP receptors phosphorylate the carboxy-terminal domain of SMAD-1,-5 and -8. Phosphorylated SMADs then translocate into the nucleus where they participate in the transcriptional regulation of target genes (99). BMPs have been implicated in the regulation of stem cell functions and the induction of cartilage and bone formation and therefore have the potential for stimulating cartilage repair (98).

Statistically significant up regulation of BMP-2 mRNA was detected one day following cartilage injury in vitro (Figure 4.2A&C). Several factors can determine the activation of

BMP signalling independently of the expression of one ligand. These include the secretion and the solubility of the ligand, its binding to matrix molecules, the presence of secreted or intracellular inhibitors and receptor regulation. To test whether the observed BMP-2 up-regulation in the explants was associated with downstream activation of the signalling pathway, immunohistochemistry was performed using an antibody that recognizes the phosphorylated form of SMAD-1/-5/-8 (Figure 4.2B). In the freshly dissected explants, 41% of the cells stained positive for Phospho-SMAD-1/5/8 and nearly all positive cells localized in the intermediate layer. In the cultured explants, we detected phospho-SMAD-1/-5-/-8 positive chondrocytes in all cartilage layers in the uninjured as well as the injured explants (83% in the uninjured versus 100% in the injured explants) (Figure 4.2B&C). These results demonstrated that BMP-2 up-regulation following cartilage injury in this explant model is associated with activation of the BMP intracellular signal transduction pathway and that cartilage itself is a target of BMP signaling. The number of Phospho-SMAD positive cells in the rested explants was intermediate between freshly dissected explants and the re-injured explants suggesting that the resting period (6 days) might not be sufficient to completely reverse the molecular response to wounding during the initial dissection of the explants. Consistent with this hypothesis, BMP-2 mRNA levels were lowest in the freshly dissected cartilage, intermediate in the uninjured cultured explants and highest in the injured explants (Figure 4.2C).

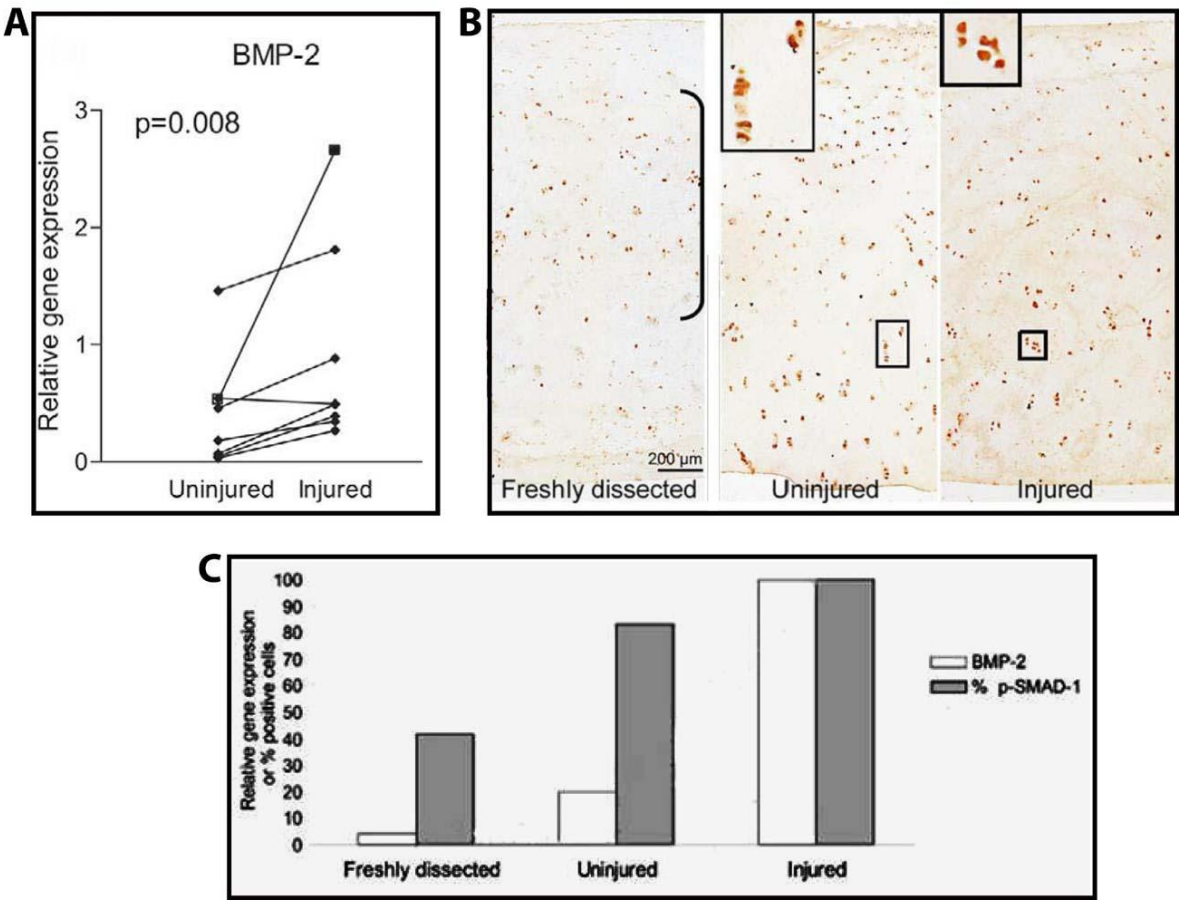

Figure 4.2: Activation of bone morphogenetic protein (BMP) pathway in vitro after cartilage injury: Real-Time RT-PCR comparing the expression levels of BMP-2 mRNA in injured and uninjured cartilage explants (A). Relative gene expression was normalized for the housekeeping gene β-actin. B, Immunostaining for phosphorylated SMAD-1/-5/-8 in freshly dissected normal cartilage (positive cells were mainly seen in the intermediate layer indicated by the bracket), injured and uninjured explants. The top insets are large magnifications of the corresponding squared areas. C, Graphic summary of the proportion of Phospho SMAD-1/-5/-8 positive cells (closed bars) and the expression of BMP-2 (open bars). Values are expressed as percent of positive cells for PSMAD and BMP-2 mRNA.

4.3 Activation of the WNT pathway in adult human articular cartilage following mechanical injury

Wnts constitute a large family of morphogens (19 Wnt ligands) that transduce their signalling through different intracellular pathways. The key event in the activation of the canonical Wnt pathway is the accumulation and the translocation of β-catenin into the nucleus, where it binds to TCF/LEF family of transcription factors, thereby activating transcription of target genes. In the absence of Wnt ligands, β-catenin is instead phosphorylated by a destruction complex and targeted for ubiquitination and subsequent proteolytic destruction through the proteosomal pathway (63).

The microarray differential gene expression screening revealed a striking up-regulation of only one of the 19 known Wnt ligands 24 hours after mechanical injury to human adult articular cartilage: Wnt16. All other Wnts were either not expressed or not regulated. Wnt16, which is known to signal through the beta catenin dependent pathway in a rat chondrocyte cell line RCS (47), was expressed at the lower limit of detection by microarray hybridization in control and freshly dissected cartilage explants but was up-regulated >20 times upon injury. The extracellular Wnt inhibitor FRZB was downregulated following injury and known transcriptional target genes of the β-catenin dependent Wnt signalling pathway such as osteoprotegerin (OPG), c-Myc, cyclin D and axin2 were up-regulated indicating activation of canonical Wnt pathway (Figure 4.3). The differential regulation of FRZB, Wnt16, and Axin2 mRNA following mechanical injury was further confirmed in 8 pairs of samples by quantitative real time RT-PCR (241).

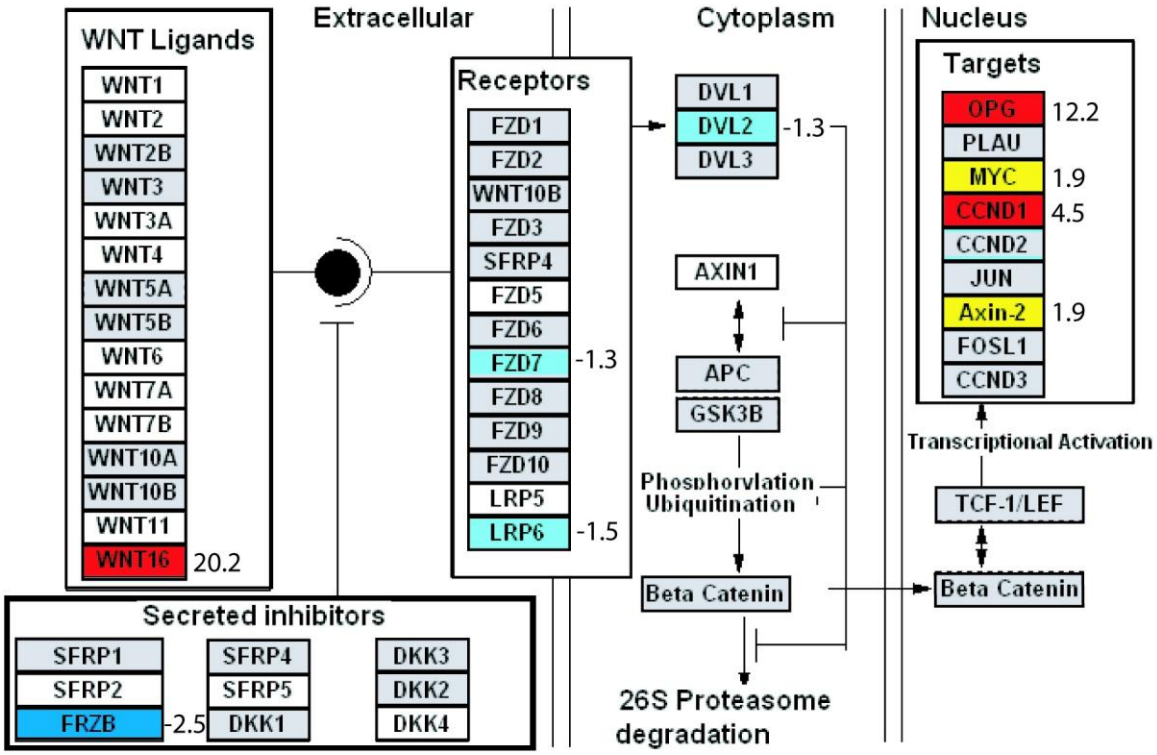

Figure 4.3: Gene modulation within the canonical Wnt pathway in adult human articular cartilage following injury. White boxes indicate genes detectable in <20% of all samples. Gray boxes indicate genes detectable in ≥20% of all samples but with no significant differences between injured and control samples. Red and yellow boxes indicate genes that were significantly ($p \leq 0.05$) up-regulated in the injured explants ≥ 2-fold or 1-2 folds respectively. Dark blue and light blue boxes indicate genes that were significantly ($p \leq 0.05$) down-regulated in the injured explants ≥ 2-fold or 1-2 folds respectively. The average fold change is shown on the right of the boxes. Figure from Dell'accio et al., 2008 (241)

The modulation of these molecules at the protein level was then investigated by immunohistochemical analysis in 3 independent pairs of explants. FRZB was present in both injured and uninjured explants but the proportion of FRZB positive cells was significantly lower in the injured explants compared to uninjured samples (Figure 4.4). Wnt16 protein was undetectable in freshly dissected as well as uninjured explants but

stained intensely in the injured ones. It was also undetectable in preserved areas of the joints with OA but highly detectable in areas with moderate to severe OA, with a territorial expression pattern suggesting that Wnt16 up-regulation takes place in vivo in cartilage pathology (Figure 4.5A).

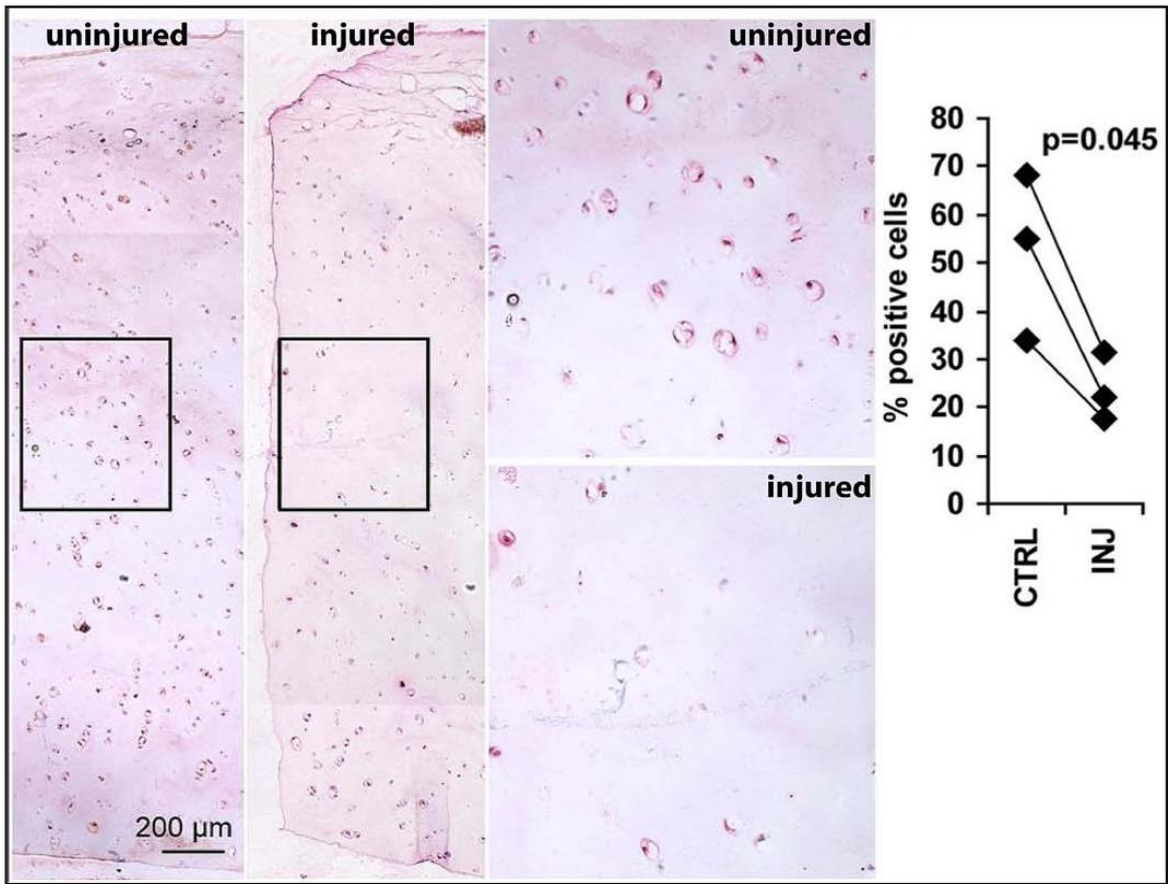

Figure 4.4: immunohistochemical staining for FRZB (red) in uninjured and injured explants 24h after injury. Larger magnification of the boxed area and the percentage of the FRZB positive cells are shown on the right

Wnt16 has been previously shown to signal through the canonical Wnt pathway which is dependent on the accumulation and the nuclear localization of β-catenin (47). To further investigate whether mechanical injury to adult human articular cartilage results in activation of Wnt signalling through the canonical pathway, I performed immunostaining for β-catenin. In the preserved (freshly isolated) and uninjured control samples, cells were either not stained or weakly stained with predominantly cytoplasmic pattern. This pattern is compatible with the known role of β-catenin in cell adhesion, in conjunction with E-cadherin (242). In the injured explants and OA samples, cells were positively stained with strong cytoplasmic and nuclear pattern suggesting accumulation, nuclear translocation and activation of β-catenin dependent Wnt signalling (Figure 4.5B). To further confirm the nuclear localization of β-catenin, I performed immunoflurescence staining for β-catenin and used conofocal microscopy for localization at the sub-cellular level. The cytoplasmic and nuclear pattern of β-catenin staining was confirmed in injured and OA samples (Figure 4.5C). To obtain quantitative comparison, β-catenin positive cells were counted regardless of the intensity of the staining. In the control samples, 46% of cells were stained weakly positive. In the injured samples, 86% of cells stained strongly positive and in the preserved cartilage areas of OA joints, β-catenin was weakly detectable in 23% of the cells and undetectable in most cells. In severely damaged areas, 94% of the cells showed strong nuclear and cytoplasmic staining (Figure 4.5D).

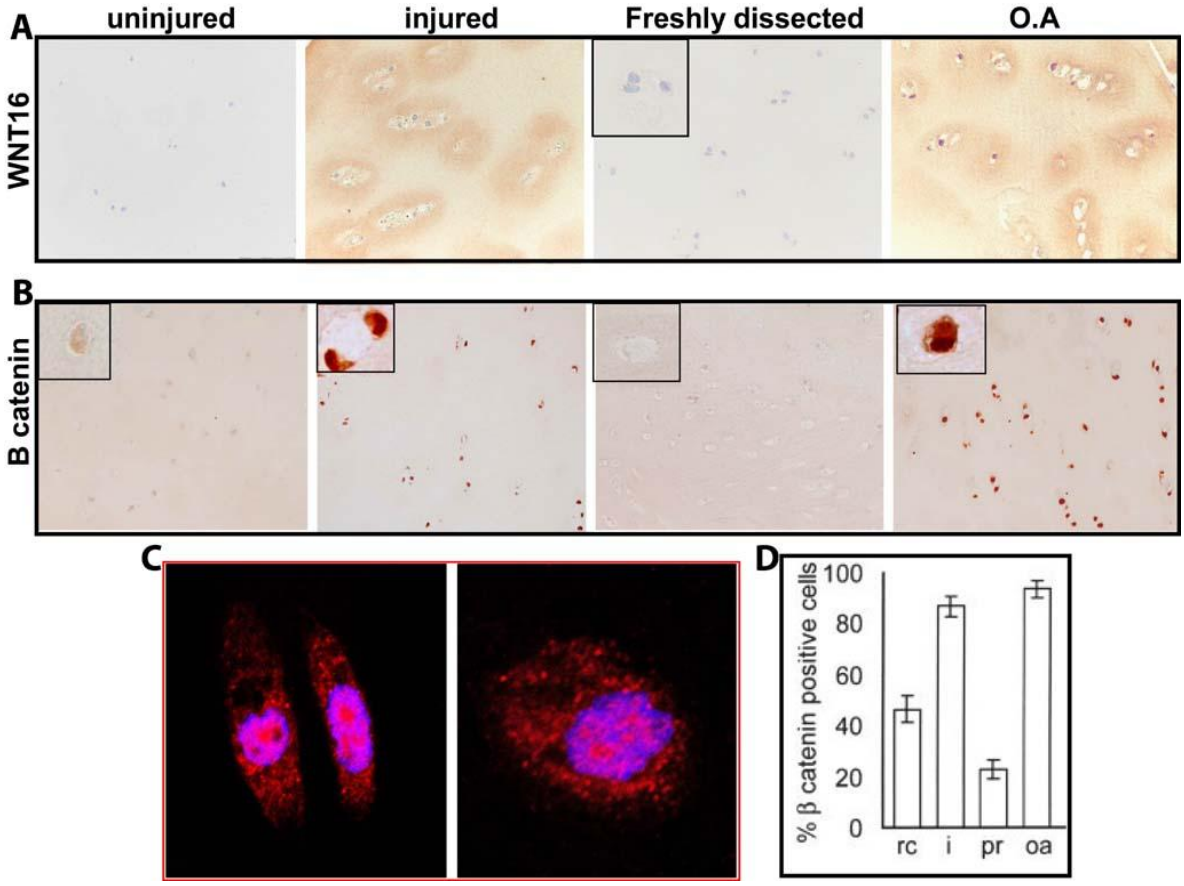

Figure 4.5: WNT signaling in injury and osteoarthritis. A and B, Immunohistochemical analysis of Wnt-16 (A) and β-catenin (B) in uninjured and injured explants, freshly dissected cartilage sample from a preserved joint area, and a cartilage sample from a damaged area of a knee with OA. The inset in A is the blocking peptide negative control for WNT16 obtained by pre-absorbing the primary antibody with Wnt16 before staining. Insets in B are higher magnification views. C, immunoflurescence staining for β-catenin in injured (left) and OA (right) samples imaged with conofocal microscopy demonstrating the nuclear localization of B catenin in OA cartilage. D, the percentage of β-catenin–positive cells in rested controls (rc), injured samples (i), freshly dissected samples from preserved joint areas (pr), and samples from areas with severe OA (oa). Positive cells were counted, regardless of the intensity of the staining, which was very faint in the control and preserved samples, and regardless of the nuclear/cytoplasmic pattern, which was strikingly nuclear in the injured and OA samples. Values are expressed as mean ± SD.

Discussion

Joint surface defects are commonly regarded as irreversible lesions that never heal spontaneously. However, acute full thickness joint surface defects that do not exceed a critical size appear to have repair capacity in animals and humans (141;142;153;236). The repair of these defects involves a coordinated process of patterning and tissue maturation that recapitulates aspects of embryonic skeletal development (153;237), thereby requiring morphogenetic signaling. In this chapter, we have demonstrated that mechanical injury in vitro can elicit the activation of two of the most important signaling pathways involved in embryonic joint development and morphogenesis namely BMP and Wnt signaling. Such modulation of morphogenetic pathways following joint surface injury might thus play a role in the activation of the repair process and in the morphogenesis of the repair tissue. BMPs are known for their anabolic effect on cartilage and therefore, have been proposed as potential therapeutic candidates for joint surface regeneration. Indeed, BMP-2 has been tested in cartilage tissue engineering approaches and although it was capable of promoting repair in an animal model of full thickness cartilage defects (243), its use in knee joints resulted in osteophyte formation and synovial hyperplasia (125;215). Further studies are still necessary to optimize the required dose/delivery system and to ensure their safety for use in cartilage repair.

Wnts have been involved in supporting the repair process in many systems (244-246) through the regulation of stem cell proliferation, migration and fate determination (247). It is thus possible that controlled activation of Wnt signaling would play a similar role in the repair of JSD. However, other previous studies have suggested that abnormal wnt signaling is also implicated in cartilage breakdown and the development of OA

(reviewed in (248)). Therefore, functional studies are necessary to evaluate the role of these molecular activations *in vivo* in the context of cartilage repair/damage.

The *in vitro* culture conditions used to maintain cartilage explants may influence their molecular response to injury, potentially introducing artifacts. In this system, the cartilage explants have already been injured upon dissection and therefore the sensitivity of the *in vitro* system to the re-injury response largely depends on the duration of the initial injury response and on its capacity to subside during the resting period. A period of 6 days was allowed to rest the tissue in culture before being re-injured however; the length of the resting period needed for optimal detection of regulation may be different for different molecules depending on the duration of their up-regulation following injury. For instance, in our experiment, the resting period did not appear to be sufficient to completely reverse the response due to the initial dissection of the explants as the expression level of BMP2 and the number of phospho-SMAD-1/-5/-8 positive cells was intermediate between the freshly dissected explants and the reinjured explants after the resting period. Moreover, the duration of the resting period allowed for the response to dissection to subside before re-injury limited the genes that could be detected to those regulated transiently after injury. This could be one reason for the poor representation of some genes that were expected to be regulated by injury such as those associated with cell proliferation or matrix remodeling.

The finding that Wnt16, which is known to play a redundant role in mouse embryonic joint morphogenesis with Wnt4 and Wnt9a (47), is the only Wnt ligand regulated in this experimental system raises the important biological issue of the specificity and/or redundancy of different Wnt ligands. However, it is possible that *in vivo* Wnt16 might not be the only Wnt ligand modulated by injury as other Wnts can either be produced

from other neighboring tissues within the joint (83;249) or their regulation in the articular cartilage upon injury is not transient and therefore could not be detected in the *in vitro* system. Wnt16 up-regulation was associated with down-regulation of the Wnt inhibitor FRZB, nuclear localization of β-catenin and up-regulation of several Wnt target genes. The functional importance of FRZB regulation in joint homeostasis is underscored by the observations that a single nucleotide polymorphism causing loss of function of the FRZB gene is associated with hip OA in humans (86) and targeted deletion of FRZB gene in mice resulted in an OA like phenotype (88).

Using microarray differential gene expression screening, we have characterized the early molecular events that occur within 24 hours after mechanical injury of adult human articular cartilage. However, it is still important to study the temporal sequence of these events, the hierarchy of different signaling molecules triggered by damage and their role in cartilage homeostasis and repair. The explant culture system relies on isolated articular cartilage and thereby focuses specifically on the cartilage-borne responses to mechanical injury and does not take into account other factors such as the presence of blood in the joint, biomechanical and inflammatory changes after injury or signaling from other joint tissues. The isolation of articular cartilage from its anatomical and functional environment and its exposure to artificial cultural conditions, limits the use of this *in vitro* model to that of a screening system, which however, requires validation in vivo. Given these limitations, the activation of candidate pathways and the expression pattern of the differentially regulated molecules needed *in vivo* validation. The *in vivo* setting was also required to investigate the function of such molecular phenomena.

In the next chapter, I will describe how I addressed these issues by generating and validating a novel joint surface injury and regeneration model in adult mice. The mouse

species was chosen because it is widely validated as a pre-clinical model and especially because it is amenable to genetic manipulation and therefore allows functional molecular studies.

Conclusions

- Morphogenetic signaling pathways such as those involving BMPs and Wnts are modulated in adult articular cartilage in response to mechanical injury.
- Articular cartilage itself is a target for such signaling.

CHAPTER 5: RESULTS

Optimization and Validation of an in Vivo murine model of joint surface injury

In order to confirm *in vivo* the molecular events described in the previous chapter and to test molecular functions in the context of repair, we needed a suitable *in vivo* model of acute mechanical joint surface injury/repair. Ideally, such model should be: (1) consistent and reproducible, (2) amenable for biological and biochemical quantification, (3) amenable for molecular analysis, (4) offer the opportunity for genetic modification. The short reproductive cycle of the mouse, ease of handling, the similarity in development and pathophysiology to humans and most importantly the ability to generate genetically modified animals made the mouse the species of choice for the *in vivo* model.

5.1. Generation and optimization of joint surface injury in mice

We decided to induce the defect in the patellar groove because the articular cartilage in this area is well exposed after patellar dislocation and thus easily accessible. In addition, it is clinically relevant as the patellar articular surface was one of the most common locations for joint surface lesions in humans (43.3%) (132;133), and the most challenging to repair with conventional methods (171). To generate a full thickness joint surface defect (JSD) in mouse patellar groove, we generated a simple device formed of a 26G needle with a glass bead placed approximately 200μm from the tip of the needle which helps in running the device longitudinally in a straight line within the patellar groove as indicated in figure 3.1D.

To optimize the surgical procedure and to validate the consistency and the reproducibility of the defects, a preliminary set of experiments were performed on mouse cadavers. Following the generation of the defects, the knee joints were decalcified, embedded in paraffin and coronally sectioned (Figure 5.1A) to measure and

compare cartilage and defect histomorphometric parameters in terms of cartilage thickness, depth, cross-sectional width (CSW) and cross-sectional area (CSA) of the JSD (Figure 5.1)

Using this approach, we identified an interval (between plane A and C) in which the articular cartilage was of uniform thickness and the defect was consistent, reproducible and full thickness (figure 5.1B-E). Within this interval, the growth plate intercepted the plane of cutting in four points providing a useful landmark for section level (plane A and C) where A is 100μm proximal to the inter-condylar notch, plane B is 100μm proximal to plane A and plane C is 100μm proximal to plane B (figure 5.1A). Outside this interval, the articular cartilage thickness varied as it gradually decreased towards the diaphysis of the femur resulting in different types of injury (Figure 5.1B-E). Therefore, all further analysis was done using sections from within the A-C interval.

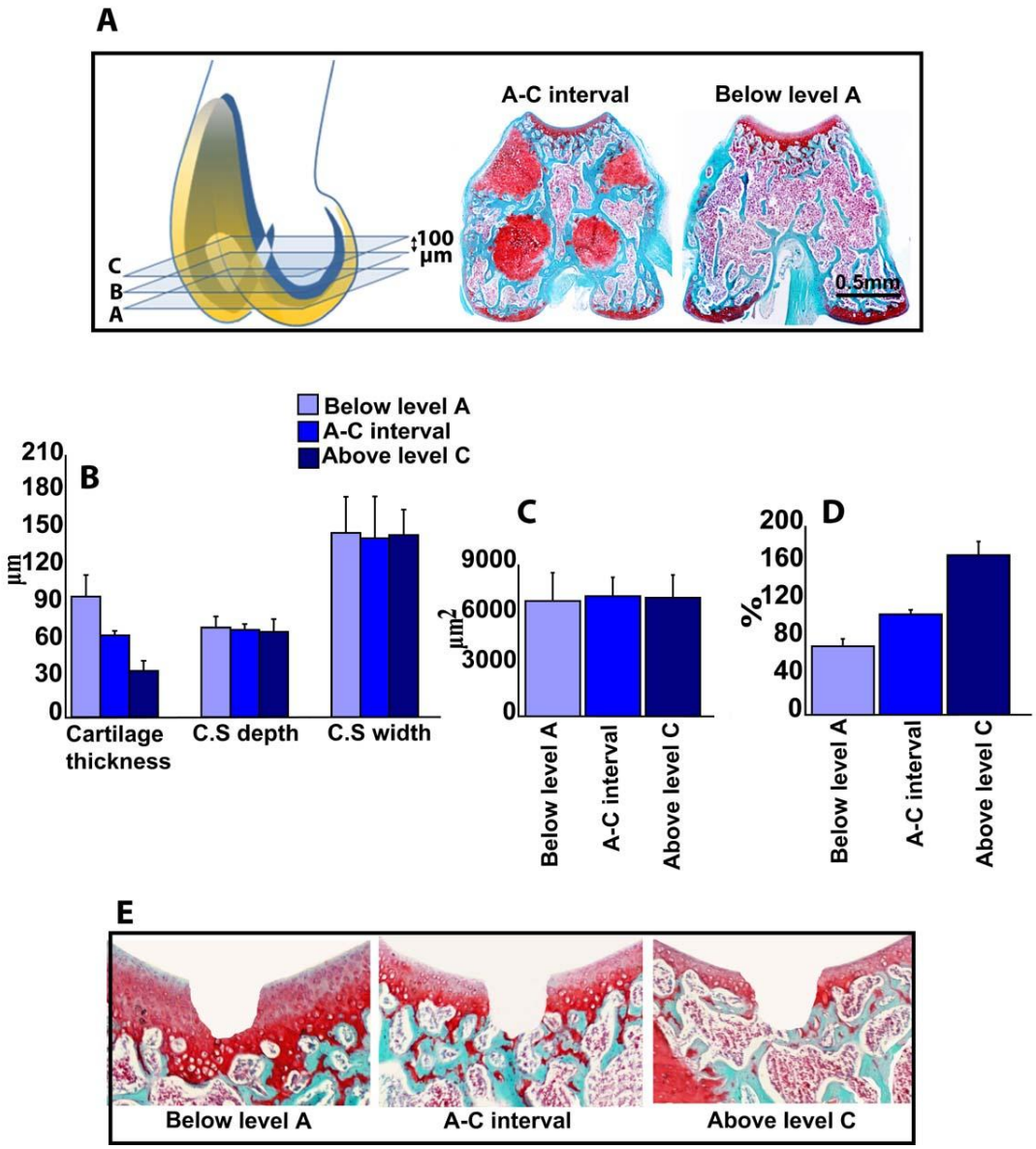

Figure 5.1: Optimization of joint surface injury in mice (A) Schematic representation of a mouse knee joint (articular cartilage in yellow and the growth plate in blue). All the sections comprised between A and C intersects the growth plate in 4 points (section A-C on the left). This landmark is absent in sections outside this interval (Section on the right). B-D Histomorphometric measurements of cartilage thickness, depth and cross sectional width of the defect (B), cross sectional area (C) and the percentage of defect depth to cartilage thickness (D) below level A, within A-C interval and above level C of injured knee joints obtained from mouse cadavers (n=3). All the values are expressed as mean ± standard error of the mean (SEM). E is Safranin O/light green staining of representative sections from the three different levels of injured mouse knee joint.

5.2. Reproducibility and consistency of JSD in different strains of mice

A second set of experiments was done in vivo using different strains of mice to histologically evaluate the nature, the extent of the injury and to assess the reproducibility and the consistency of the experimental JSD. The same histomorphometric parameters of cartilage thickness and injury size were then measured and compared limiting the analysis to A-C intervals within the patellar groove of each mouse (Table 5.1). The thickness of the articular cartilage within the analyzed interval was comparable in C57BL/6 and DBA/1 mice but significantly higher in MRL/Mpj mice (figure 5.2.A). Depth, CSW, and CSA of the defects were very consistent and highly reproducible within the same joint, and across different mice with no statistically significant difference between all the strains analysed (Figure 5.2.A and B). Importantly, in all operated C57BL/6 and DBA/1 mice, the defects were consistently full thickness within the analysed interval. However, the joint surface injury induced in MRL/Mpj was partial thickness due to the relatively higher thickness of the articular cartilage (Figure 5.2.C &D) and therefore, they were excluded from any further analysis.

The variability within A-C interval in C57BL/6 and DBA/1 mice was further evaluated calculating the coefficient of variation (in percent) for each histomorphometric parameters and confirming the consistency of JSD (Table 5.1). In addition, only within this interval, sections intercepted the epiphyseal growth plate in 4 points (Fig 5.1A), thereby providing a landmark recognizable on histological sections further confirming the accuracy of the stringent sampling protocol which allowed a remarkable level of consistency.

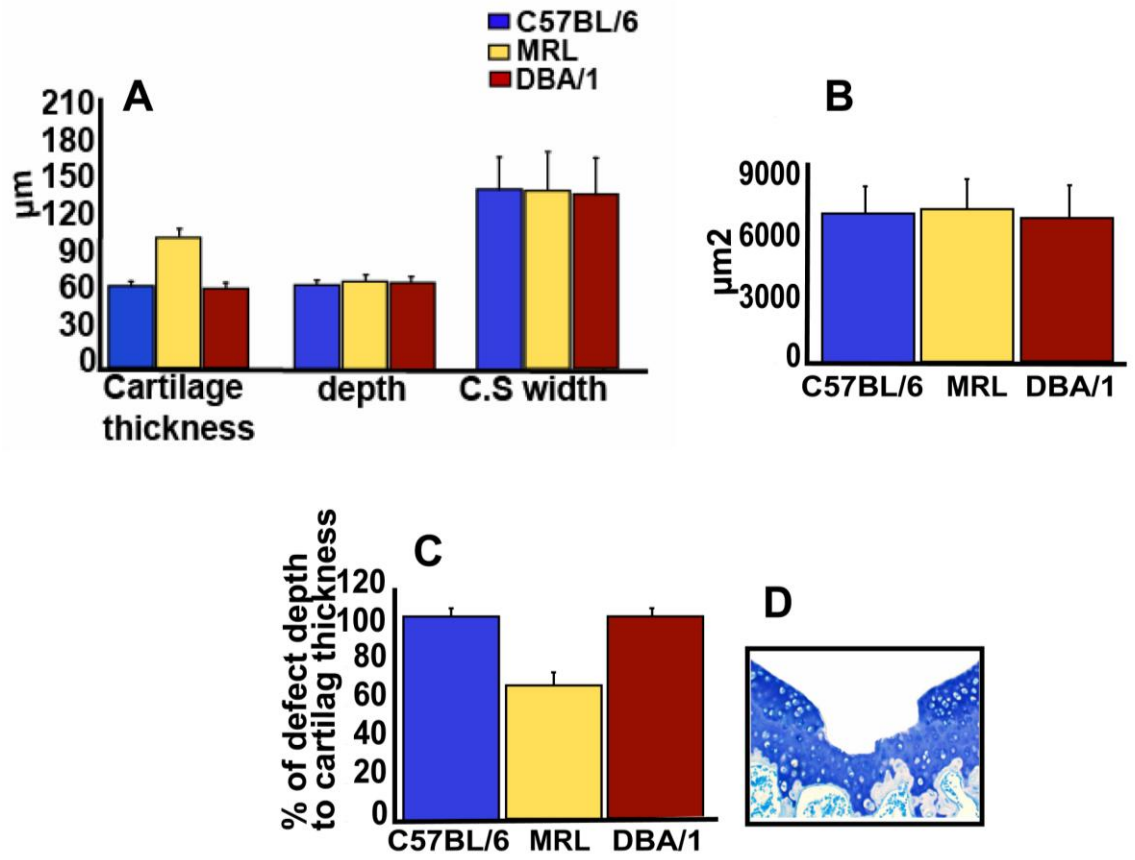

Figure 5.2: Consistency and reproducibility of surgically induced full thickness defect. Histomorphometric measurements of cartilage thickness, depth and cross sectional width of the defect (A), cross sectional area (B) and the percentage of defect depth to cartilage thickness (C) within A-C interval in C57BL/6 (n=9), MRL/MPJ (n=5) and DBA/1 mice (n=5). D, Toluodine Blue staining of section MRL/Mpj knee joints after injury. All the values are expressed as mean ± standard error of the mean (SEM).

Table 5.1: The mean and the standard error of the mean (SEM) of histomorphometric measurements

	Depth	Cross Sectional Width	Cross Sectional Area	% of defect depth to cartilage thickness
C57BL/6	**69.78 ± 4.33µm CV=6.4%**	**149.55 ± 26.29µm CV=19%**	**7302.4 ± 1258.05µm^2 CV=18.9%**	**106.37% ± 4.28**
DBA/1	**70.36 ± 3.84µm CV=5.3%**	**141.31 ± 29.37µm CV=22.3%**	**6988.2 ± 1541.56µm^2 CV=23.3%**	**104.64 %± 2.58**

CV= coefficient of variation

5.3. Structural outcome of joint surface injury in different mouse strains

Having optimized an injury model which is reproducible in two different mouse strains, this allowed a comparison of the outcome between these strains. The scope of this experiment was to investigate whether there is a genetic component in the capacity to repair joint surface defect and to identify a strain that has good repair capacity. This would therefore enable the use of the model to study the role of specific genes in joint surface repair and their influence in outcome determination. The outcome of joint surface injury was then compared in C57BL/6 and DBA/1 strains, because of their well known differences in skeletal biology (250) and in their susceptibility to OA in surgically induced joint instability model (DMM) (26).

The histological time course analysis showed no difference between the two adult strains one day after injury as evaluated by histomorphometry (Figure 5.2) and histology (Figure 5.3A). At 1 week time point, undifferentiated spindle shaped cells partially filled the defects in DBA/1 mice. By 4 weeks, the tissue filling the defects in DBA/1 mice consisted of chondrocytes surrounded by Safranin O stained matrix. However, this repair tissue lacked the typical architecture of normal articular cartilage as the superficial, intermediate, and deep layers were not morphologically distinguishable and the bone front had not reached the level of the osteochondral boundary as in the surrounding cartilage. After 8 weeks, there was a complete filling of the defects with well organized Safranin O positive hyaline-like cartilage (Figure 5.3A). Polarized light microscopy showed continuity of the collagen network between repair tissue and original cartilage,

thereby indicating integration; however, superficial irregularities and fibrillar discontinuity were sometimes observed (Figure 5.3B).

In contrast, the lesions induced in C57BL/6 mice healed poorly as undifferentiated fibroblast-like cells invaded only the bottom of the defects four weeks after injury. At later time points, defects were partially filled with thin cancellous bone covered by a superficial layer of fibrous tissue (Figure 5.3A). In addition C57BL/6 mice displayed progressive features of OA in the articular cartilage of the patellar groove as early as 1 week after injury. Initially, these features included small hypo- or a-cellular areas, surface fibrillation and faint Safranin O staining adjacent to the experimental defect. Subsequent progression included cluster formation, clefts, focal lesions and loss of Safranin-O metachromasia. Later on, these features extended to cartilage areas far from the experimental injury (Figure 5.3C).

At all time points analyzed, no histological differences in the articular cartilage of the patellar groove were detected within the interval analyzed between the sham operated and non-operated controls from both strains as evaluated by H&E and SO staining (Figure 5.3).

The number of mice analyzed at different time points is shown in table 5.2

.

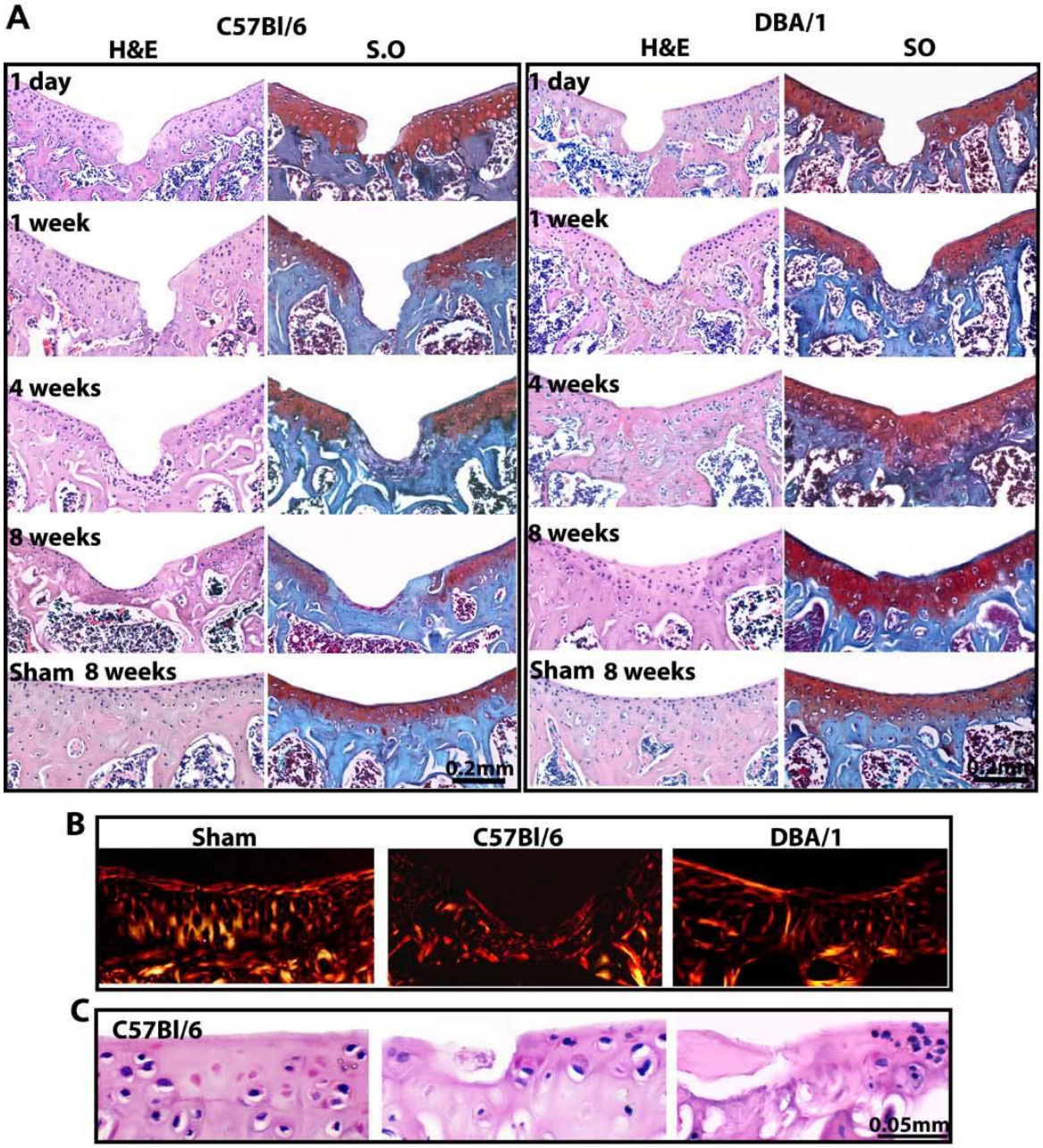

Figure 5.3: Time course histological analysis after joint surface injury. A, H&E (left) and Safranin O (right) staining of sections from sham operated and injured joints of 8 weeks old C57BL/6 and DBA/1 mice at the indicated time points. B, Polarized light microscopy of sections from sham operated, injured C57BL/6 and DBA/1 mice 8 weeks after surgery. C, Higher magnification of H&E stained sections from injured C57BL/6 showing areas away from the experimental lesion with various degrees of OA.

Table 5.2: The number of mice killed per time point

Strain	Age	No. of animals	Time point
DBA/1	8 weeks	15	8 weeks
C57Bl/6	8 weeks	15	8 weeks
DBA/1	8 weeks	5	1 day
C57Bl/6	8 weeks	5	1 day
DBA/1	8 weeks	5	1 week
C57Bl/6	8 weeks	5	1 week
DBA/1	8 weeks	5	4 weeks
C57Bl/6	8 weeks	5	4 weeks

5.4. Quantitative assessment of cartilage injury outcome

The main aim of generating a mouse model of joint surface injury was the use of the model in investigating the function of individual molecules using mouse genetics. Therefore, quantitative outcome measures are needed to easily compare mutant strains and wild type littermates. Two well validated histological scoring systems (188;238;239) were applied in the mouse model to assess the quality of cartilage repair tissue and the degree of osteoarthritis in DBA/1 and C57BL/6 mice at four and eight weeks time points as previously described in Materials and Methods chapter. The repair scores in DBA/1 mice were statistically significantly lower (indicating better repair) than C57BL/6 at 4 and 8 weeks after injury (Figure 5.4A). The modified Mankin score confirmed the absence of OA features in DBA/1, similar to uninjured and sham controls, whereas C57BL/6 developed OA already at 4 weeks after injury (Figure 5.4B).

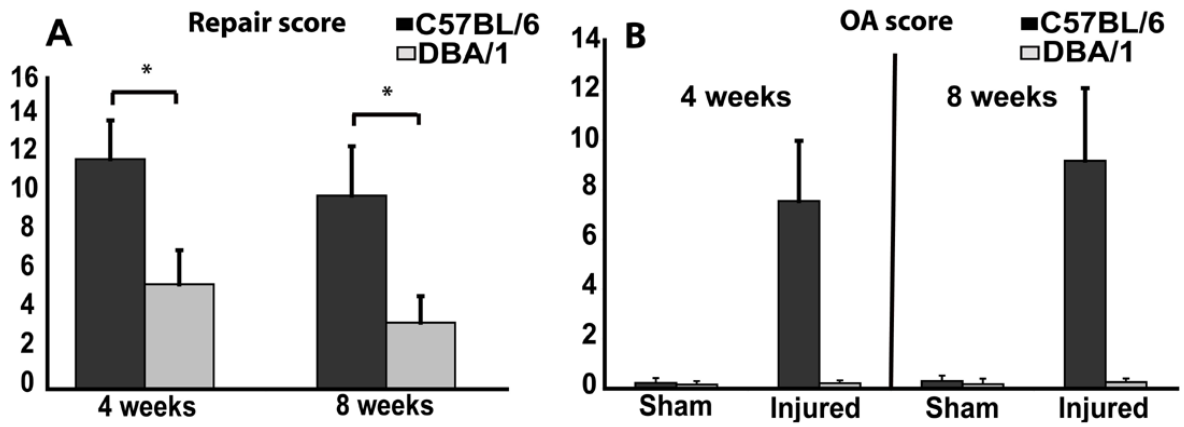

Figure 5.4: Quantitative assessment of cartilage injury outcome. Repair score (A) and modified Mankin score (B) at 4 (n=5) and 8 (n=15) weeks time points. Low score in (A) indicated better repair and high score in B indicated more severe OA. All the values are expressed as mean ± standard error of the mean (SEM). * = $P<0.05$.

5.5. The outcome of joint surface injury in aged mice

Age is a factor influencing the outcome of JSD in humans (143;251) and animal models (148) with older individuals being less likely to have spontaneous healing. To investigate the effect of ageing, we challenged 8-month old C57BL/6 and DBA/1 mice in this model. Aged animals from both strains reproducibly failed to repair the defect. However, whereas C57BL/6 mice developed severe diffuse knee OA, DBA/1 mice did not show any sign of OA at any time points analyzed (Figure 5.5) suggesting that the failure of repair alone might not be the main cause for OA development and that the two processes might be uncoupled.

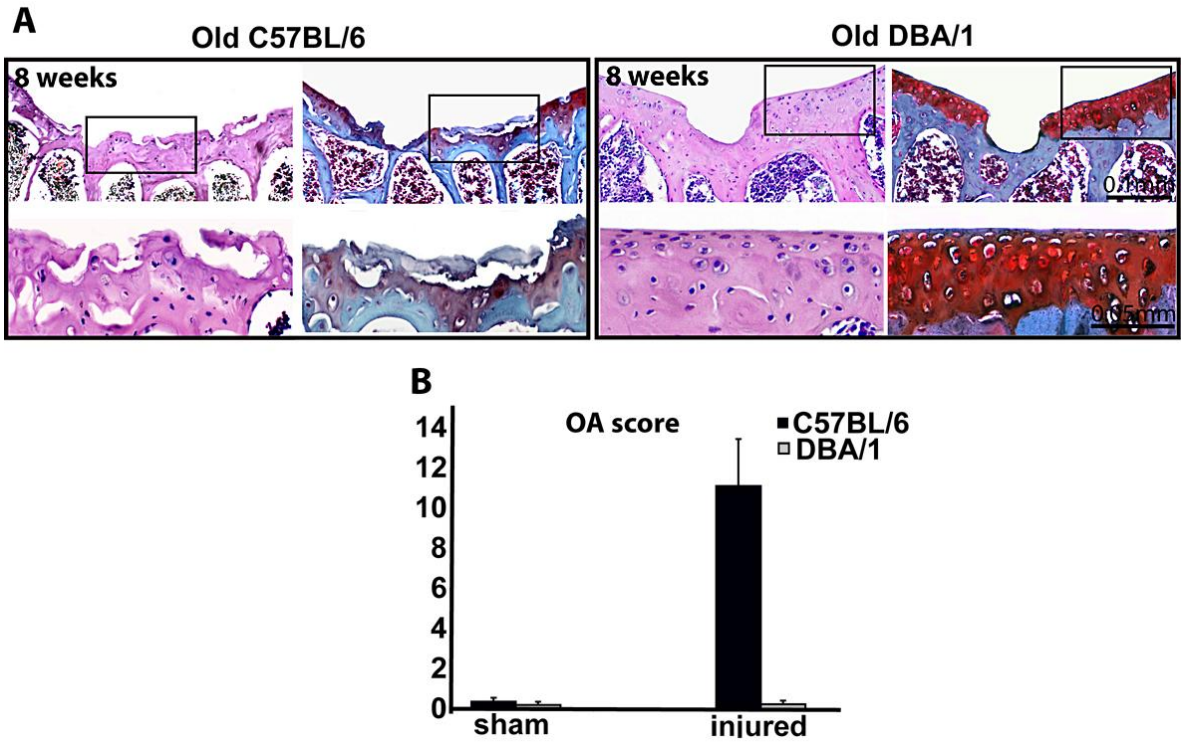

Figure 5.5: Structural outcome in aged mice. A, H&E (left) and Safranin O (right) staining of sections from injured joints of 8 month old C57BL/6 and DBA/1 mice 8 weeks after surgery. The lower panel shows higher magnification of the areas squared in the upper panel. B, modified Mankin score at 8 weeks time points (n=15).All the values are expressed as mean ± standard error of the mean (SEM).

Discussion

In this chapter, we have developed and validated a murine model of cartilage regeneration in which the outcome of joint surface injury is strain and age dependent. Since the repair of JSD depends largely on their size and depth (143;149;251), the reproducibility of the injury in our model was an important concern that was successfully addressed with a rigorous sampling technique. A high reproducibility and consistency of the injury was achieved by combining a well controlled sampling technique within a selected anatomical area and the design of a simple and reliable device to induce the injury. Importantly, all the defects were full thickness in all C57B/6 and DBA/1 mice and slightly deeper than 100% of the cartilage thickness. Such consistency was largely ensured by the resistance offered by the subchondral bone, the resilience of the 26 gauge needle used to make the device, and the presence of the glass bead which by adapting to the concavity of the patellar groove, allowed the tip of the needle to run reproducibly in the centre of the patellar groove.

In this model, the full thickness injury in adult DBA/1 mice resulted in consistent regeneration of articular cartilage as early as four weeks after creation of the defect with further maturation of the repair tissue at the 8 weeks time points. However, long term studies are still needed to evaluate the durability of this repair tissue. In contrast, age matched C57BL/6 mice displayed poor repair response and developed features of PTOA. This observed difference in the healing capacity between the two strains of mice mirrors the different repair capacity of human individuals and suggests that joint surface defects may trigger a cascade of events that will ultimately results in either joint repair

or failure. These events could be probably initiated and controlled by genetically determined programs.

The time course histological analysis showed that non differentiated spindle-like cells filled the lesions in DBA/1 mice at 1 week whereas in C57BL/6, morphologically similar cells appeared in the defects after 4 weeks when chondrogenesis had already occurred in DBA/1 mice. This delay in populating the wound could be due to differences reported in proliferation rate, cell surface epitopes and differentiation potential between bone marrow mesenchymal stem cells (MSCs) isolated from C57BL/6 and DBA/1 with higher chondrogenic potential of DBA/1 MSCs (252). Additional potential mechanism could be a delayed activation/migration of mesenchymal progenitors in response to cartilage signals released by injured cartilage. In the previous chapter (Chapter 4), we have demonstrated that genes encoding morphogens and other signaling molecules are activated in human adult articular cartilage after mechanical injury. Failure of either the cartilage to deploy such response to injury or the mesenchymal progenitor/stem cells to respond to such signaling molecules may contribute to the delay of C57BL/6 mesenchymal cells in filling the defect and thus to the poor repair outcome.

In addition to the poor repair observed in C57BL/ mice after joint surface injury, they also displayed progressive degradation of the surrounding articular cartilage. No signs of OA were seen in any of the control or sham-operated joints and thus it is unlikely that these OA features developed spontaneously or as a result of joint instability induced temporarily during surgery. The secondary OA development after cartilage injury in C57BL/6 mice might be one of the reasons for repair failure. It is unclear whether the two processes are causally related or they represent two distinct processes. The outcome of joint surface injury in old DBA/1 mice where neither repair nor OA were observed

suggests that these two processes might be, at least in part, uncoupled as the repair failure in these mice did not lead to secondary OA development and the absence of OA did not promote the regenerative process. In humans, 30% of JSD that have been detected in healthy asymptomatic individuals remained stable during the 2 year follow-up study without any further worsening or evidence of repair (143). These data in humans and animals suggest that the mechanisms responsible for the restoration of joint homeostasis and prevention of PTOA development after injury might be different from those initiating and promoting endogenous repair. However, the relationship and the importance of these processes for one another are not clearly defined.

It is well established that with age, the regenerative potential of most tissues deteriorate due to a combination of age-dependent changes in the tissue itself, in the local progenitor cells and in the environmental cues that participate in tissue homeostasis and repair. In our study, aged mice from both strains completely failed to repair the defect even with a scar tissue. Aging is known to induce structural, molecular, cellular and mechanical changes in articular cartilage that involve age related decline in the proliferative and anabolic response of chondrocytes to growth factor stimulation as well as reduction in the levels of growth factors (11). These changes may adversely affect the attempt to repair the articular cartilage and contribute to the risk of its degeneration by decreasing the ability of the cells to maintain and repair the tissue. However, it is still necessary to investigate the earlier events that were associated with this repair failure in aged animals and to better understand how the age related changes can influence the ability of the tissue to preserve and restore itself.

The different repair outcome seen in DBA/1 and C57BL/6 mice after the induction of joint surface injury has provided the opportunity to investigate and compare the events

that might take place differently in the two strains and thus help in identifying factors that may participate in outcome determination. The next chapter describes a systematic time point analysis of the events associated with joint surface damage and subsequent repair / OA development.

Conclusions

- We have generated and validated a consistent and reproducible in vivo murine model of joint surface injury and repair with strain and age dependent outcome.
- The model is amenable to outcome quantification, and genetic manipulation. This will give the opportunity to study the function of individual molecules/genes in the context of adult joint surface healing/degeneration.

CHAPTER 6: RESULTS

Characterization of the injury response in young C57Bl/6 and DAB/1 mice

In the previous chapter we have described the generation and validation of a novel in vivo murine model in which the outcome of joint surface injury is strain dependent. Chondrocyte apoptosis, proliferation and ECM remodelling have been described in previous literature to be associated with JSI in humans and animal models (223;253). To investigate and better understand the reasons for the different healing outcome in DBA/1 and C57BL/6 mice, we have monitored and compared aspects of these features *in vivo* in a time course analysis.

6.1. Apoptosis

Apoptosis has been associated with acute cartilage injury (220;223) and with OA (254). Hence Apoptosis has been often proposed as a pathogenic mechanism of cartilage breakdown in OA (255). In the injured joints, apoptotic cells were identified in the proximity of the injury and at the edge of articular cartilage at day one in young mice of both strains (Figure 6.1.A). In consecutive H&E stained section, pyknotic nuclei were present in the same areas (Figure 6.1.C). In subsequent time points, chondrocyte apoptosis in DBA/1 mice progressively decreased and nearly disappeared at 4 and 8 week time points (Figure 6.1A&B), whereas in C57BL/6 mice, after an initial decrease, apoptosis persisted, mainly around areas of cartilage degeneration, with statistically significant difference to DBA/1 mice (Figure 6.1.A-C). In the articular cartilage of the sham and non-operated knee joints, we did not detect any TUNEL-positive cells at any time points analyzed (Figure 6.1A).

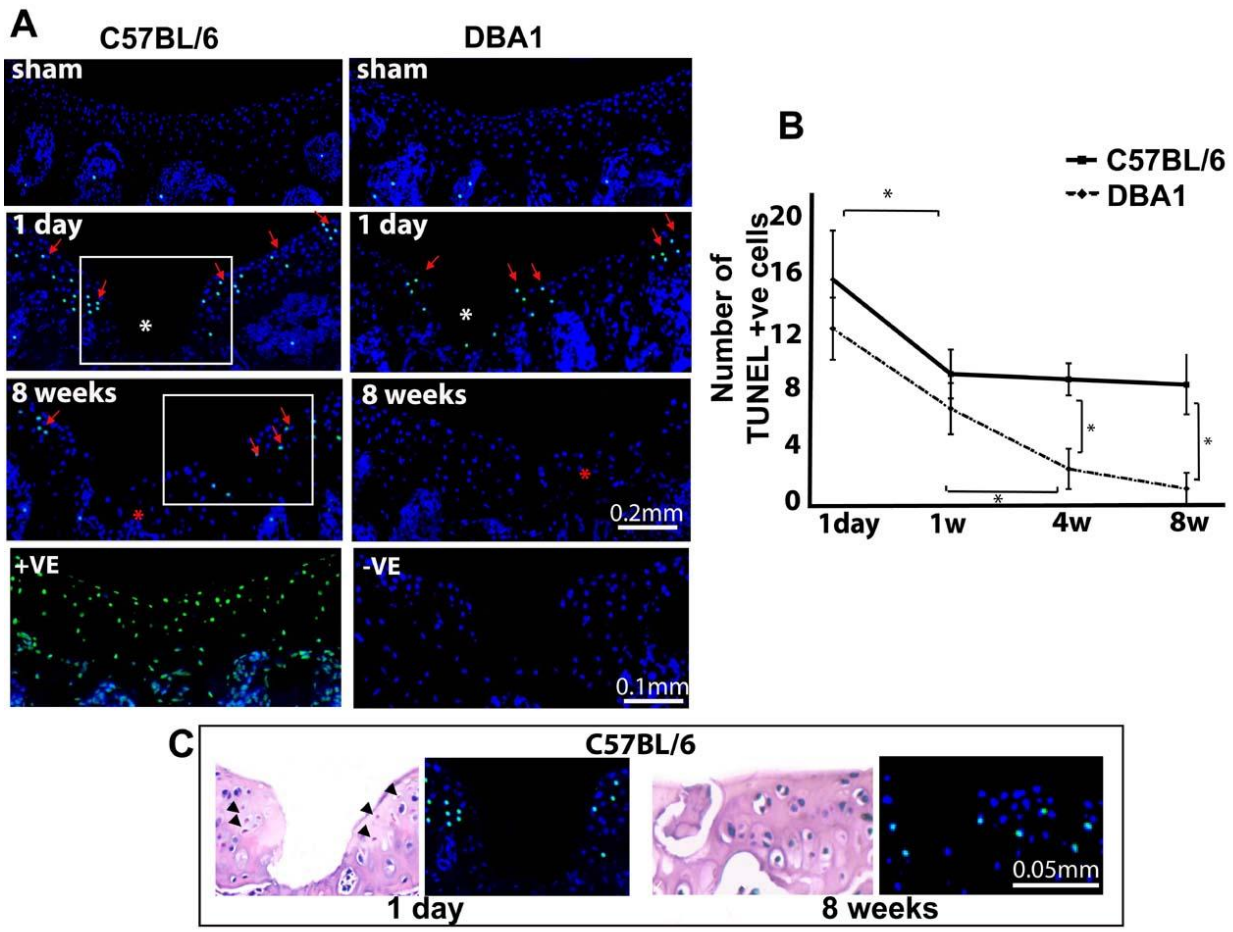

Figure 6.1: Cell death. A, TUNEL assay in sham-operated and injured joints of young mice at 1 day and 8 weeks after injury as well as the positive and negative controls. Red arrows indicate apoptotic nuclei (green). Nuclei are counterstained with DAPI (blue). The asterisk indicates the injury site. B, Numbers of apoptotic cells at different time points comparing both strains. The values are expressed as mean and standard deviation of 3 different operated mice using 3 sections from each joint.*=$P<0.05$. C, higher magnification of the areas squared in (A) at 1 day and 8 weeks time points respectively, and H&E staining of a consecutive section. Pyknotic nuclei are indicated with black arrowheads.

6.2. Proliferation:

To investigate whether mechanical cartilage injury can induce cellular proliferation within the joint, an antibody against phosphorylated Histone H3 (PHH3) was used to detect cells in the mitotic (M) phase of the cell cycle (256). Although chondrocyte proliferation has been reported to take place following injury (223;257), we only detected scattered proliferating cells within the repair tissue at 1 and 4 weeks following injury in DBA/1 mice but not in the articular cartilage adjacent to the injury in either of the two strains (Figure 6.2A&B). The synovial membrane of both strains also exhibited cells undergoing proliferation only at the one week time point with no statistically significant difference between the 2 strains (Figure 6.2C&D). No proliferating cells were identified either in the articular cartilage or in the synovial membrane of sham operated or non-operated controls.

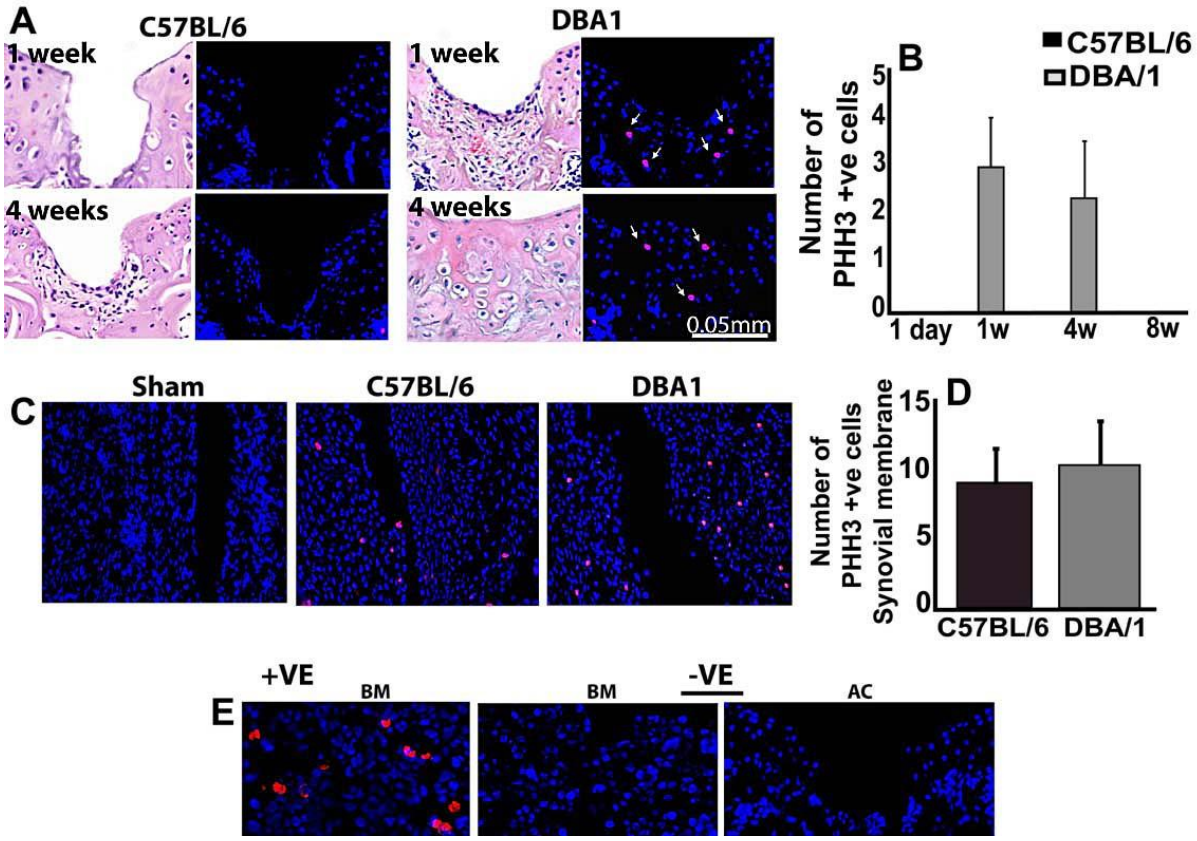

Figure 6.2: Cell proliferation. Phosphohistone H3 immunoflurescence and H&E staining of a consecutive section at 1 and 4 weeks time points (A). White arrows indicate Proliferating cells (red). Nuclei are counterstained with DAPI (blue). The numbers of proliferating cells counted in the articular cartilage of 3 mice using 3 sections from each joint are shown as mean and standard deviation (B). PHH3 immunoflurescence (C) and the count of the positive cells in the synovial membrane (D) at one week time point. As positive control we chose bone marrow areas in which there were several proliferating cells and negative control (E) was section treated with isotype matched non immune antibodies the primary antibody. BM=Bone marrow and AC= Articular cartilage.

6.3. Synovitis

Synovitis is not only a feature of inflammatory arthritis, but also takes place in OA and following trauma (258). Persistent high grade synovitis is a main feature of destructive arthritis in which synovial inflammation causes joint surface damage (94). On the other hand, synovium-residing progenitor cells have been postulated to take part in the repair of JSD (259). It is well known that persistent local inflammation inhibits repair in several systems (260;261), and therefore, a different degree of synovitis or its persistence might have been a determinant factor in the outcome of joint surface injury. Synovitis was quantified by histomorphometric analysis measuring the area of the synovial membrane in control, sham operated and injured joints in the two strains. All operated joints (sham and injured) from both strains exhibited transient synovial hyperplasia that was observed at the one week time point and resolved by the 4 weeks time point (Figure 6.3A&B). Although this analysis is incomplete, still it provides an idea of the inflammatory component of the injury reaction. The synovial thickening was not limited to the injured knees but was also present in the sham operated joints and therefore it is not specific to cartilage injury. No difference was observed between sham operated and injured knee joints from the two strains. Hence, based on this simple analysis, the amount of synovitis at this specific time point could not explain the different outcome but it is still possible that a different inflammatory response may play a role in repair outcome.

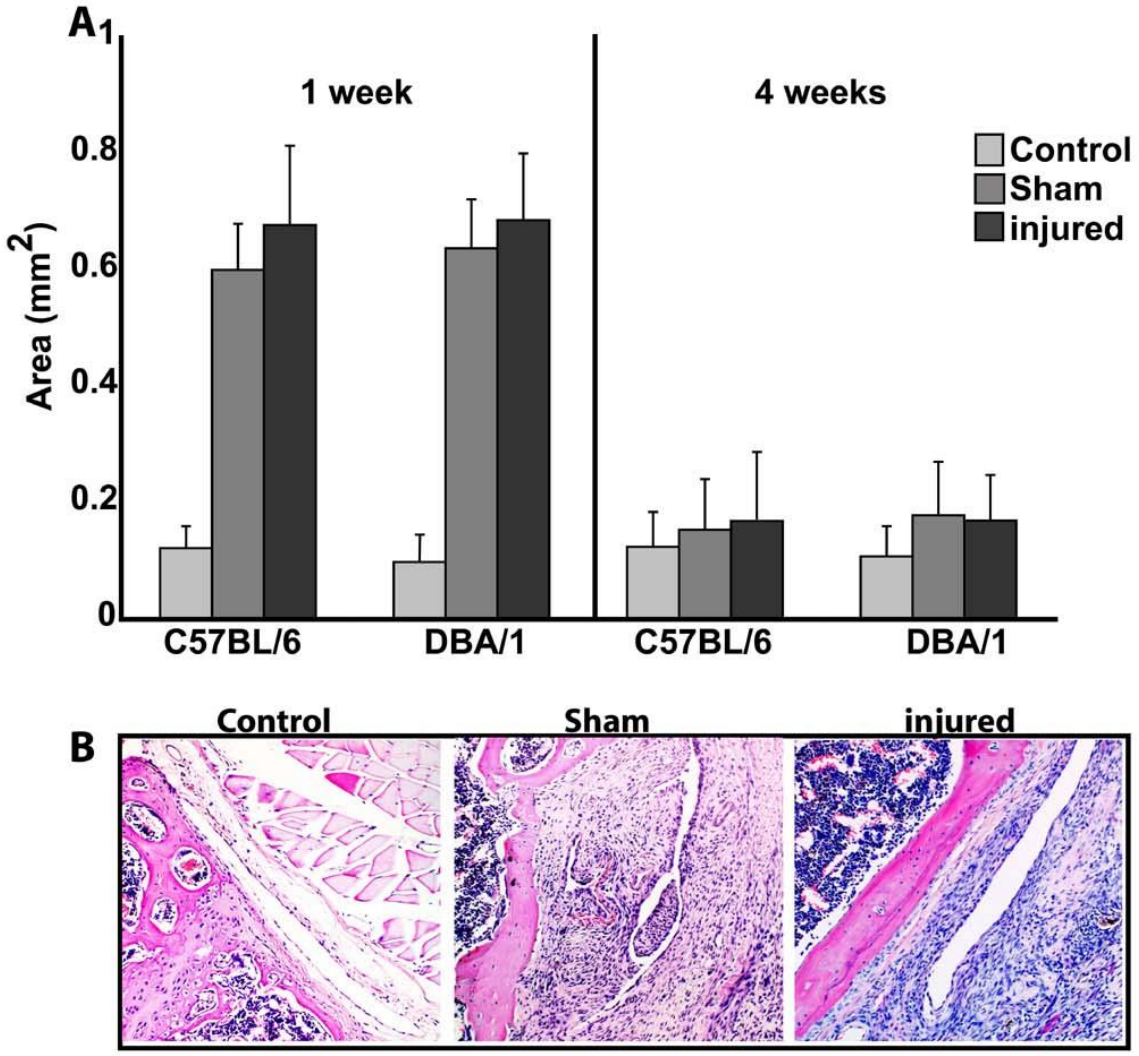

Figure 6.3: Inflammatory response to arthrotomy: A, Quantitative histomorphometric assessment of synovial thickening 1 and 4 weeks after surgery in C57BL/6 and DBA/1mice. B, Representative H&E stained sections from control, Sham operated and injured knee joints at the one week time point.

6.4. Matrix remodelling

Remodelling of the cartilage ECM has been the focus of extensive research in cartilage biology and its importance has been confirmed in outcome determination in a murine model of osteoarthritis (32). For the critical homeostatic role played by the matrix component of the cartilage, it is possible that ECM remodelling may also affect the repair process following cartilage injury and hence the final outcome of cartilage injury could be determined by the balance between synthetic and catabolic activities. Therefore, the remodelling of the two major components of cartilage matrix (type II collagen and aggrecan) was compared after injury in the two strains of mice.

6.4.1. Type II collagen Neo-synthesis

Type II Collagen is composed of three subunit polypeptide chains intertwined in triple helical configuration. During biosynthesis, each polypeptide chain is synthesized with extra registration peptides (telopeptide) on both the amino- and carboxyl terminal ends to prevent premature intra-cellular precipitation and assembly of the procollagen molecule. After its extracellular transport, the N and C- telopeptides are released by procollagen peptidase enzyme allowing tropocollagen to assemble into polymeric collagen fibrils (15). Therefore, to monitor type II collagen neo-synthesis, we immuno-stained the C-terminal telopeptide cleaved from type II procollagen molecules using anti CPII antibody (262). In the control and sham-operated joints, the collagen C-telopeptide was detected in the mineralized deep layer of the articular cartilage (Figure 6.4A). Following injury, pericellular CPII staining was observed in the superficial and intermediate zones. In these areas, collagen type II neo-synthesis peaked one week after

injury in both strains, but subsequently declined in C57BL/6, while it persisted in DBA/1 mice for at least 8 weeks and became confined to the newly formed cartilage (Figure 6.4A, B). The number of CPII-positive chondrocytes was statistically significantly higher in DBA/1 mice at 4 and 8 weeks time points (Figure 6.4B). The positive and negative controls are shown in Figure 6.4C.

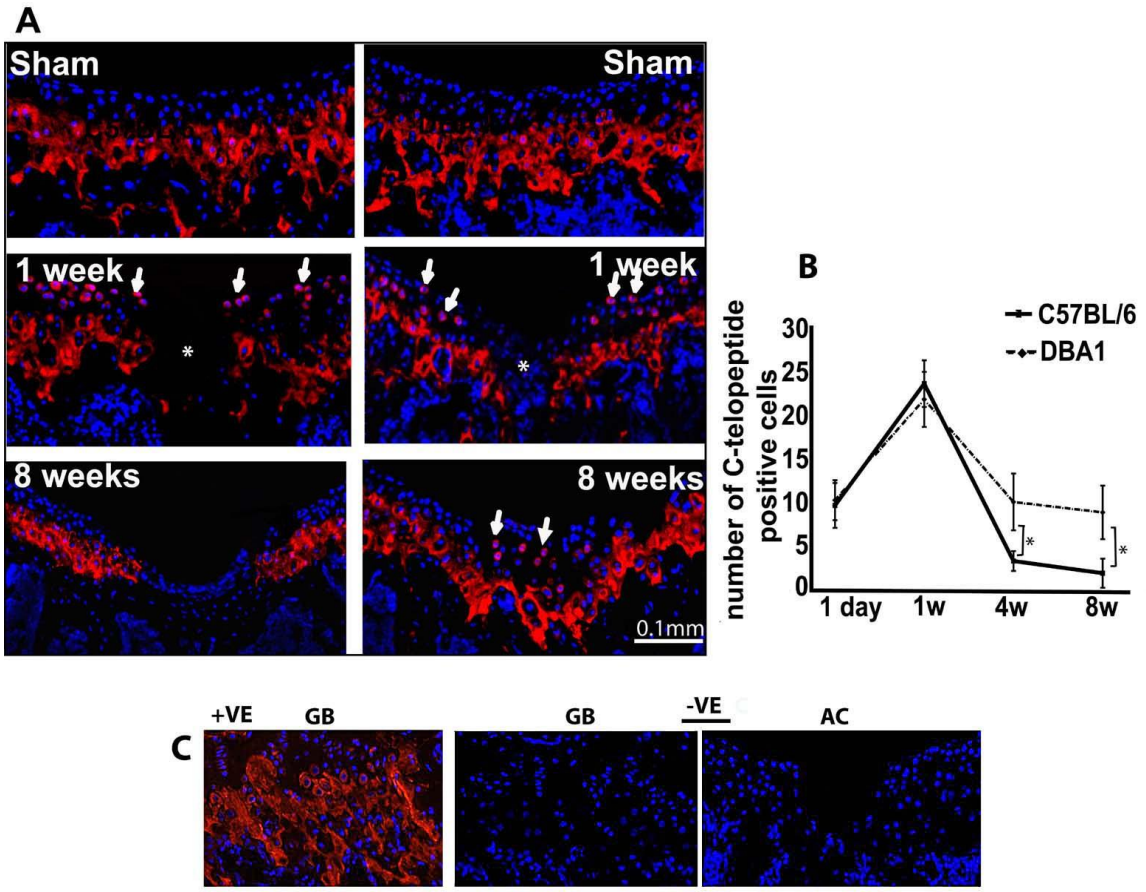

Figure 6.4: Collagen synthesis: A, Immunoflurescence staining for type II collagen C telopeptide (A) in eight week old C57BL/6 (left) and DBA/1 (right). Type II collagen C-telopeptide is shown in red and nuclei are counterstained with DAPI (blue). B, The number of C-telopeptide positive chondrocytes within the superficial and intermediate layer. The values from 3 different mice from each strains at the indicated time point are expressed as mean and standard deviation * $P<0.05$. C, Positive (left) and negative (middle and right) controls for CPII immunostaining. As a positive control, I used growth plate cartilage in which the antigen had been already reported to be present. Negative control was sections in which isotype matched non immune antibodies were used instead of the primary antibodies. GB=Growth plate and AC= Articular cartilage.

6.4.2. Type II collagen degradation

Type II collagen degradation was then compared in both strains utilizing anti C1,2C (Col2-3/4C_{short}) antibody that recognizes the carboxy-terminal end of the collagenase-generated fragment of type II collagen. Intact uninjured articular cartilage from sham and non-operated joints showed weak pericellular C1,2C staining in both C57BL/6 and DBA/1 young mice (Figure 6.5A). As early as 1 week and for at least 8 weeks following injury, immunostaining increased in both strains. The repair tissue in DBA/1 mice, however, displayed a weaker staining than the adjacent cartilage (Figure 6.5A). The positive and negative controls are shown in Figure 6.5B.

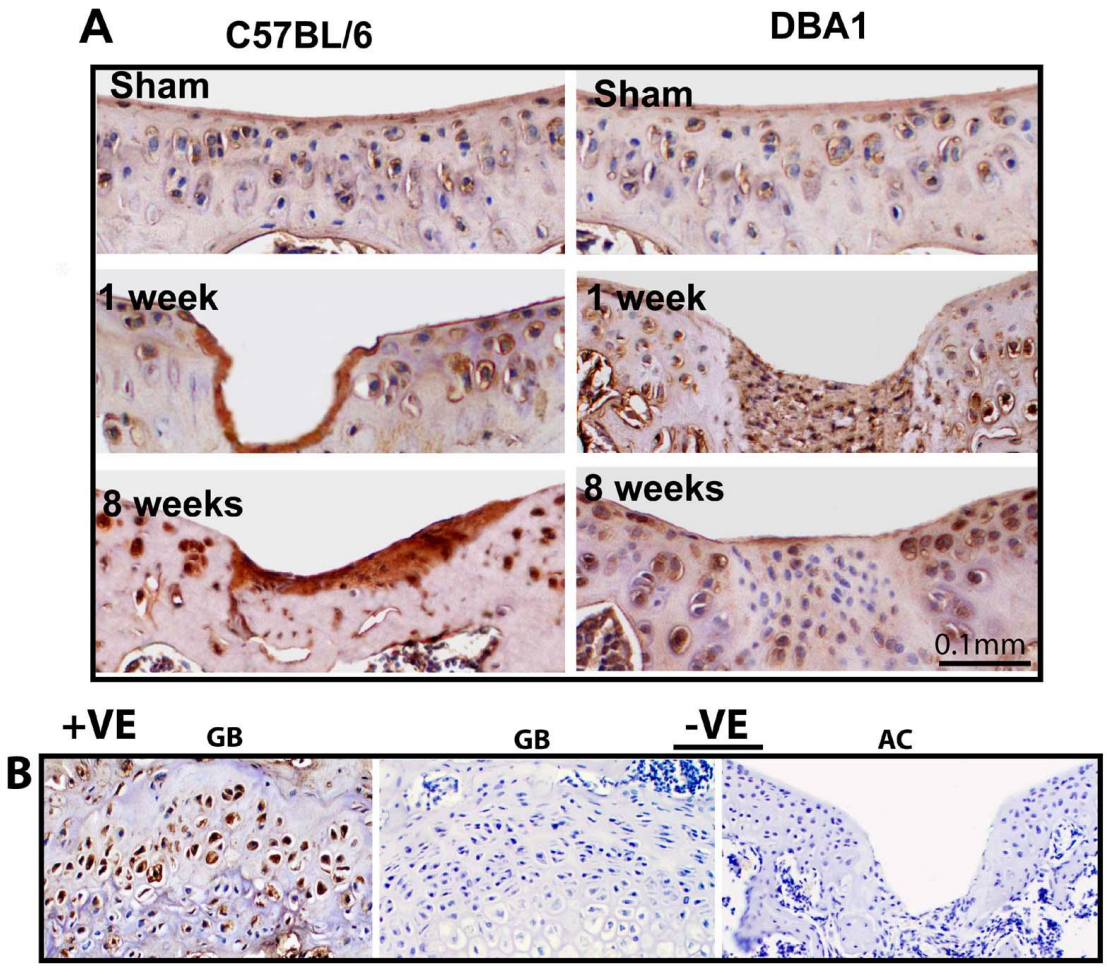

Figure 6.5: Collagen degradation. A, immunostaining of C1,2C neoepitope in sham and injured C57BL/6 (left) and DBA/1 (right) at the indicated time points. Negligible staining is seen in the repair tissue in DBA/1 mice. B, Positive (left) and negative (middle and right) controls for C1,2C immunostaining. GB=Growth plate and AC= Articular cartilage.

6.4.3. Aggrecanase and MMPs mediated aggrecan cleavage

Proteoglycan turnover is central to cartilage homeostasis and proteoglycan cleavage has been shown to be a crucial event in OA development (32). Proteoglycan remodeling has also been argued as an important element for cartilage repair. Therefore, we have compared in the two mouse strains the modalities of proteoglycan degradation utilizing two antibodies that recognize neoepitopes generated by aggrecan (the major proteoglycan in cartilage) when cleaved by aggrecanases and metalloproteinases MMPs (TEGE^{373} and VDIPEN) respectively. In sham and non-operated control joints, both strains exhibited similar staining patterns (Figure 6A&7A). As early as one day after injury and thereafter, C57BL/6 mice displayed increased TEGE^{373} staining and low levels of VDIPEN. An opposite expression pattern was detected in DBA/1 mice with weak TEGE^{373} and intense VDIPEN staining (Figure 6A&7A). These findings indicate that aggrecan is prevalently degraded by aggrecanases in the C57BL/6 and by metalloproteinases in DBA/1 strain thereby confirming the critical role of aggrecanases in cartilage destruction and suggest that a controlled level of MMP-mediated aggrecanolysis may be needed for cartilage homeostasis, and possibly repair.

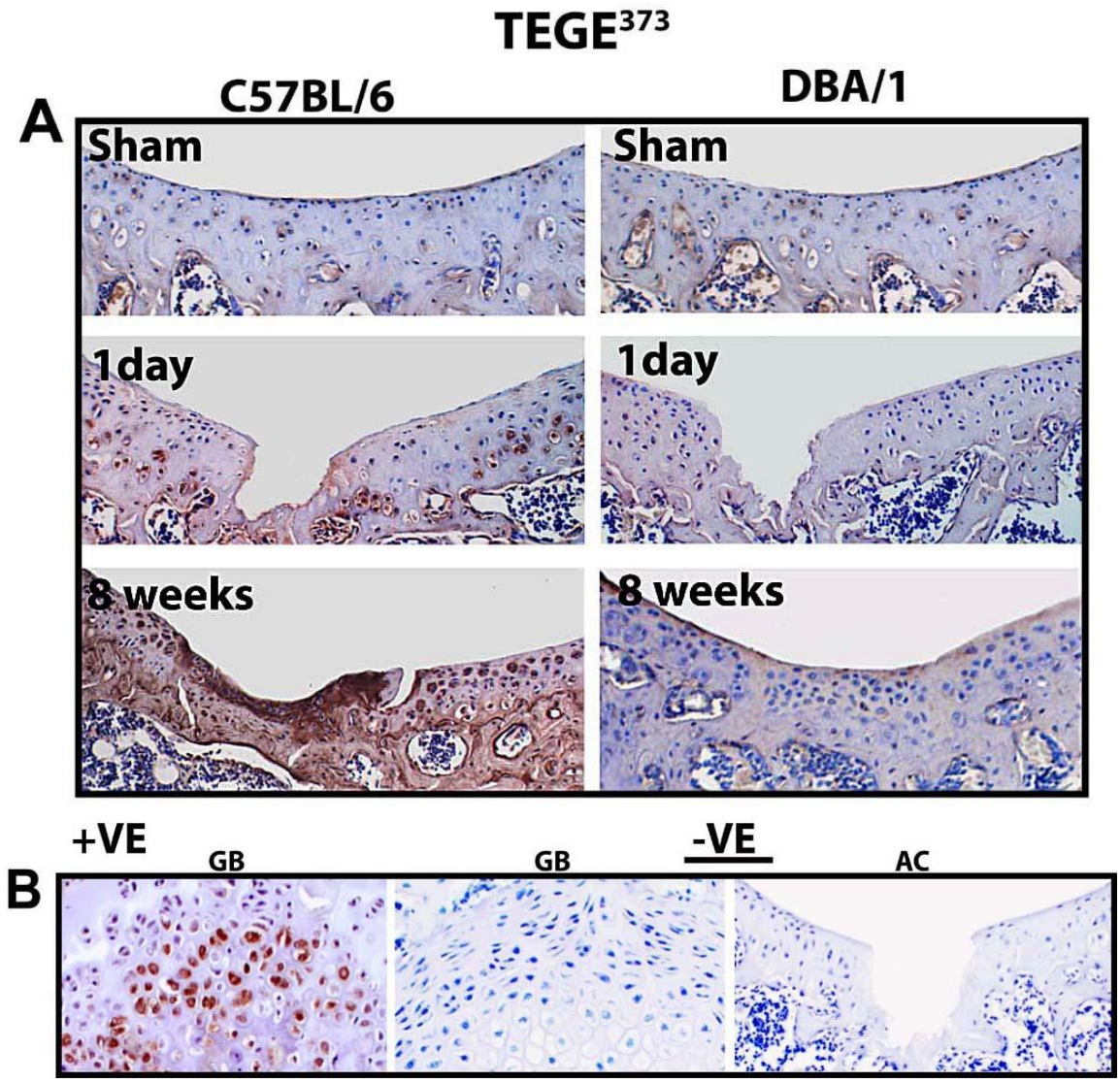

Figure 6.6: Aggrecanase mediated aggrecan degradation. A, Immunostaining of aggrecanase ($TEGE^{373}$) generated neoepitope (brown) in the articular cartilage of eight week old C57BL/6 and DBA/1. Nuclei are counterstained with Hematoxylin (blue). B, Positive (left) and negative (middle and right) controls for $TEGE^{373}$ immunostaining. GB=Growth plate and AC= Articular cartilage.

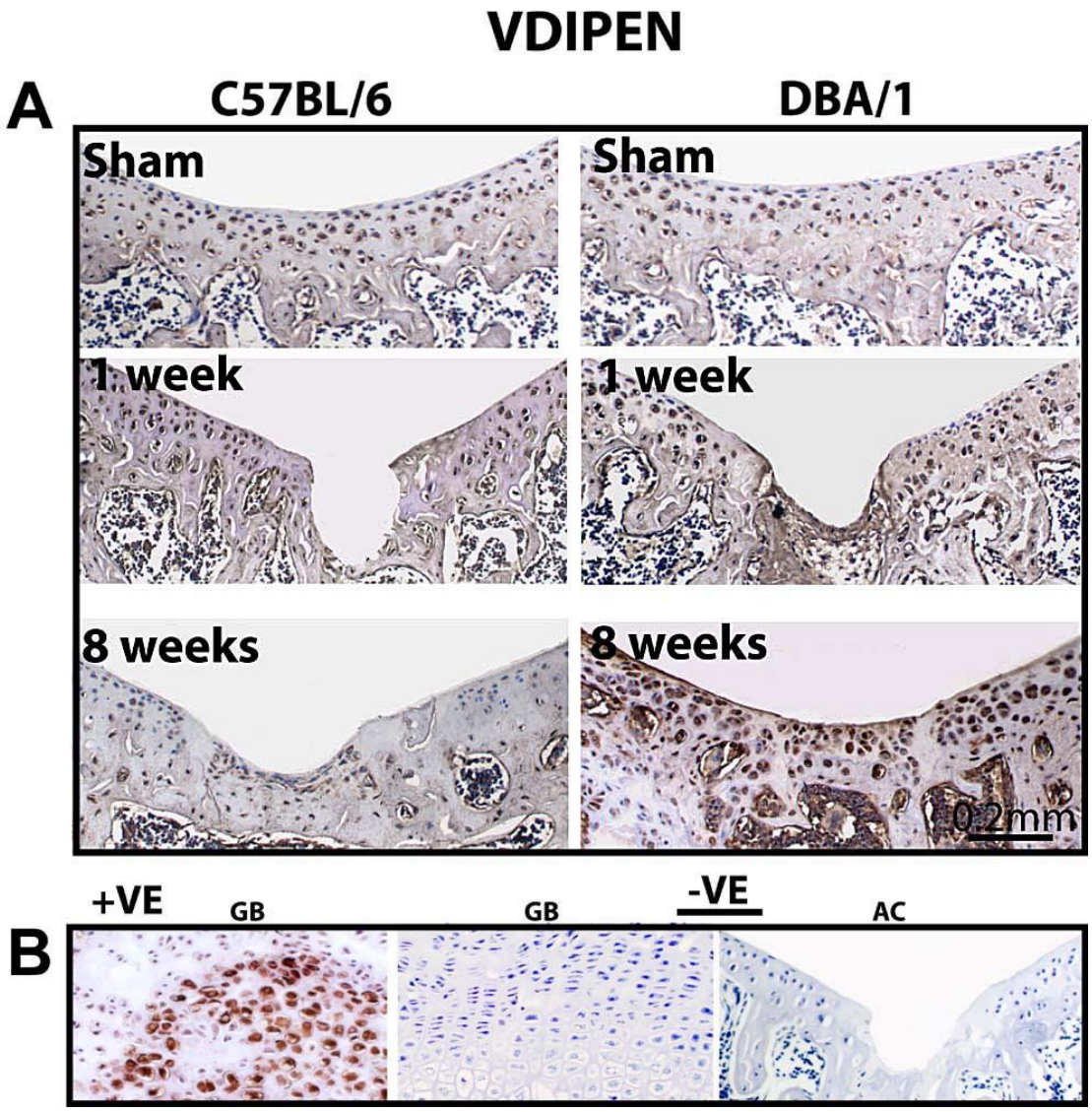

Figure 6.7: MMPs mediated aggrecan degradation. **A,** Immunostaining of MMPs (VDIPEN) generated neoepitope (brown) in the articular cartilage of eight week old C57BL/6 and DBA/1. Nuclei are counterstained with Hematoxylin (blue). B, Positive (left) and negative (middle and right) controls for VDIPEN immunostaining. GB=Growth plate and AC= Articular cartilage.

Discussion

We have demonstrated in this chapter that joint surface damage can trigger a series of cellular and extra-cellular events including apoptosis, proliferation and matrix changes. These events were regulated differently in DBA/1 and C57BL/6 mice resulting in the different outcome observed in both strains.

Chondrocyte apoptosis progressively resolved in DBA/1 mice and persisted in C57BL/6 for at least 8 weeks. Chondrocyte death following mechanical injury and its potential role in the pathogenesis of osteoarthritis have been described in several studies (220;223;254;263). However, apoptotic cells may play a positive role in the repair responses by releasing chemo-attractants for stem/progenitor cells such as HMGB1 (264). Therefore, it is possible that controlled chondrocyte apoptosis, in the initial phases of repair, may play a similar function after cartilage injury; however, it could be detrimental if not tightly regulated and inappropriately prolonged. Our experimental setup does not allow us to discriminate whether the prolonged apoptosis in C57BL/6 is determining or a consequence of repair failure.

Proliferation in the cartilage surrounding the injury site has been reported following mechanical trauma (223;257). We did not detect chondrocyte proliferation in the articular cartilage surrounding the injury. However, proliferating cells were identified within the repair tissue in DBA/1 mice at 1 and 4 weeks post-surgery. This discrepancy with previous literature could be due to differences in the experimental conditions, the time points analyzed and the detection systems used. In this study, we examined the phosphorylation of Histone H3 which is tightly correlated with the chromosome condensation phase during mitosis, thereby representing a snapshot of cells in M phase

of cell cycle (256). Conversely, incorporation of labeled nucleosides marks all the cells undergoing DNA duplication during the labeling period. Furthermore, cell proliferation in adult tissues occurs at a very low rate, and may take place in a short time-span after injury, thus our time points might have missed proliferation within the cartilage surrounding the injury. It is also possible that cells might first migrate from the surrounding cartilage and then divide within the repair tissue. Surrounding tissues such as bone marrow and synovium have been proposed to contribute cells to the reparative process in different in vivo injury models (153;259). Indeed, proliferating cells were seen in the synovial membrane of both strains one week following injury suggesting a possible role for the synovial membrane in the repair process. Additionally, PHH3 positive cells were also identified in the bone marrow of injured and sham operated joints. The fact that bone marrow contains continuously proliferating hematopoietic stem cells may explain our findings however, it can not be excluded that bone marrow MSCs may be contributing to the process of cartilage regeneration. The origin of the cells populating the defects and ultimately forming the repair cartilage in DBA/1 mice remains to be clarified.

It is well known that the inflammatory response to trauma is an essential phase for repairing the damaged tissue however, if prolonged; it can impair the healing process and results in local destruction (261). Synovial inflammation, involving lymphocytic infiltration and overexpression of pro-inflammatory mediators, is a common feature in OA and a factor that likely causes an imbalance between the catabolic and anabolic activities of the chondrocytes (265). Mild transient synovial thickening was observed in all joints following arthrotomy suggesting that it is a surgery related reaction rather than a response to cartilage injury. Synovitis peaked one week after surgery and completely

resolved at the 4 week time points in both strains and is therefore unlikely to account for their different outcome. However, we can not exclude the possibility that differences in the composition of the inflammatory infiltrate, different cytokine profiles and dynamics of resolution might all be factors influencing the regeneration outcome and therefore more studies are still needed to further characterize and compare these factors in both strains.

This study shows a prompt activation of matrix remodeling after injury within the repair tissue in DBA/1 mice and in the remaining cartilage in both strains. Matrix remodeling has been described in response to injury (223;266), during OA (20;267) and in human repair cartilage tissue obtained from autologous chondrocyte implantation (21). Interestingly, in this study, DBA/1 mice maintained a high level of Collagen type II neo-synthesis and a low collagen catabolic activity for 8 weeks after injury. However, C57BL/6 mice exhibited a reverse pattern with progressive decrease in the number of CP II positive cells and intense Col2-3/4C_{short} staining. Aggrecan degradation was predominantly driven by aggrecanases in C5BL/6 mice and by metalloproteinases in DBA/1 mice.

Recently, ADAMTS-5 has been identified as the main aggrecanase in mouse cartilage and its ablation protected the mice from OA induced by DMM (32). Similarly, mutants harboring a genetic allele of the aggrecan gene that blocks aggrecanase-mediated cleavage were also protected when challenged in DMM model, but, interestingly, mice harboring an aggrecan mutant allele that is resistant to MMP-mediated cleavage developed more severe OA than their wild-type littermates (16). Moreover, MMP9-deficient mice were more susceptible to OA than their wild-type littermates in the same model (26). Taken together, these data and our results confirm the critical role

of aggrecanases in cartilage destruction and suggest that a controlled level of MMP-mediated aggrecanolysis may be needed for cartilage repair, as MMPs proteolysis can facilitate cell migration, regulate tissue architecture, release and activate ECM bound growth factors and signaling molecules (23). A caveat, in the interpretation of our data, is that aggrecan cleaved by aggrecanases may be internalized (268) and thereby no longer available for MMP cleavage even in the presence of active MMPs. This may explain why, in C57BL/6, although several MMPs can cleave collagen and aggrecan, we only detected cleaved type II collagen. Another explanation for this discrepancy is that different MMPs may be responsible for aggrecan and collagen type II cleavage.

The above mentioned cellular responses to cartilage injury are thought to be part of a more complex signaling triggered by joint surface damage, possibly activating and regulating the reparative process or contributing to PTOA development. In chapter 4, we have characterized the molecular response of human articular cartilage to injury in vitro and showed modulation of genes encoding signaling molecules and morphogens. In the next chapter, we will use the mouse model of joint surface injury/repair to validate these findings in vivo.

Conclusions

- The different repair outcome in C57BL/6 and DBA/1 mice was associated with different regulation of apoptosis, proliferation and matrix remodelling
- Specific measurable parameters of anabolism and catabolism may be used as biomarkers to predict the ability of cartilage to heal and the likelihood of post-traumatic OA development
- These assays may be used to identify mechanisms by which a specific gene can influence the regenerative process.

CHAPTER 7: RESULTS

In vivo validation of the molecular response of articular cartilage to injury

Acute mechanical injury to adult human articular cartilage results in an early molecular response with activation of several signalling morphogenetic pathways. Although the in vitro model of cartilage injury used in this study is a well validated system, it has several drawbacks and limitations. For instance, the cartilage tissue has already been injured upon dissection and isolated from its anatomical and functional environment and instead exposed to artificial cultural conditions. The in vivo model of joint surface injury and repair offers the opportunity to validate in vivo the differential expression of genes reported to be modulated upon cartilage injury in vitro by microarray screening. In particular, we focused on pathways known to play a role in embryonic skeletogenesis and joint morphogenesis such as BMP and Wnt pathways.

7.1. Modulation of BMP pathway in vivo following joint surface injury

In our in vitro experiments, BMP2 mRNA was upregulated in the injured human cartilage explants with phosphorylation of SMAD-1/-5/-8 indicating activation of BMP pathway. To investigate whether the regulation of the BMP pathway demonstrated in vitro also took place following injury in vivo, we utilized our new in vivo murine injury model. Immunohistochemical staining for BMP-2 was done on sections from mouse knee joints comparing the sham versus the injured at different time points following injury. BMP-2 was intensely detected in the extracellular matrix of the injured articular cartilage in both strains as early as one day and at least for 8 weeks post-surgery. At later time points, however, the staining became less diffuse especially in C57BL/6 mice. The articular cartilage of the sham operated knees showed faint pericellular staining (Figure 7.1A). The ECM-associated staining pattern was not unexpected as BMP2 is known to

bind strongly to Heparan sulfate proteoglycans (HSPGs) through the heparin binding domain at its N-terminus (269).

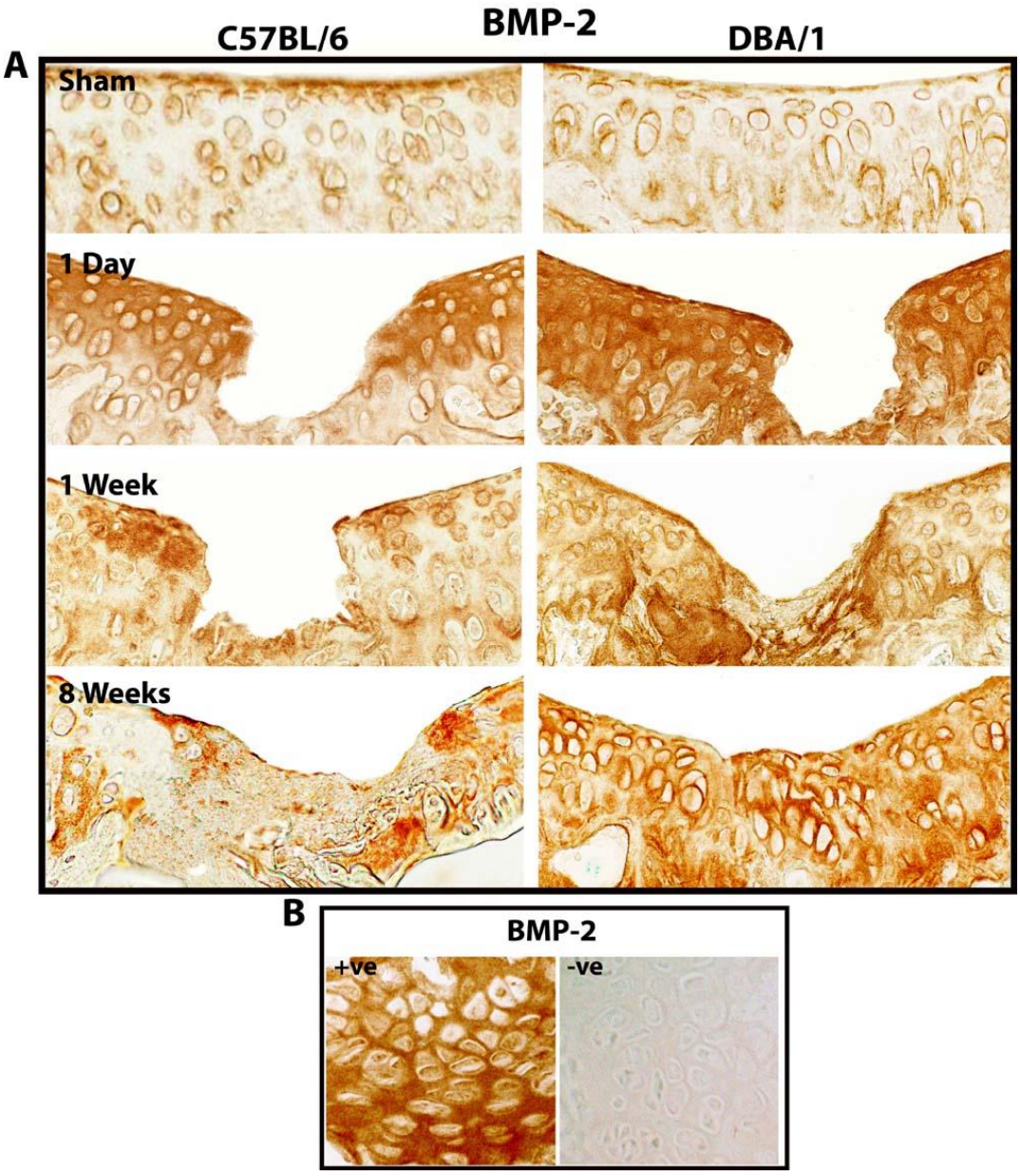

Figure 7.1: BMP2 activation after mechanical cartilage injury in the murine in vivo model: A, immunostaining for BMP-2 in the sham and injured C57BL/6 and DBA/1 mice at the indicated time points. The positive and negative controls for BMP-2 in the growth plate cartilage are shown in B. The negative control sections were treated with an isotype matched non- immune primary antibody.

As activation of BMP signaling activates the phosphorylation of the intracellular signaling mediators SMAD-1/-5/-8, we performed immuno-staining using an antibody that detects the phosphorylated form of SMAD-1/-5/-8. In the injured joints, phospho-SMAD-1/-5/-8 positive cells can be identified both in injured articular cartilage one day following the injury (Figure 7.2A). In contrast, no phosphorylated SMAD-1/-5/-8 were detected in the sham operated joints (Figure 7.2A) indicating that the activation of BMP signaling is a mechanism specific to cartilage injury. The BMP pathway is known to be active in cartilage of the growth plate where it plays an important role in regulating the process of endochondral bone formation (270). Therefore, growth plate cartilage was used as an internal positive control for both BMP2 (Figure 7.1B) and PSMAD (Figure 7.2B) immunostaining.

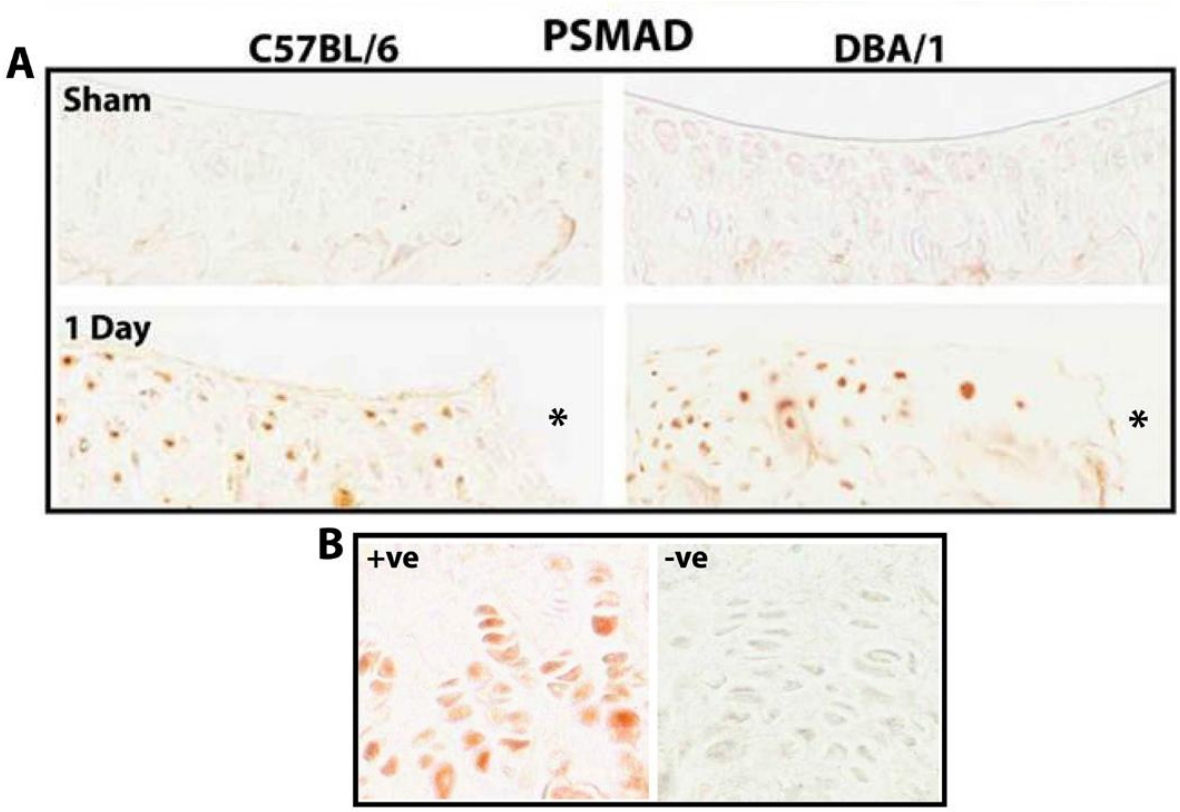

Figure 7.2: PSMAD immunostaining in both stains in injured and sham operated joints. Positive cells were identified in injured articular cartilage one day after surgery (A). The asterisks indicate the site of injury. The positive and negative controls for PSMAD in the growth plate cartilage are shown in the lower inset (B). The negative control sections were treated with an isotype matched non- immune primary antibody.

7.2: Modulation of Wnt signalling in the in Vivo mouse model of joint surface injury

The experiments done using the in vitro model of cartilage injury showed a consistent injury-associated up-regulation of Wnt16 as well as activation of the canonical Wnt signalling pathway. To test whether the same phenomena also takes place in vivo after cartilage injury, modulation of Wnt signalling was studied in the murine in vivo model of joint surface injury.

In keeping with the in vitro data from human cartilage explants, the secreted Wnt inhibitor FRZB was markedly decreased in the articular cartilage of injured knees in C57BL/6 and DBA/1 mice (Figure 7.3A). Wnt16 was also sharply upregulated 24h after cartilage injury at both protein (Figure 7.3A) and mRNA (Figure 7.3B) level. It was interesting to notice that Wnt16 was not detected at the sham operated joints, where injury to the synovial membrane and the joint capsule occur and result in synovitis comparable to those of injured joints. This demonstrates a high level of specificity of the Wnt16 response to cartilage injury but not to other joint tissues. This data also indicate that Wnt16 up-regulation after cartilage injury is conserved across species.

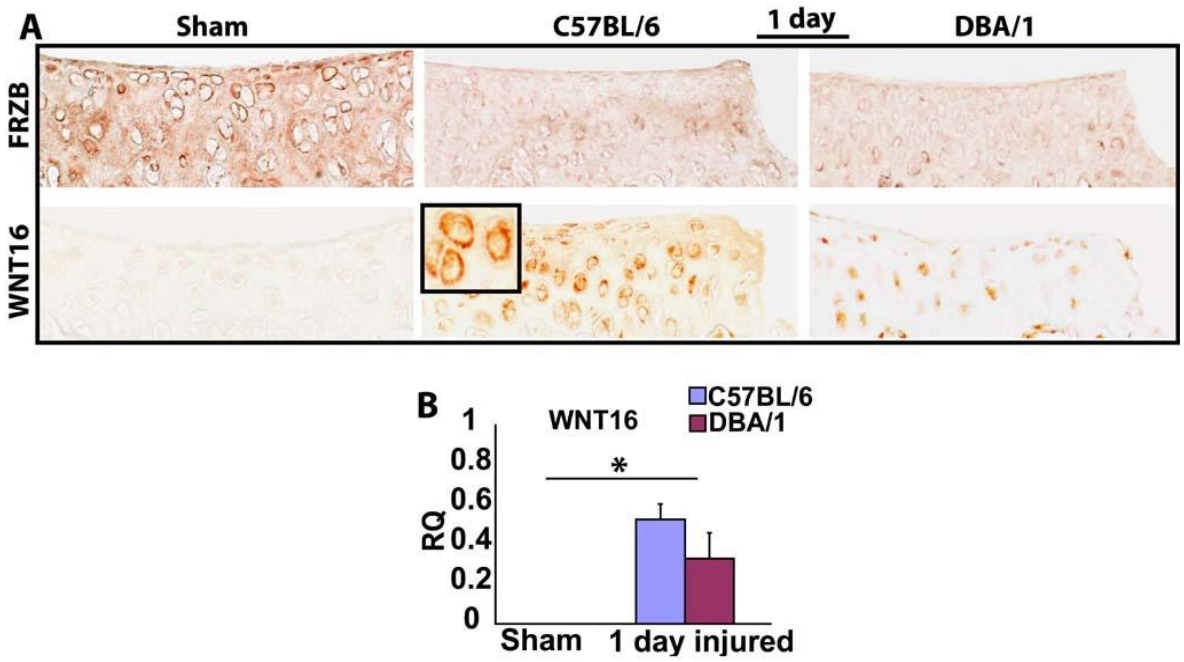

Figure 7.3: Wnt16 up-regulation and FRZB downregulation are reproduced in vivo in a mouse model of cartilage injury: immunohistochemical staining for the Wnt antagonist FRZB and Wnt16 (A) and quantitative real time PCR analysis of Wnt16 (B) in the sham operated and injured knee joints of C57BL/6 and DBA/1 mice one day after injury. The inset in A is showing high magnification view and Values in B are expressed as mean and standard deviation. *p <0.05.

To investigate whether this molecular regulation is associated with activation of the β catenin-dependent wnt signalling pathway as in the in vitro experiments, immunostaining for β catenin was performed comparing the injured versus the sham operated knee joints. Cytoplasmic accumulation and nuclear localization of β-catenin was observed in the articular cartilage of injured joints from both mouse strains whereas chondrocytes in sham operated joints only exhibited weak staining mostly associated with the cell membrane (Figure7.4A). To investigate if β-catenin accumulation after injury is associated with up-regulation of TCF/LEF1 target genes, gene expression analysis of the Wnt target genes Axin2 (271) and Osteoprotegerin (OPG) (272) was

performed. Axin2 mRNA was significantly up-regulated in both strains one day after cartilage injury (Figure 7.4B) confirming the activation of Wnt signaling through the canonical pathway in vivo. Our experimental conditions did not reveal significant differences in OPG expression at protein (Figure 7.4A) or mRNA (Figure 7.4C) level between injured joints and sham operated controls.

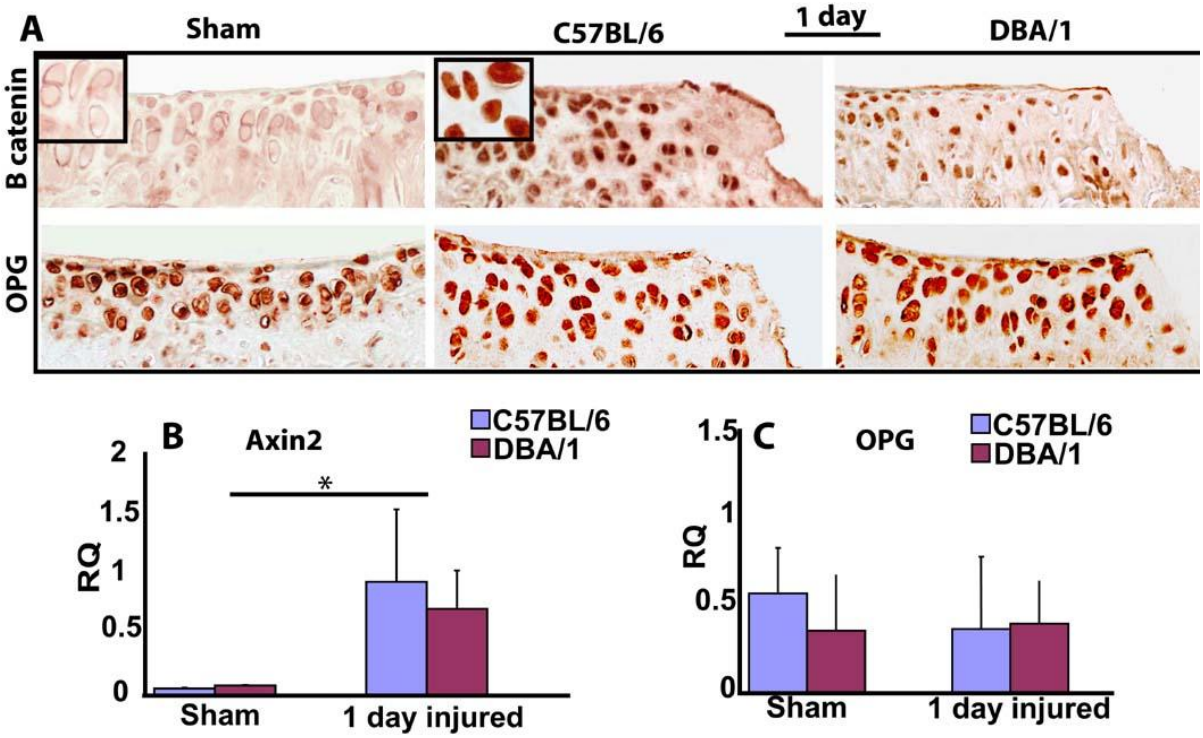

Figure 7.4: Activation of the canonical Wnt pathway upon joint surface injury in vivo: A, Immunostaining for β-catenin (upper panel) and OPG (Lower panel). B-C, quantitative real time PCR analysis for Axin2 (B) and OPG (C) in sham operated controls and injured joints of C57BL/6 and DBA/1 one day after injury. The insets in A are showing high magnification view and values in B and C are expressed as mean and standard deviation. *p <0.05.

Wnt4 and Wnt9a are co-expressed with Wnt16 in the joint interzone during embryogenesis and are known to activate the canonical Wnt signalling (47). To evaluate if these genes might contribute to the reported activation of the canonical Wnt signalling *in vivo*, modulation of these Wnt ligands was studied after cartilage injury in vivo by gene expression analysis. Wnt4, but not Wnt9a, mRNA was significantly upregulated in vivo after joint surface injury in both strains (Figure 7.5A&B) indicating a possible role in Wnt activation through the canonical pathway.

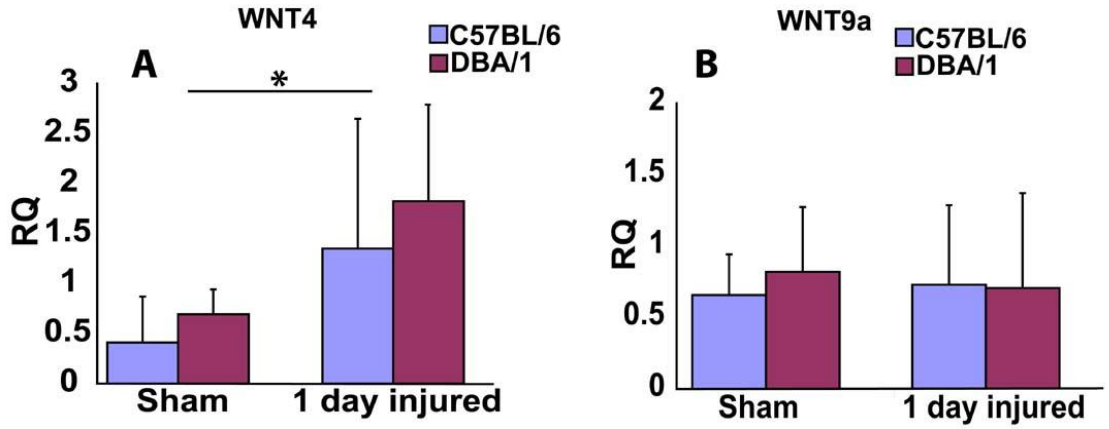

Figure 7.5: Injury associated modulation of Wnt ligands involved in synovial joint formation. Quantitative real time PCR analysis of the Wnt ligands WNT4 (A), WNT9a (B) in sham operated and injured joints from C57BL/6 and DBA/1 mice at day one time point. Values are expressed as mean and standard deviation. *p <0.05.

To explore the dynamics of wnt16 up-regulation and activation of the β catenin-dependent Wnt pathway in C57BL/6 and DBA/1 mice 8 weeks after injury, Wnt16 and β-catenin immunostaining were performed on sections obtained from both strains. This experiment revealed that at this late time point wnt 16 was detectable at very low levels and β-catenin exhibited a cytoplasmic granular pattern of staining in both strains tested (Figure 7.6).

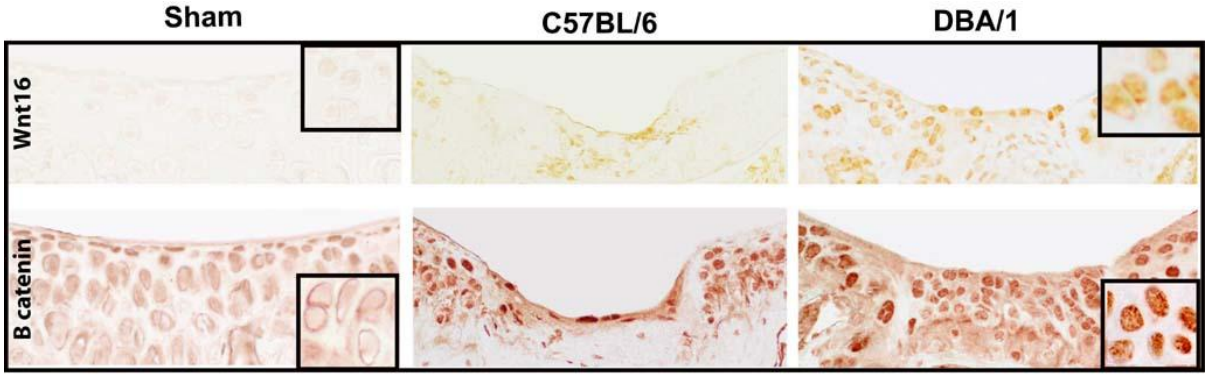

Figure 7.6: Regulation of Wnt16 and β catenin activation at late time points: Immunohistochemical staining for Wnt16 (upper panel) and β catenin (Lower panel) in sham operated joints (Left) and injured C57BL/6 (Middle) and DBA/1 (Right) at 8 weeks following cartilage injury. The insets are high magnification images showing the cellular pattern of staining at the indicated time points.

7.3: Effect of activation of the canonical Wnt pathway on mouse articular cartilage explants

To investigate the possible effects of canonical Wnt signalling activation in mouse articular cartilage, articular cartilage explants from the femoral heads were isolated, stimulated with recombinant Wnt3a (known agonist for the canonical pathway) for either 24 or 48 hours and RNA was extracted for gene expression analysis. This stimulation was effective as shown by the up-regulation of the target gene Axin2 (Figure 7.7.A). Wnt3a treatment also up-regulated OPG mRNA (Figure 7.7B) and significantly increased Col2A (Figure 7.7C) and aggrecan (Figure 7.7E) mRNA without significant effect on Col10 expression (Figure 7.7D) after 24 hours. The effect of stimulation was lost after 48 hours (Figure 7.7) indicating that activation of the Wnt signalling pathway, in this system is short-lived.

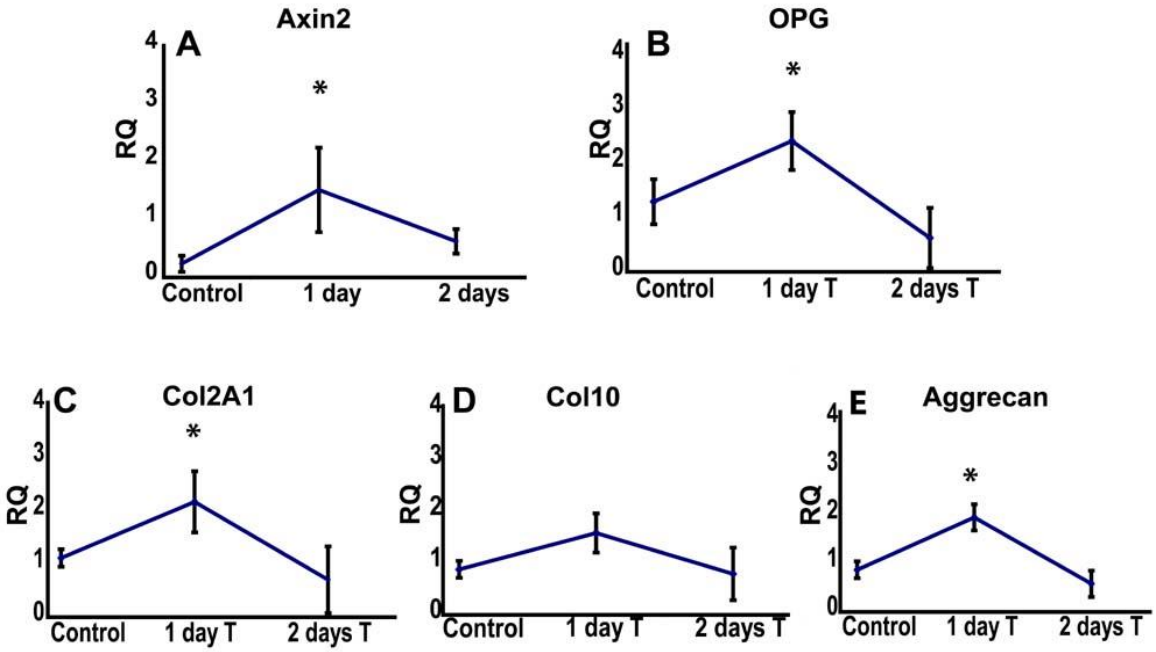

Figure 7.7: Effect of the canonical Wnt pathway activation on mouse articular cartilage explants*:* Real time PCR analysis for axin2 (A), OPG (B), Col2A (C), Col10 (D) and aggrecan (E) in mouse cartilage explants following stimulation with recombinant Wnt3a or the vehicle of the proteins (0.1%BSA-PBS). Values are expressed as mean and standard deviation.

Under our experimental conditions, activation of the canonical pathway in articular cartilage explants resulted in up-regulation of cartilage markers Col2A and aggrecan suggesting an anabolic effect. Similar results were observed when treating adult human articular cartilage explants with LiCl (an inhibitor of GSK3) indicating that this effect may be conserved across species (273). Up-regulation of aggrecan and Col10 mRNA was also reported in articular chondrocytes isolated from β-catenin cAct mice in which β-catenin is constitutively activated (95). Activation of wnt signalling in our experimental setup was transient possibly due to subsequent repression of the pathway through negative feedback regulatory mechanisms (56). This transient activation might

not be sufficient to significantly alter the expression of certain genes such as Col10 that may require persistent longer activation of Wnt signalling.

In other in vitro systems, however, the activation of Wnt pathway induced downregulation of cartilage marker genes aggrecan and Col2A (274) suggesting that different experimental in vitro conditions may result in variable responses and highlighting the necessity for the in vivo validation.

7.4: Identification of the target cells of the canonical Wnt signalling in the adult joint environment

To identify cells in which Wnt pathway is active following cartilage injury, we used BAT-gal (β-catenin activated transgene driving expression of nuclear β-galactosidase reporter) mouse line as a readout of β-catenin activity (275). These mice express β-galactosidase under the transcriptional control of TCF/LEF1 responsive elements and therefore cells with active wnt signalling can be demonstrated using X-Gal staining (275). The joint surface injury model was performed in 8 weeks old BAT-gal mice (FVB genetic background) and X-GAL staining was done at different time points in the injured and sham operated joints. Up-regulation of β-galactosidase was present in a subset of cells within the bone marrow spaces around the injury site only at the one day time point. Later on, these cells disappeared despite filling of the defects with undifferentiated cells after one week and repair of the wound with cartilaginous tissue after 8 weeks (Figure 7.8).

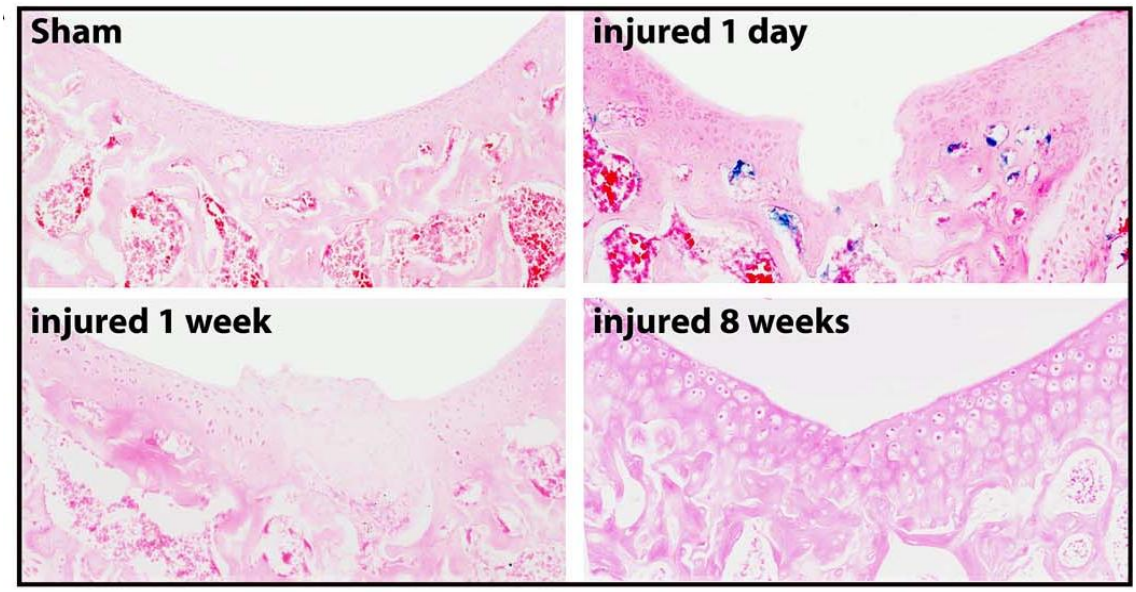

Figure 7.8: BAT-gal expression at different time points following cartilage injury. X-gal staining was performed and sections were counterstained with eosin. X-GAL positive cells are shown in blue.

Further phenotypic and functional characterization of these cells is still needed to identify the nature of the cells and to investigate whether they are involved in the reparative response. Such investigations were outside the scope of this thesis however, two possibilities are worth discussing because of their possible implication in repair processes. The first one is that the canonical wnt signalling plays a role in the maintenance of the stem cell pool and in the regulation of healing process in several systems (247;276;277) and therefore cellular targets of this pathway within injured joints (β-galactosidase positive cells) may represent joint progenitor cells contributing to joint surface repair. The second is that the wnt pathway also has an important role in bone remodelling especially through RANK-RANKL-OPG axis which blocks osteoclastogenesis and ultimately bone resorption (94;278). Therefore, it is also possible

that the β-galactosidase positive cells are pre-osteoclasts targeted by the activated Wnt signalling after cartilage injury.

7.5: Suitability of BAT-GAL mice as a reporter for Wnt signalling in adult cartilage

Unexpectedly, in spite of the already mentioned positivity of β catenin immunostaining in injured cartilage, no X-GAL positive cells were identified in the articular cartilage of BAT-GAL mice after injury (Figure 7.9A). To test whether β-catenin accumulated in BAT-GAL mice as was the case in DBA/1 and C57BL/6 strains, β-catenin immunostaining was performed on sections obtained from these mice. As with the other two strains, cytoplasmic accumulation and nuclear localization of β-catenin was observed in the articular cartilage of BAT-GAL mice one day after injury and in growth plate chondrocytes with the absence of X-GAL staining (Figure 7.9A).

To further investigate the reliability of BAT-GAL expression to reflect the Wnt/ β-catenin activity in cartilage tissue, BAT-GAL femoral heads were stimulated in vitro with Wnt3a (well characterized Wnt ligand that signals through the canonical pathway) for either one or two days. Again, no X-GAL staining was seen in the cartilage explants following stimulation (Figure 7.9B) despite the up-regulation of Axin2 (Figure 7.9C) that suggests the activation of the canonical Wnt pathway. These results indicate that the expression of nuclear β-galactosidase reporter does not mirror the activation of Wnt signalling in cartilaginous tissue of adult mice and thus BAT-GAL mice are not suitable as reporter for the canonical Wnt pathway activation in adult mouse cartilage

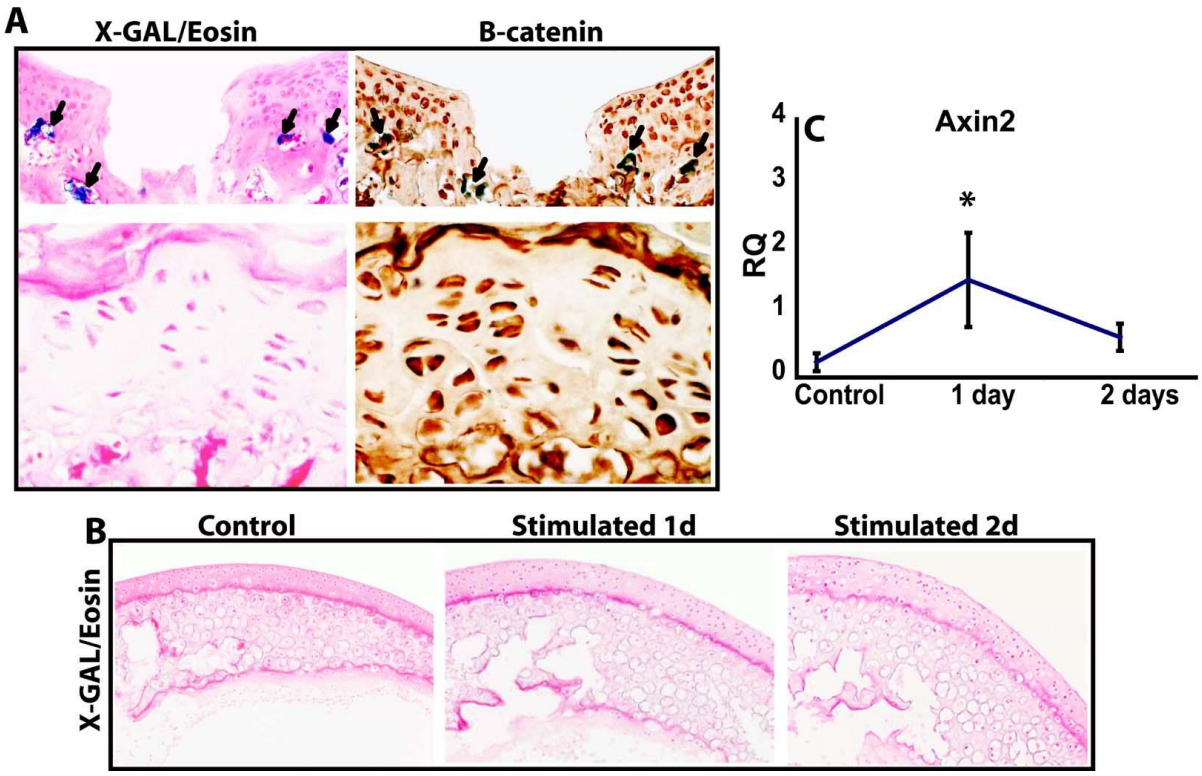

Figure 7.9: BAT- GAL mice as a reporter for WNT signaling in adult cartilage: A, X-GAL staining (arrow) in injured articular cartilage and in the growth plate (left) and β-catenin immunostaining of a consecutive section (right). B, X-GAL staining of un- stimulated (control) and WNT3a stimulated BAT-GAL articular cartilage dissected from femoral heads. Sections were counterstained with eosin. Real time PCR analysis for axin2 (C) in mouse cartilage explants following stimulation with recombinant WNT3a or the vehicle of the proteins (0.1%BSA-PBS). Values are expressed as mean and standard deviation.

7.6: Validation of Axin2 KI mice as reporters for Wnt signalling

Axin2 mRNA was upregulated after injury in adult human cartilage explants and in mice with joint surface defects. Knock-in (KI) mice in which a lacZ cassette replaces exon 2 of the axin2 gene can be used as a reporter for axin2 and since the expression of axin2 is under the control of Wnt signaling and Axin2 may even be a universal Wnt transcriptional target, these mice may serve as a useful Wnt reporter (279). In addition, Axin2 is a repressor of the canonical wnt signalling and therefore these mutants are expected to display increased Wnt/β-catenin signalling thereby providing the opportunity to study the effect of excessive wnt activation on joint regeneration/OA development after injury.

Axin2 KI mice were subjected to either arthrotomy (sham operated) or arthrotomy and joint surface injury (injured) and mice were killed 1, 3 and 7 days after surgery and X-GAL staining was performed. B-galactosidase expression was detected in chondrocytes and bone marrow cells in the sham operated joints (Figure 7.10) but surprisingly disappeared completely one day after cartilage injury (Figure 7.10). This could be caused by either disruption of a regulatory element within the exon that was removed affecting axin-2 promoter activity and rendering these mice unsuitable as reporter for Wnt signalling or by suppression of the Wnt signalling in Axin2 KI mice following joint surface injury. To further investigate whether canonical Wnt pathway is modulated in Axin2 KI mice, β-catenin immunostaining was performed on sections obtained from these mice. No cytoplasmic accumulation or nuclear localization of β-catenin was observed in articular cartilage after injury (Figure 7.10) not only suggesting the

unsuitability of these mice as Wnt reporter in adult life, but also that disruption of Axin2 might have interfered with the activation of the canonical Wnt signalling.

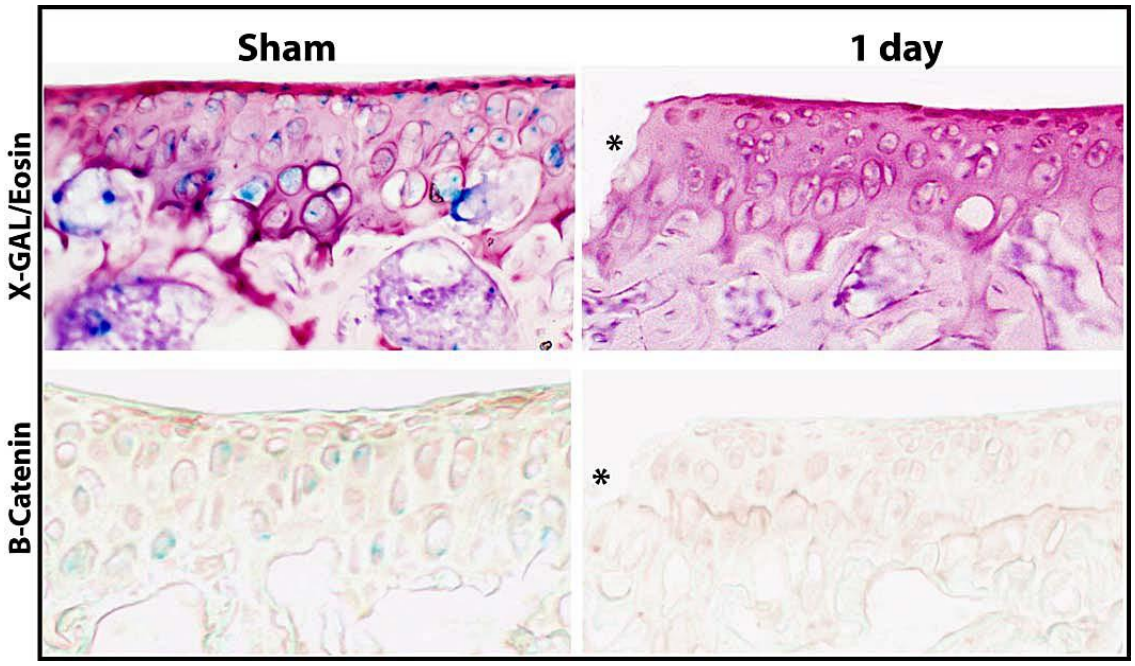

Figure 7.10: Axin2 KI mice in the joint surface injury model: X-Gal staining (upper panel) and β-catenin immunostaining (lower panel) of sham operated (left) and injured (right) knee joints (positive X-GAL cells appear in either blue when sections counter-stained with eosin or green when sections immunostained for β-catenin). Asterisks point to the site of injury.

Discussion

In this chapter, we have validated *in vivo* the molecular response of articular cartilage to acute mechanical injury that has been previously characterized *in vitro*. In agreement with the *in vitro* data from adult human articular cartilage explants, joint surface injury *in vivo* was also associated with activation of the BMP and Wnt pathways which are known to play a crucial role in joint development, morphogenesis and homeostasis. These findings not only confirm the *in vitro* data but also suggest that such response to injury is evolutionary conserved.

BMP-2 was upregulated in articular cartilage following injury *in vivo* in C56BL/6 and DBA/1 mice concomitant with phosphorylation of SMAD-1/-5/-8 indicating modulation of BMP signaling. BMP-2 was detected in the injured articular cartilage in both strains for at least 8 weeks post-surgery suggesting that some of the molecular signals triggered by joint surface injury might not be transient and instead be needed for a long time to regulate and co-ordinate the different components of the repair process. BMPs are known to elicit an anabolic response in articular cartilage both in vitro (119) and in vivo (123;124). Therefore, it is possible that the presence of BMP-2 in C57BL/6 mice at late time points might represent an anabolic effort to resist structural damage to cartilage after injury. The persistence of BMP-2 up-regulation for long periods after injury *in vivo* might explain our previous *in vitro* data in which the expression level of BMP-2 mRNA and the number of PSMAD-1/-5/-8 positive cells in the rested explants were intermediate between the freshly isolated explants and the injured ones and further support our conclusion that the resting period was not sufficient to completely reverse the response due to the initial dissection of the explants.

In addition to the modulation of BMP signaling, our *in vivo* and *in vitro* studies showed up-regulation of Wnt16 ligands and associated activation of the canonical Wnt pathway. However, in contrast to the *in vitro* data in which other Wnt ligands including Wnt4 and Wnt9a (known to co-expressed with Wnt16 in the prospective joints during embryonic skeletogenesis) were not regulated upon injury, Wnt4 mRNA was upregulated *in vivo* after joint surface injury in both strains. Besides the many differences between the 2 experimental systems, one possible explanation for this discrepancy is that if Wnt4 up-regulation following injury persists for more than 6 days, it would not be detected in the microarray experiment as long lasting gene regulation induced by dissection will not subside within the 6 days of the resting period and therefore, after being reinjured, rested-control and injured samples will have similar gene expression levels. Such regulation would instead be revealed by comparing the injured and rested control to the freshly dissected explants but since both rested controls and injured explants are exposed to cultured conditions whereas the freshly dissected explants are not, it is not possible to discriminate between genes regulated by injury and genes regulated by exposure to culture conditions. Another discrepancy between the *in vitro* microarray data and the *in vivo* validation was seen in the expression of OPG following injury. OPG mRNA was upregulated in injured adult human articular cartilage but, under our experimental conditions, no significant differences were found either in mRNA or protein level between injured mouse joints and sham operated controls. This could be due to differences related to species or the time point of activation. In addition, OPG is constitutively expressed at high level in bone and cartilage in vivo. This might have masked an up-regulation following injury.

At later time points after *in vivo* joint surface injury, Wnt16 expression subsided, but β catenin accumulation persisted and acquired a cytoplasmic granular pattern. β catenin is a dual function protein that plays a crucial role in regulating both Wnt signal transduction and cell adhesion through binding to the cytoplasmic domain of cadherins and linking it to the actin cytoskeleton (242). The different regulation of β-catenin at early and late time points following cartilage injury could be due to activation of Wnt signalling probably required earlier for stem cell regulation and cell fate determination and the adhesive functions required later for organizing tissue architecture and morphogenesis. A detailed *in vivo* characterization of the expression pattern and dynamics of all Wnt ligand and other components of the pathway including target genes and binding partners of β-catenin following cartilage injury in both strains is still needed to better understand the involvement of the Wnt pathway in outcome determination after JSI.

Wnt proteins are pleiotropic signalling molecules and their functions are highly context dependent. For instance, this study as well as others (273);(95) has demonstrated that activation of the canonical Wnt pathway resulted in up-regulation of cartilage marker genes aggrecan and Col2A mRNA suggesting an anabolic response whereas under different experimental conditions, it induced downregulation of aggrecan and Col2A (274) and stimulated the expression of catabolic genes such as MMPs and ADAMTSs (91). Furthermore, activation of the canonical Wnt signalling has been shown to suppress chondrogenesis in some systems (274;280) but promotes it under other experimental models (281;282). In this regard, it is also interesting that both gain and loss of function of β-catenin in adult articular chondrocytes resulted in an OA like phenotype although through different mechanisms. The most likely explanation of these

apparently contrasting data is that tight spatiotemporal regulation of the pathway is necessary for joint homeostasis.

Wnt signalling has been implicated in the regulation of stem cell maintenance, proliferation, migration and fate decision (247). Thus, tracking Wnt pathway activity following cartilage injury in vivo (where adult articular cartilage interacts with neighbouring tissues within the joints) might lead to the identification of joint specific targets of Wnt modulation that might contribute to joint surface repair. Challenging BAT-GAL mice in the in vivo model of JSI however showed no *lac*Z expression in articular cartilage following injury or upon treatment with Wnt3a ligand despite the up-regulation of the Wnt target gene Axin2. It is unlikely that the failure to identify X-Gal positive cells in injured and Wnt treated articular cartilage was due to lack of penetration efficacy of the staining into the tissues as the same negative results were obtained with performing the staining either in whole mount or in individual sections and in addition, positive cells were identified within deeper bone marrow spaces. Previous studies have reported instances in which BAT-Gal reporter mice failed to label sites of Known Wnt/β catenin signalling in the skin and pancreas (283;284). Transgenic TCF reporters are designed to detect the canonical Wnt dependent transcriptional activation through TCF. However, β catenin can activate Wnt target genes in a TCF-independent manner (285) and TCF can activate transcription in the absence of Wnt signalling (286) generating false negative or false positive results. Furthermore, TCF is known to interact with co-repressors to directly inhibit transcription in the absence of Wnt signalling (287). Therefore it is possible that Wnt signalling events that direct the de-repression of TCF target genes, but not trigger activation by TCF, might not be detected by TCF reporters which can not sense changes in repression (288).

Unexpectedly, Axin2/LacZ knock-in mice failed to up-regulate β-galactosidase expression or to accumulate β-catenin in articular cartilage following injury. These results suggest that Axin2 might be required for the activation of Wnt signalling. It has been demonstrated that Axin2 is required for the initial signalling cascade and specifically in the phosphorylation of LRP6 at the cell membrane via its ability to recruit GSK-3 (289). Therefore, it is possible that the disruption of the axin2 gene in this animal model might have compromised the activation of the pathway following injury.

These results indicate that the BAT-GAL and Axin2/LacZ knock-in mice are unsuitable as Wnt reporters in adult articular cartilage. However, despite the inability to track wnt target cells, we have demonstrated that mechanical injury to adult articular cartilage *in vivo* results in reactivation of morphogenetic pathways. This *in vivo* reproducibility of the signalling events previously observed in human cartilage following injury provides an opportunity to explore the function of different molecules in joint surface regeneration/degeneration after injury. In the next chapter, we have used the in vivo murine model of JSI to investigate whether the injury induced up-regulation of Wnt16 was required for cartilage repair in this model.

Conclusions

❖ Morphogenetic pathways such as BMP and Wnt are modulated following mechanical injury in vivo

❖ BAT-GAL and Axin2/LacZ knock-in mice are not suitable as reporters for the canonical wnt pathway activation in adult articular cartilage.

CHAPTER 8: RESULTS

Functional validation of Wnt16 in cartilage regeneration and development of OA in vivo

The experiments so far have confirmed that the gene modulations that we described following injury to human cartilage explants are also reproduced *in vivo* in the mouse model of acute joint surface injury/repair. Thus this model gives the opportunity to address the function of different molecules modulated in response to injury and hence we decided to use it to study the requirement of Wnt16 for cartilage repair.

Wnt16 was the only Wnt ligand to be up-regulated in human adult articular cartilage following injury. This up-regulation was confirmed in vivo using the mouse model of joint surface injury/repair and was associated with cytoplasmic accumulation and nuclear localization of β-catenin and up-regulation of gens encoding Wnt target genes such as Axin2 in vitro and in vivo. The regulation of Wnt16 after cartilage injury may play a role in activating a repair response or it could be a pathogenic mechanism contributing to cartilage degradation and PTOA development or it could be just an adaptive response to injury. The aim of this chapter was to investigate the function of Wnt16 in the context of joint surface regeneration/degeneration.

8.1: Requirement of Wnt16 for joint surface repair

Wnt16 deficient mouse mutants were obtained through a collaboration with Professor Jing Yu and Professor Andrew McMahon (Harvard University, Boston USA) on a mixed background (backcrossed 5 times onto the 129SvEv strain starting from a 129/C57BL/6 background) and appeared phenotypically normal and fertile. Heterozygous mice were then intercrossed to generate homozygous mutants and wild type littermates for comparison. There was no difference in the skeletal morphology of adult 10 weeks old Wnt16 null mice compared to wild type mice (Figure 8.1A-C).

Furthermore, the standard histological analysis of the knee joint tissue did not reveal any morphological difference between the KO mice and their WT controls (Figure 8.1D & E).

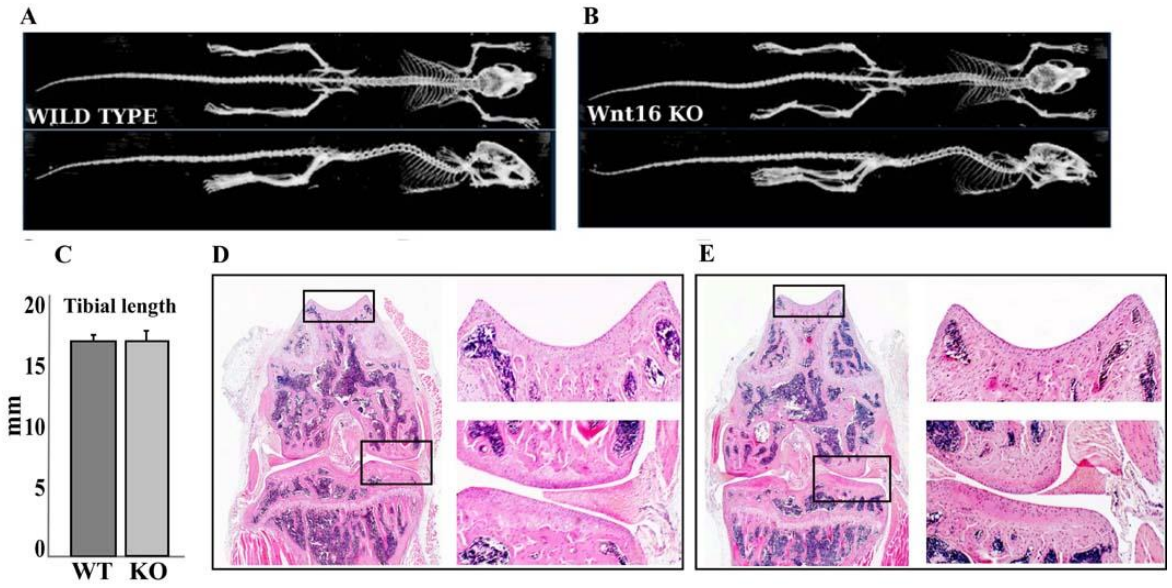

Figure 8.1: Wnt16 null mice have normal skeletal and joint morphology: 3D reconstruction of the skeleton of adult male $Wnt16^{+/+}$ (A) and $wnt16^{-/-}$ (B) showing no obvious abnormalities. (C) The measurement of adult WT and KO mice tibial length. (D-E) are H&E staining of sections from WT (D) and KO (E) knee joints showing normal structures. Boxed areas of the patellar groove and tibio-femoral joints at left are shown in higher magnifications at right.

To investigate whether Wnt16 plays a functional role in the repair process of joint surface defects, adult Wnt16 homozygous null mutants and wild type littermates were challenged in the in vivo model of joint surface injury. Eight weeks following injury, the animals were killed and the outcome was evaluated histologically and quantified by histological scoring systems (188;238;239). Unfortunately, in this background, the regeneration in wild type mice was poor and variable with filling of most of the defects

with non cartilaginous tissue that stained negative for SO staining (Figure 8.2A). On the other hand, most of the Wnt16 null mice failed to repair the defect with any tissue (Figure 8.2B). The repair scores (Figure 8.2C) were better in WT mice although not statistically significantly. Mild degree of post-traumatic OA was observed in both WT and KO mice with no statistical significant difference in Mankin scores (Fig. 8.2D)

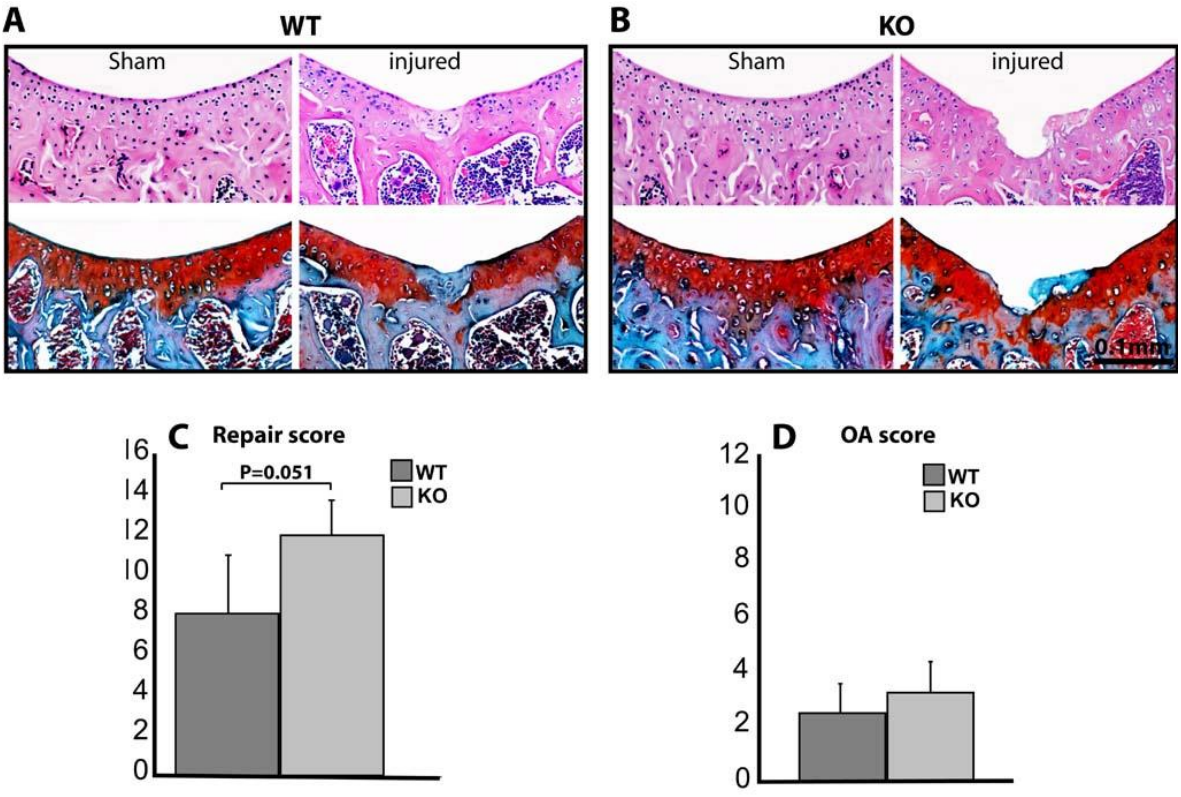

Figure 8.2: Wnt16 KO mice in joint surface injury model: (A-B), H&E (upper panel) and Safranin O (lower panel) staining of sections from sham and injured WT 129FvEv mice (A) and Wnt16 KO mice (B) 8 weeks after injury. (C-D), repair scores (C) and modified Mankin scores (D) of WT (n=6) and KO (n=5) at 8 weeks time points. Low score in C indicated better repair and high scores in D indicated more severe OA. All values are expressed as mean ± standard error of the mean (S.E.M).

These preliminary results show that this injury model is unsuitable for mice on this mixed 129/C57BL/6 background. Despite this and the generally poor repair in WT animals (poorly differentiated tissue filling most defects, Figure 8.2), the outcome was generally worse in mutants with no tissue filling the defect, thereby resulting in a difference that was approaching statistical significance. This suggests that in the appropriate background (pure DBA/1) we might be able to observe a clearer phenotype. The backcrossing of Wnt16 mice into the DBA/1 background is currently in progress in our laboratory.

8.2: Wnt16 expression in murine OA

Wnt16 was upregulated upon injury in vitro in adult human cartilage explants and in vivo in mice. This up-regulation was not exclusive to the acute mechanical injury model but was also relevant to osteoarthritis as Wnt16 was abundantly present in human osteoarthritic cartilage but was undetectable in preserved cartilage areas of the same joint.

To test whether Wnt16 is also regulated in osteoarthritis in mice, we utilized an OA mouse model in which osteoarthritis is induced by surgical destabilization of the medial meniscus (DMM) (32). This model is relevant to human OA since meniscal instability is well known to lead to OA in humans (160) and it has been validated in the 129SvEv genetic background (158) and therefore, if the Wnt16 up-regulation was also present in mice, this model could be used to test its function in the context of OA development. Wnt16 was undetected in the sham operated control knees but upregulated in murine

osteoarthritis as early as 2 days following the surgical destabilization of the medial meniscus (Figure 8.3)

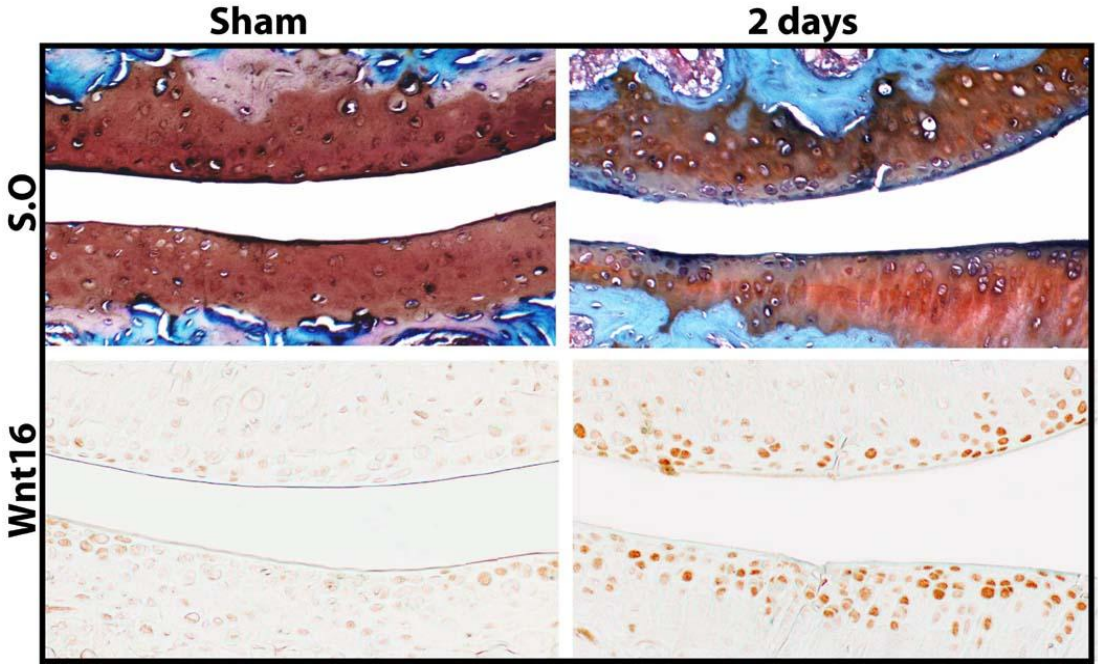

Figure 8.3: Wnt16 in instability induced OA model: S.O (upper panel) and immunostaining for Wnt16 (lower panel) in sections from sham operated or destabilized knee joints 2 days following DMM.

8.3: Development of OA in WT and Wnt16$^{-/-}$ mice

Encouraged by the confirmation of Wnt16 up-regulation in the DMM model of OA, we sought to investigate whether such regulation has a role in OA development by challenging Wnt16 null mice and wild type littermates in the surgically induced instability model of OA (DMM). The mice were killed 8 weeks after surgery and the outcome was analysed histologically and the degree of osteoarthritis was assessed with two well established OA scoring systems by two independent observers blinded to the genotype of the mice.

Neither Wnt16 null mice nor the wild type littermates developed spontaneously any feature of OA (Figure 8.4). However, following destabilization of medial meniscus, Wnt16$^{-/-}$ mice developed more severe OA than their wild type littermates. Fibrillations, moderate loss of articular cartilage and loss of proteoglycans were the main features observed in WT mice (Figure 8.4A) whereas, deep lesions, major loss of cartilage and diffuse hypocellularity were a hallmark of OA developed in Wnt16 deficient mice (Figure 8.4B). Both the Mankin (Figure 8.4C) and the Chambers' (Figure 8.4D) OA scores were statistically significantly higher in Wnt16-/- mice compared to their wild type littermates in the medial compartments. As expected in this model, a mild degree of OA was observed in the lateral compartment without difference between WT and KO mice (Figure 8.4 A-D). These data shows that Wnt16 is required for cartilage homeostasis in challenge conditions and suggests a role in cartilage protection against breakdown in osteoarthritis.

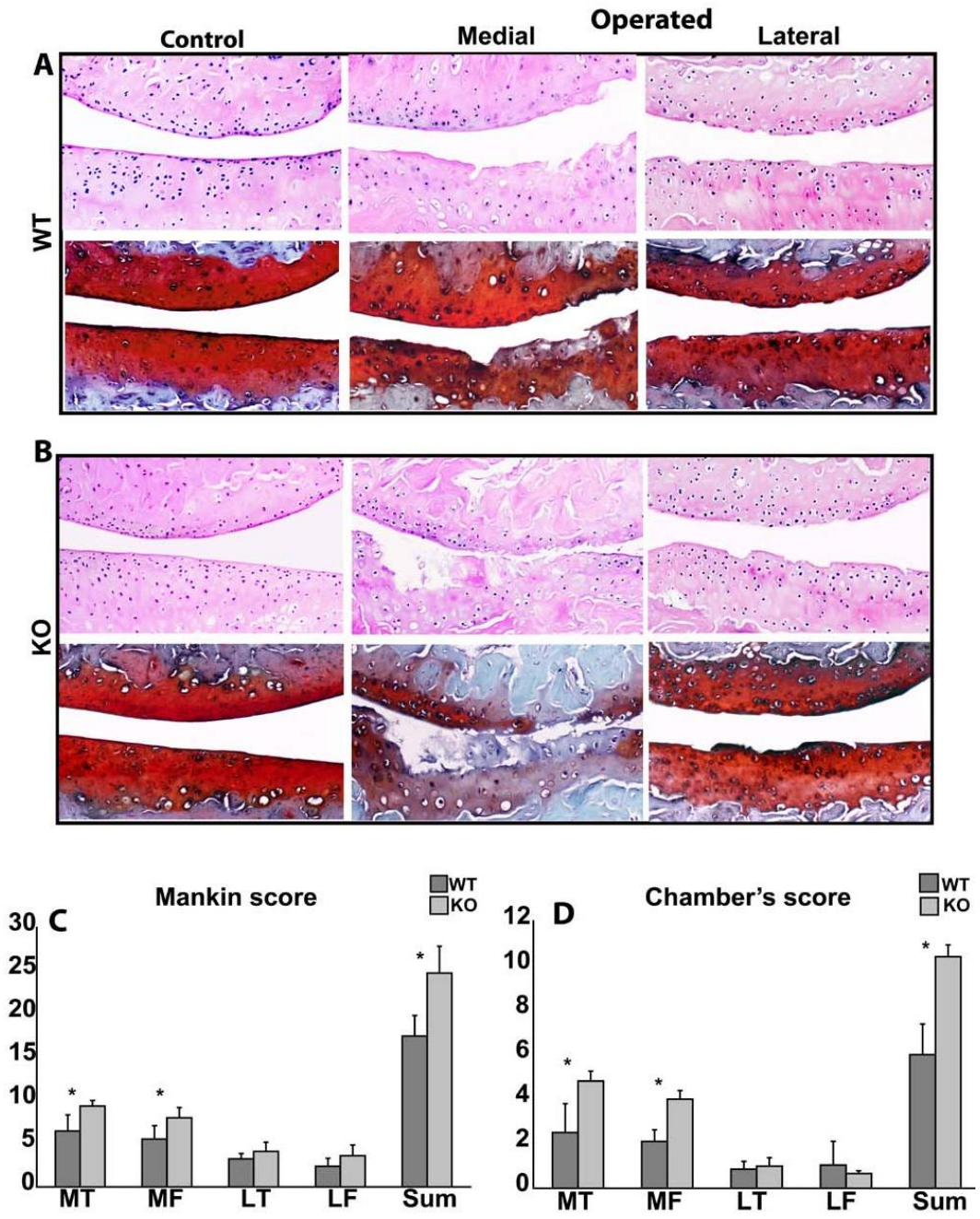

Figure 8.4: OA development in male Wnt16 null mice and WT littermates: A-B, Representative H&E (upper panel) and S.O (lower panel) stained sections from control and challenged "operated " wild type (A) and Wnt16$^{-/-}$ mice (B) 8 weeks after medial meniscus destabilization. C-D, Mankin (C) and Chambers' (D) scores of challenged WT (n=4) and Wnt16$^{-/-}$ mice (n=4). Higher scores indicate more severe OA. Values are expressed as mean and standard error of the mean (S.E.M). **P*=<0.05. MT=Medial Tibia. MF=Medial femur. LT=Lateral Tibia. LF=Lateral Tibia.

Epidemiological studies have demonstrated sex-related differences in human OA development with higher prevalence in men before the age of 50. However, after menopause the incidence and the severity of the disease increase significantly in women (290). This is in keeping with male mice developing more severe OA than female in DMM model (291), which is regularly performed in young animals.

To investigate whether the more severe OA outcome of wnt16 deficient mutants was sex dependent, joint instability was surgically induced by DMM in female Wnt16 null mice and wild type littermates. Mice were then killed at 8 weeks following surgery and cartilage degradation was evaluated histologically and graded by the Modified Mankin and Chambers scoring systems.

As expected, wild type female mice developed milder OA than males but OA was more severe in $Wnt16^{-/-}$ female mice as compared to their wild type littermates. Superficial fibrillation and localized loss of proteoglycans were observed in WT mice (Figure 8.5A), while extensive fibrillation and deep erosions extending to the calcified cartilage were seen in Wnt16 deficient mice (Figure 8.5B). OA developed almost exclusively within the medial compartment. A statistical significant difference between medial tibial and femoral OA scores of WT and KO mice was shown by both Mankin (Figure 8.5C) and Chamber (Figure 8.5D).

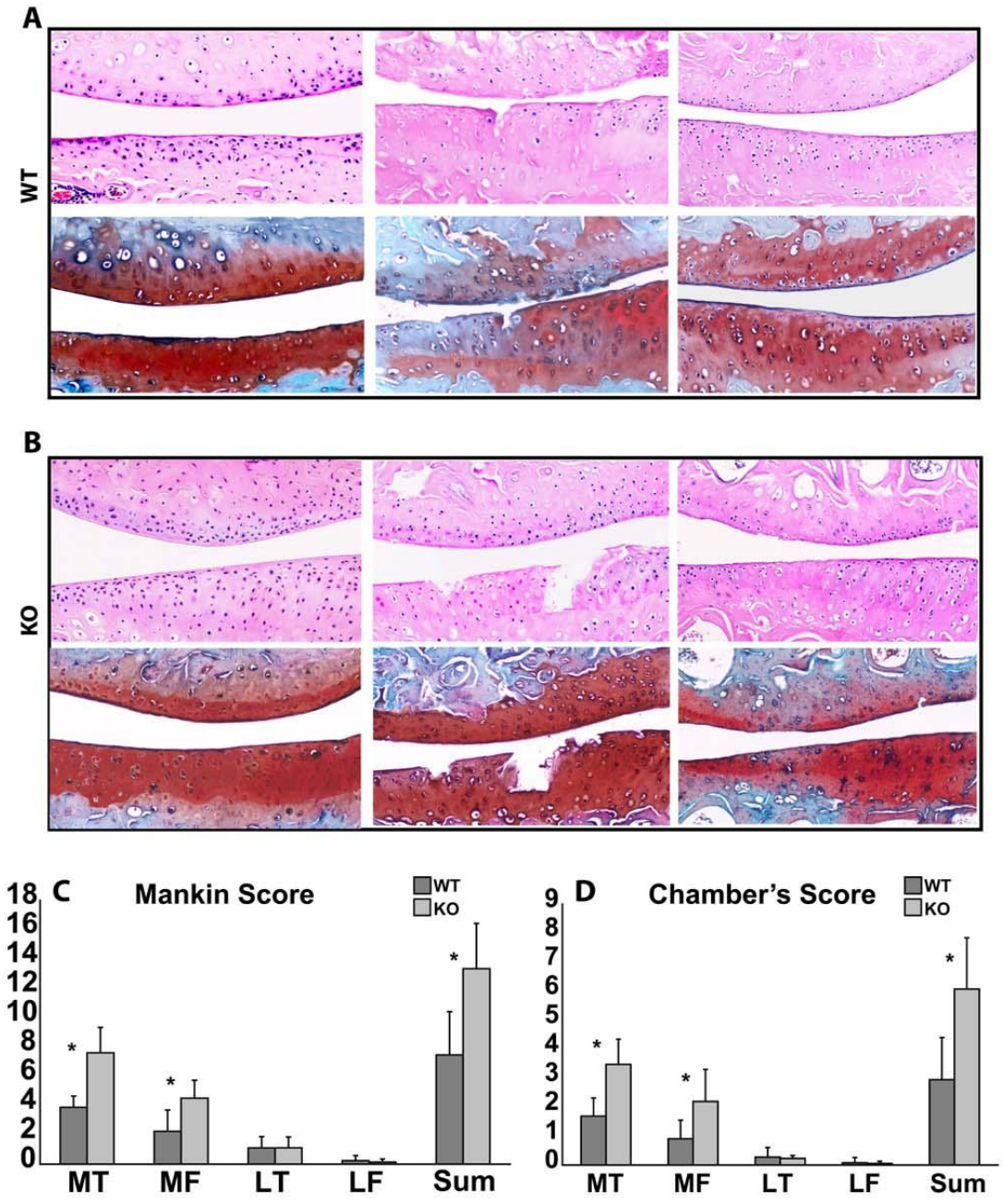

Figure 8.5: OA development in female Wnt16 null mice and WT littermates: A-B, Representative H&E (upper panel) and S.O (lower panel) stained sections from control and challenged "operated " wild type (A) and Wnt16$^{-/-}$ mice (B) 8 weeks after medial meniscus destabilization. C-D, Mankin (C) and Chambers' (D) scores of challenged WT (n=6) and Wnt16$^{-/-}$ mice (n=6). Higher scores indicate more severe OA. Values are expressed as mean and standard error of the mean (S.E.M). **P*=<0.05. MT=Medial Tibia. MF=Medial femur. LT=Lateral Tibia. LF=Lateral Tibia.

OA was more severe in 129SvEv wild type male mice than females after DMM. The summed mean scores of male mice were more than two folds higher than that of the female mice using both the Mankin (Fig. 8.6A) and Chambers (Fig. 8.6B) scoring systems at 8 weeks after surgery. Interestingly, the same ratio was observed between summed OA scores of males and females Wnt16$^{-/-}$ mice (Fig. 8.6). Both male and female Wnt16 deficient mice developed significantly more severe OA lesions than their wild type littermates. The mean summed scores for Wnt16$^{-/-}$ mice were nearly 1.5 fold higher than that for wild type mice in both sexes (Fig. 8.6).

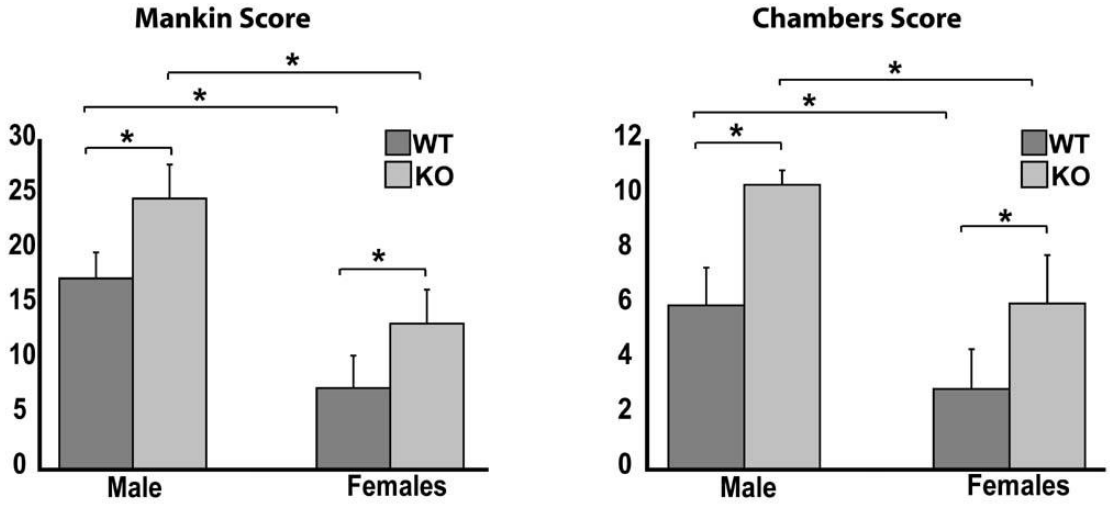

Figure 8.6: OA severity in male and female mice: Summed Mankin (A) and Chambers (B) histological scores for Wnt16$^{+/+}$ and Wnt16$^{-/-}$ mice 8 weeks after DMM in males and females. The values are expressed as the mean of the highest 3 sections scores ± SEM. * = P<0.05.

Discussion

In this chapter, we have investigated the involvement of Wnt16 in joint surface repair and homeostasis and showed preliminary results that suggest a chondroprotective role for Wnt16 in vivo. Wnt16, along with other Wnt ligands such as Wnt4 and Wnt9a, are expressed in the developing synovial joints where they play an essential role in joint specification and formation (47). In adult cartilage, however, Wnt16 is not expressed in normal joints but re-expressed only upon mechanical cartilage injury with activation of the canonical Wnt pathway. These data points to the tissue specificity of this ligand in the biological context of cartilage injury since neither Wnt16 nor β-catenin were upregulated in sham operated joints which were subjected to arthrotomy and patellar dislocation without cartilage injury.

The absence of overt developmental skeletal abnormalities in Wnt16 deficient mice could be explained by the presence of other Wnt family members such as Wnt4, Wnt9a which could potentially compensate the loss of Wnt16 activity during embryonic development. The targeted disruption of Wnt4 also did not show any skeletal phenotype (80) but deficiency of both Wnt4 and Wnt9a resulted in joint fusions and synovial chondroid metaplasia (292) thereby, supporting the existence of functional redundancy, at least during development, between these different Wnt ligands.

The preliminary functional validation of Wnt16 following cartilage injury showed better histological repair response of WT mice compared to Wnt16 null mice. Although this difference was not statistically significant, it still suggests that Wnt16 might have a role in promoting/supporting the repair response. Failure to detect significant differences could be due to insufficient number of mice or the inability of the scoring system to

distinguish between inferior repair tissue (seen in WT mice) and total absence of repair tissue (seen in KO littermates). Further studies in DBA/1 background are still necessary to first confirm these preliminary results and then to elucidate the molecular and cellular mechanisms through which Wnt16 supports the repair process. Thereafter, the ability of Wnt16 to improve regeneration of chronic joint surface lesions in strains with poor repair should be explored.

Wnt16 up-regulation was also relevant to osteoarthritis as it was abundantly present in human cartilage affected by OA and expressed after destabilization of medial meniscus in an instability induced model of OA. In this model, Wnt16 deficient mice developed more severe OA compared to wild type littermates in a sex-independent fashion suggesting that Wnt16 might has a chondroprotective effect that, after chronic injury, can not be compensated.

Although, the skeleton of Wnt16 deficient mice was indistinguishable from that of wild type mice in CT scans and their joint tissue appeared normal on histological examination, it is still possible that subtle differences in their joint architecture might have rendered them more susceptible to OA after induction of joint instability. Therefore, more detailed quantitative comparison of the skeleton of mutants and wild type mice as well as investigating the ability of exogenous Wnt16 delivery to reverse the OA phenotype in $Wnt16^{-/-}$ mice to levels seen in $Wnt16^{+/+}$ mice are required to confirm that the more severe OA seen in Wnt16 null mice is not due to any developmental defect that may influence the development of OA after DMM but rather due to a critical role of Wnt16 in cartilage degradation/regeneration taking place during OA development. Wnt16 might suppress some mechanisms of cartilage breakdown and/or enhance the anabolic/regeneration mechanisms. The biological processes and molecular mechanisms

leading to more severe OA development in Wnt16 null mutants following DMM remain to be investigated.

Conclusions

- Wnt16 is expressed after DMM and plays a role in outcome determination in experimental osteoarthritis.

CHAPTER 9

General Discussion

Traumatic cartilage lesions represent a common symptomatic and disabling problem (130;131) that often requires surgical intervention to relieve pain and to prevent possible evolution towards secondary OA (293). However, the evidence that full thickness articular cartilage defects can sometimes heal spontaneously (141-143) (151;236) demonstrates that adult joints possess repair machinery that, under appropriate conditions, can lead to anatomical and functional restoration. The absence of relevant pre-clinical animal models of joint surface regeneration suitable for molecular studies and genetic manipulation has represented a bottleneck for the understanding of the molecular and cellular mechanisms regulating joint surface healing and consequently the development of novel therapeutics to enhance/support this repair process. In this study, we have developed and characterized a novel murine model in which the repair outcome of a well controlled, consistent and reproducible full thickness JSD is dependent on the strain and the age of the mice and we have used this model to study the role of wnt16 regulation in the homeostatic response of articular cartilage to injury.

In this in vivo model, adult DBA/1 mice reproducibly healed experimental joint surface lesions, whereas age-matched C57BL/6 healed poorly and instead developed features of secondary osteoarthritis. This strain-dependent ability to repair cartilage and prevent progression towards PTOA demonstrates that there are genetic factors that govern the response of articular cartilage to injury and hence participate in outcome determination. This animal model of joint surface injury/repair could therefore represent a valuable tool to elucidate the molecular basis for articular cartilage regeneration and to address the functionality and hierarchy of molecules involved in the response to injury through the use of suitable genetically modified mice.

The natural history of JSD is so far unpredictable given the high variability in the repair capacity and the susceptibility to cartilage degeneration among human population (143;251). This variability was reproduced in the inbred mouse strains and was associated with different regulation of measurable anabolic and catabolic parameters. Such parameters could thus be used as biomarkers to predict the outcome of joint surface injury. The ability of cartilage to heal after injury and to prevent further degradation in mice correlated with a decline in cell death, persistent proliferation, type II collagen neo-synthesis, less type II collagen degradation, less aggrecanase and more MMP- induced aggrecan degradation. These data point to a potential window for therapeutic intervention to prevent posttraumatic OA with inhibitors of apoptosis and inhibitors of aggrecanases and/or MMPs that are being developed and tested in preclinical and clinical studies (294-296).

The relationship between susceptibility to OA and capacity for repair are not well understood. It is known that C57BL/6 mice develop spontaneous OA with ageing (297) and they are more susceptible than DBA/1 to OA induced by medial meniscus destabilization (DMM) (26). However, spontaneous OA appears in C57BL/6 mice only after their first year of age, and no signs of OA were present in control or sham-operated joints in our study. It is therefore unlikely that pre-existing osteoarthritis or joint instability inadvertently induced during surgery were the causes for repair failure. On the other hand, the generation of a JSD in C57BL/6 mice precipitated the appearance of secondary OA features as early as 1 week after injury. At 4 weeks, when the OA features in C57BL/6 mice had advanced, there was also a clear difference in repair outcome compared to DBA/1. It is possible that the rapid development of secondary OA may have conditioned repair failure. Our experimental setup does not discriminate

whether the failure of repair and the development of OA are causally related, or if they represent distinct processes resulting from an inferior joint homeostatic mechanism in C57BL/6 than in DBA/1mice. However, the observation that aged DBA/1 mice did not repair and did not develop OA either, under our experimental conditions and at the time points examined, demonstrates that repair failure alone may not be sufficient for the development of secondary OA and suggests that the two processes may be, at least in part, uncoupled. In this regard, it must be stressed that this model is not a model of primary OA, but rather a model of joint surface injury and repair that provides the opportunity to investigate the function of the injury- regulated genes in that acute context. However, the occurrence of post-traumatic OA in C57BL/6 mice suggests that it could be also used to study the mechanism by which repair influences progression of post-traumatic secondary OA and vice versa.

One important determinant of repair outcome could be local inflammation (261). Indeed, DBA/1 mice are responsive to inflammatory arthritis models such as type II collagen-induced arthritis leading to extensive new tissue formation and joint ankylosis whereas C57BL/6 mice are resistant (298). A modest infiltrate was present in the synovial membrane of the sham and injured mice from both strains during the first week following surgery suggesting that it is not specific to cartilage injury but rather a reaction to the surgical procedure. However, it is possible that different regulation of the inflammatory response may play a role in repair outcomes.

The repair of JSDs encompasses highly coordinated biological events that require a fine tuning of diverse processes including cellular apoptosis, proliferation and tissue patterning regulated in a temporal-spatial manner however, the molecular mechanisms regulating this process are poorly understood. We have demonstrated that mechanical

injury to adult articular cartilage resulted in a robust response with reactivation of morphogenetic pathways such as BMP and Wnt (241). In addition, previous studies have demonstrated the release of fibroblast growth factor 2 (FGF-2) from injured articular cartilage (216) and showed a chondroprotective role of this growth factor in vivo (299). Taken together, these data support our hypothesis that injured articular cartilage can be a source of signaling molecules that might participate in determining the outcome of joint surface defect.

BMPs are known to elicit an anabolic response in articular cartilage both in vitro (119) and in vivo (123;124), and it has been shown that it is required for joint homeostasis in adulthood (300). Indeed, targeted deletion of the gene encoding BMP receptor 1A in the articular cartilage of mice resulted in joint surface degeneration resembling OA (128) and polymorphism in BMP-2 gene was associated with increased susceptibility to OA development (122). Moreover, BMPs play a crucial role in regulating the recruitment of progenitor cells and promoting their differentiation into the chondrogenic lineage during embryonic skeletogenesis. Finally, the expression of BMP-2 mRNA was linked to the capacity of in vitro expanded adult human articular chondrocytes to form stable cartilage in vivo that is resistant to vascular invasion and endochondral bone formation (176). Therefore, the recruitment of chondroprogenitors, the regulation of chondrogenesis and cartilage ECM synthesis as well as the preservation of the phenotypic stability of articular chondrocytes could all be potential roles of BMP signaling in JSD repair. Indeed, BMPs including BMP-2 have been tested in experimental cartilage tissue engineering approaches (209) and several systems for their delivery including gene therapy have been evaluated (301) with encouraging results. However, if over-expressed can cause detrimental side effects such as ectopic bone formation and osteophyte (215).

Therefore, their potential for clinical use strongly depends on the use of optimum safe levels as well as on the use of efficient and safe delivery systems.

The function of the canonical Wnt signaling in the context of joint surface injury/repair is still poorly understood. Several lines of evidence in many systems have demonstrated that the activation of Wnt signaling enhances wound healing (302), supports repair (244-246) and promotes limb regeneration in regenerating animals (303) through regulating stem cell maintenance, proliferation, migration and fate determination (247). It is therefore possible that the Wnt pathway might have a similar function in the repair of JSDs. However, other studies have suggested a role of abnormal Wnt signaling in the pathogenesis of osteoarthritis. For example, Allelic variants of the Wnt inhibitor FRZB (86), Wnt co-receptor LRP5 (89) and WISP (90) were associated with the development of OA in humans. Furthermore, the Wnt pathway has been involved in cartilage destruction by regulating matrix degradation (91), chondrocyte apoptosis and dedifferentiation (92). In this regard, it is interesting that both gain and loss of function of β-catenin in adult skeleton results in cartilage loss and OA development (95;96). These data imply that Wnt signaling is pivotal in regulating chondrocyte survival and maintenance in postnatal life and that controlled balance between positive and negative signals is required for joint homoeostasis and repair but such mechanisms that are set into action to support repair in adulthood may also play a pathogenic role when not appropriately regulated.

The modulation of the Wnt pathway has been an attractive therapeutic strategy to modify disease progression in arthritis and to enhance repair in many tissues (304). Although constitutive activation of Wnt pathway can lead to abnormal cell growth and

cancer (305), its tightly controlled modulation might have therapeutic benefit in regenerative medicine (306). Given the complexity of the Wnt signaling with the involvement of many agonists, receptors and antagonists (63), it is important to select a relevant tissue specific target in order to limit the undesirable side effects. Our data demonstrate a high level of specificity of Wnt16 in the biological context of cartilage injury. Wnt16 was the only Wnt ligand to be modulated in adult human cartilage following injury indicating ligand specificity and was re-expressed in mice following cartilage injury or meniscal destabilization but not following sham operation where injury to joint capsule and synovial membrane occur indicating tissue specificity. Moreover, despite the expression of several Wnt ligands in the joint environment and their modulation during OA, the absence of Wnt16 was not compensated following DMM and resulted in more severe OA in Wnt16 null mice as compared to wild type littermates indicating its functional specificity. The identification of a very specific ligand such as Wnt16 represents an opportunity to support cartilage homeostasis and repair with minimum side effect/toxicity. The presence of suitable mouse models of joint surface injury/repair and OA, together with the availability of Wnt16 deficient mutant mice will allow addressing the functionality of Wnt16 in vivo during the process of cartilage regeneration/degradation. Subsequently, this knowledge can be exploited for the development of novel molecular therapeutics to improve joint surface healing in cell-free in situ tissue engineering approaches.

Appendix

Ethylenediaminetetraacetic acid (EDTA_pH 8.0

20g of EDTA were dissolved in 80ml H_2O. NaOH was used to adjust the pH. Distilled water was added to the final volume of 100 ml. The solution was stored at room temperature and diluted to 4% to be used

Toluidine blue

0.1% Toluidine blue (Sigma, UK) in 0.1M acetate buffer, pH 5. To prepare acetate buffer, mix 14.8ml of stock A (0.6ml glacial acetic acid MW 60.05 in100cm distilled water) to 35.2ml of stock B (0.82g sodium acetate anhydrous MW 82 in 100cm distilled water) and bring it to 100ml with distilled water.

Safranin O

0.2% in distilled water with 0.2M glacial acetic acid = 1,2 ml glacial acetic acid + 20ml 1% SO bring to 100ml.

Light green

0.5% in 500ml distilled water with 1ml glacial acetic acid.

X-gal staining solution

Final staining Reagents	**Stock**	**To make 1ml**
X-Gal 1mg/ml	50mg/ml	20µl
10X PBS	10 X	100µl
5mM Potassium ferrocyanide	50mM (211mg/10ml)	100µl
5mM Potassium ferricyanide	50mM	100µl
5mM EGTA	0.5M	10µl
2mM MgCl2	1M	2µl
0.02% NP-40	1	20µl
Water		648µl

Sodium Citrate Buffer

Dissolve 2.94g Sodium Citrate in 1L of distilled water and adjust pH to 6.

10x PBS

Add 80g sodium chloride (NaCl), 2g potassium chloride (KCl), 14.4g sodium phosphate diphasic (Na_2HPO_4) and 2.4g potassium phosphate monobasic (KH_2PO_4) to 1L distilled water and adjust pH to 7.4.

HRP Avidin-Biotin Complex (DAKO)

10 μl of Solution 1 were added to 1 ml of TBS pH 7.6, and mixed well. Another 10 μl of solution 2 were added and mixed well. The ABC complex was prepared at least 45' before use.

Tris Acetic acid EDTA (TAE buffer 50X)

242 of Tris base, 57.1ml of acetic acid and 18.6g of EDTA were dissolved in 800ml of distilled water. Distilled water was added to the final volume of 1L and the solution was stored at room temperature and diluted to 1X before use.

Radio Immuno Precipitation Assay (RIPA) buffer

Final concentration	Reagents for 200ml
150mM NaCl	1.75g NaCl
1% NP-40	2ml NP-40
0.5% deoxycholc acid	1g deoxycholc acid
0.1% SDS	1ml 20% SDS
50mM Tris pH 8	6.67ml 1.5M Tris pH 8
Distilled water	Fill to 200ml d water

Tris-Glycine transfer buffer

Tris base (12 mM) 1.45 g, Glycine (96 mM) 7.2 g and Methanol (20% final concentration) 200 ml were dissolved in 800ml of distilled water. Distilled water was added to the final volume of 1L

Publications

(1) **Eltawil NM**, De Bari C, Achan P, Pitzalis C, Dell'accio F, A novel in vivo murine model of cartilage regeneration. Age and strain-dependent outcome after joint surface injury. Osteoarthritis Cartilage, 2009 Jun; 17 (6):695-704.

Accompanied by Editorial; Lories RJ, Luyten FP, Progress towards a molecular basis for joint surface repair. Osteoarthritis Cartilage, 2009 Jun;17 (6):693-4.

Evaluated as "must read" in Faculty of 1000 by Linda Sandell. Faculty of 1000 Medicine, 15 May 2009. Evaluations for Eltawil NM et al., *Osteoarthritis and Cartilage*. http://www.f1000medicine.com/article/id/1160512/evaluation

(2) Dell'accio F, DeBari C, **Eltawil NM**, Vanhummelen P, Pitzalis C. Molecular response of articular cartilage to injury by microarray screening. Wnt16 expression and signalling after injury and in osteoarthritis. Arthritis Rheum 2008 May; 58(5):1410-21.

Accompanied by Editorial; Vincent TL, Saklatvala J. Is the response to injury relevant to osteoarthritis? Arthritis Rheum. 2008 May; 58 (5):1207-10.

(3) Dell'Accio F, De Bari C, **El Tawil NM**, Barone F, Mitsiadis TA, O'Dowd J, et al. Activation of WNT and BMP signaling in adult human articular cartilage following mechanical injury. Arthritis Res.Ther. 2006; 8:R139.

(4) Hughes C, Faurholm B, Dell'accio F, Manzo A, Seed M, **Eltawil N** et al. Human single chain fragment variable (scFv) that specifically targets arthritic cartilage. Arthritis Rheum 2010. In press

References

(1) Allan DA. Structure and physiology of joints and their relationship to repetitive strain injuries. Clin Orthop Relat Res 1998;(351):32-38.

(2) Huber M, Trattnig S, Lintner F. Anatomy, biochemistry, and physiology of articular cartilage. Invest Radiol 2000; 35(10):573-580.

(3) Poole AR, Kojima T, Yasuda T, Mwale F, Kobayashi M, Laverty S. Composition and structure of articular cartilage: a template for tissue repair. Clin Orthop Relat Res 2001;(391 Suppl):S26-S33.

(4) Schumacher BL, Block JA, Schmid TM, Aydelotte MB, Kuettner KE. A novel proteoglycan synthesized and secreted by chondrocytes of the superficial zone of articular cartilage. Arch Biochem Biophys 1994; 311(1):144-152.

(5) Bhosale AM, Richardson JB. Articular cartilage: structure, injuries and review of management. Br Med Bull 2008; 87:77-95.

(6) Schmid TM, Linsenmayer TF. Immunohistochemical localization of short chain cartilage collagen (type X) in avian tissues. J Cell Biol 1985; 100(2):598-605.

(7) Archer CW, Francis-West P. The chondrocyte. Int J Biochem Cell Biol 2003; 35(4):401-404.

(8) Poole CA, Flint MH, Beaumont BW. Morphological and functional interrelationships of articular cartilage matrices. J Anat 1984; 138 (Pt 1):113-138.

(9) Chi SS, Rattner JB, Matyas JR. Communication between paired chondrocytes in the superficial zone of articular cartilage. J Anat 2004; 205(5):363-370.

(10) Gonzalez S, Fragoso-Soriano RJ, Kouri JB. Chondrocytes interconnecting tracks and cytoplasmic projections observed within the superficial zone of normal human articular cartilage--a transmission electron microscopy, atomic force microscopy, and two-photon excitation microscopy studies. Microsc Res Tech 2007; 70(12):1072-1078.

(11) Martin JA, Buckwalter JA. Aging, articular cartilage chondrocyte senescence and osteoarthritis. Biogerontology 2002; 3(5):257-264.

(12) Guilak F, Alexopoulos LG, Upton ML, Youn I, Choi JB, Cao L et al. The pericellular matrix as a transducer of biomechanical and biochemical signals in articular cartilage. Ann N Y Acad Sci 2006; 1068:498-512.

(13) Vincent TL, McLean CJ, Full LE, Peston D, Saklatvala J. FGF-2 is bound to perlecan in the pericellular matrix of articular cartilage, where it acts as a chondrocyte mechanotransducer. Osteoarthritis Cartilage 2007; 15(7):752-763.

(14) Eyre DR. Collagens and cartilage matrix homeostasis. Clin Orthop Relat Res 2004;(427 Suppl):S118-S122.

(15) Stenzel KH, Miyata T, Rubin AL. Collagen as a biomaterial. Annu Rev Biophys Bioeng 1974; 3(0):231-253.

(16) Little CB, Meeker CT, Golub SB, Lawlor KE, Farmer PJ, Smith SM et al. Blocking aggrecanase cleavage in the aggrecan interglobular domain abrogates cartilage erosion and promotes cartilage repair. J Clin Invest 2007; 117(6):1627-1636.

(17) Knudson CB, Knudson W. Cartilage proteoglycans. Semin Cell Dev Biol 2001; 12(2):69-78.

(18) Hildebrand A, Romaris M, Rasmussen LM, Heinegard D, Twardzik DR, Border WA et al. Interaction of the small interstitial proteoglycans biglycan, decorin and fibromodulin with transforming growth factor beta. Biochem J 1994; 302 (Pt 2):527-534.

(19) Rosenberg K, Olsson H, Morgelin M, Heinegard D. Cartilage oligomeric matrix protein shows high affinity zinc-dependent interaction with triple helical collagen. J Biol Chem 1998; 273(32):20397-20403.

(20) Bay-Jensen AC, Andersen TL, Charni-Ben TN, Kristensen PW, Kjaersgaard-Andersen P, Sandell L et al. Biochemical markers of type II collagen breakdown and synthesis are positioned at specific sites in human osteoarthritic knee cartilage. Osteoarthritis Cartilage 2007.

(21) Roberts S, Hollander AP, Caterson B, Menage J, Richardson JB. Matrix turnover in human cartilage repair tissue in autologous chondrocyte implantation. Arthritis Rheum 2001; 44(11):2586-2598.

(22) Visse R, Nagase H. Matrix metalloproteinases and tissue inhibitors of metalloproteinases: structure, function, and biochemistry. Circ Res 2003; 92(8):827-839.

(23) Page-McCaw A, Ewald AJ, Werb Z. Matrix metalloproteinases and the regulation of tissue remodelling. Nat Rev Mol Cell Biol 2007; 8(3):221-233.

(24) Kevorkian L, Young DA, Darrah C, Donell ST, Shepstone L, Porter S et al. Expression profiling of metalloproteinases and their inhibitors in cartilage. Arthritis Rheum 2004; 50(1):131-141.

(25) Okada Y, Shinmei M, Tanaka O, Naka K, Kimura A, Nakanishi I et al. Localization of matrix metalloproteinase 3 (stromelysin) in osteoarthritic cartilage and synovium. Lab Invest 1992; 66(6):680-690.

(26) Glasson SS. In vivo osteoarthritis target validation utilizing genetically-modified mice. Curr Drug Targets 2007; 8(2):367-376.

(27) Brewster M, Lewis EJ, Wilson KL, Greenham AK, Bottomley KM. Ro 32-3555, an orally active collagenase selective inhibitor, prevents structural damage in the STR/ORT mouse model of osteoarthritis. Arthritis Rheum 1998; 41(9):1639-1644.

(28) Sandy JD, Flannery CR, Neame PJ, Lohmander LS. The structure of aggrecan fragments in human synovial fluid. Evidence for the involvement in osteoarthritis of a novel proteinase which cleaves the Glu 373-Ala 374 bond of the interglobular domain. J Clin Invest 1992; 89(5):1512-1516.

(29) Lohmander LS, Neame PJ, Sandy JD. The structure of aggrecan fragments in human synovial fluid. Evidence that aggrecanase mediates cartilage degradation in inflammatory joint disease, joint injury, and osteoarthritis. Arthritis Rheum 1993; 36(9):1214-1222.

(30) Tortorella MD, Burn TC, Pratta MA, Abbaszade I, Hollis JM, Liu R et al. Purification and cloning of aggrecanase-1: a member of the ADAMTS family of proteins. Science 1999; 284(5420):1664-1666.

(31) Abbaszade I, Liu RQ, Yang F, Rosenfeld SA, Ross OH, Link JR et al. Cloning and characterization of ADAMTS11, an aggrecanase from the ADAMTS family. J Biol Chem 1999; 274(33):23443-23450.

(32) Glasson SS, Askew R, Sheppard B, Carito B, Blanchet T, Ma HL et al. Deletion of active ADAMTS5 prevents cartilage degradation in a murine model of osteoarthritis. Nature 2005; 434(7033):644-648.

(33) Gendron C, Kashiwagi M, Lim NH, Enghild JJ, Thogersen IB, Hughes C et al. Proteolytic activities of human ADAMTS-5: comparative studies with ADAMTS-4. J Biol Chem 2007; 282(25):18294-18306.

(34) Glasson SS, Askew R, Sheppard B, Carito BA, Blanchet T, Ma HL et al. Characterization of and osteoarthritis susceptibility in ADAMTS-4-knockout mice. Arthritis Rheum 2004; 50(8):2547-2558.

(35) Dean DD, Martel-Pelletier J, Pelletier JP, Howell DS, Woessner JF, Jr. Evidence for metalloproteinase and metalloproteinase inhibitor imbalance in human osteoarthritic cartilage. J Clin Invest 1989; 84(2):678-685.

(36) Sahebjam S, Khokha R, Mort JS. Increased collagen and aggrecan degradation with age in the joints of Timp3(-/-) mice. Arthritis Rheum 2007; 56(3):905-909.

(37) Baker AH, Edwards DR, Murphy G. Metalloproteinase inhibitors: biological actions and therapeutic opportunities. J Cell Sci 2002; 115(Pt 19):3719-3727.

(38) Saklatvala J. Tumour necrosis factor alpha stimulates resorption and inhibits synthesis of proteoglycan in cartilage. Nature 1986; 322(6079):547-549.

(39) Lotz M, Blanco FJ, von KJ, Dudler J, Maier R, Villiger PM et al. Cytokine regulation of chondrocyte functions. J Rheumatol Suppl 1995; 43:104-108.

(40) Mankin HJ, Jennings LC, Treadwell BV, Trippel SB. Growth factors and articular cartilage. J Rheumatol Suppl 1991; 27:66-67.

(41) Hui W, Rowan AD, Cawston T. Modulation of the expression of matrix metalloproteinase and tissue inhibitors of metalloproteinases by TGF-beta1 and IGF-1 in primary human articular and bovine nasal chondrocytes stimulated with TNF-alpha. Cytokine 2001; 16(1):31-35.

(42) Goldring MB, Tsuchimochi K, Ijiri K. The control of chondrogenesis. J Cell Biochem 2006; 97(1):33-44.

(43) Akiyama H. Control of chondrogenesis by the transcription factor Sox9. Mod Rheumatol 2008; 18(3):213-219.

(44) Karsenty G, Wagner EF. Reaching a genetic and molecular understanding of skeletal development. Dev Cell 2002; 2(4):389-406.

(45) Francis-West PH, Parish J, Lee K, Archer CW. BMP/GDF-signalling interactions during synovial joint development. Cell Tissue Res 1999; 296(1):111-119.

(46) Hartmann C, Tabin CJ. Wnt-14 plays a pivotal role in inducing synovial joint formation in the developing appendicular skeleton. Cell 2001; 104(3):341-351.

(47) Guo X, Day TF, Jiang X, Garrett-Beal L, Topol L, Yang Y. Wnt/beta-catenin signaling is sufficient and necessary for synovial joint formation. Genes Dev 2004; 18(19):2404-2417.

(48) Brunet LJ, McMahon JA, McMahon AP, Harland RM. Noggin, cartilage morphogenesis, and joint formation in the mammalian skeleton. Science 1998; 280(5368):1455-1457.

(49) Niedermaier M, Schwabe GC, Fees S, Helmrich A, Brieske N, Seemann P et al. An inversion involving the mouse Shh locus results in brachydactyly through dysregulation of Shh expression. J Clin Invest 2005; 115(4):900-909.

(50) Edwards JC, Wilkinson LS, Jones HM, Soothill P, Henderson KJ, Worrall JG et al. The formation of human synovial joint cavities: a possible role for hyaluronan and CD44 in altered interzone cohesion. J Anat 1994; 185 (Pt 2):355-367.

(51) Pacifici M, Koyama E, Shibukawa Y, Wu C, Tamamura Y, Enomoto-Iwamoto M et al. Cellular and molecular mechanisms of synovial joint and articular cartilage formation. Ann N Y Acad Sci 2006; 1068:74-86.

(52) Dowthwaite GP, Edwards JC, Pitsillides AA. An essential role for the interaction between hyaluronan and hyaluronan binding proteins during joint development. J Histochem Cytochem 1998; 46(5):641-651.

(53) Pitsillides AA, Archer CW, Prehm P, Bayliss MT, Edwards JC. Alterations in hyaluronan synthesis during developing joint cavitation. J Histochem Cytochem 1995; 43(3):263-273.

(54) Koyama E, Shibukawa Y, Nagayama M, Sugito H, Young B, Yuasa T et al. A distinct cohort of progenitor cells participates in synovial joint and articular cartilage formation during mouse limb skeletogenesis. Dev Biol 2008; 316(1):62-73.

(55) Pacifici M, Koyama E, Iwamoto M. Mechanisms of synovial joint and articular cartilage formation: recent advances, but many lingering mysteries. Birth Defects Res C Embryo Today 2005; 75(3):237-248.

(56) Miller JR. The Wnts. Genome Biol 2002; 3(1):REVIEWS3001.

(57) Willert K, Brown JD, Danenberg E, Duncan AW, Weissman IL, Reya T et al. Wnt proteins are lipid-modified and can act as stem cell growth factors. Nature 2003; 423(6938):448-452.

(58) Bradley RS, Brown AM. The proto-oncogene int-1 encodes a secreted protein associated with the extracellular matrix. EMBO J 1990; 9(5):1569-1575.

(59) Secchiero P, Melloni E, Corallini F, Beltrami AP, Alviano F, Milani D et al. Tumor necrosis factor-related apoptosis-inducing ligand promotes migration of human bone marrow multipotent stromal cells. Stem Cells 2008; 26(11):2955-2963.

(60) Reichsman F, Smith L, Cumberledge S. Glycosaminoglycans can modulate extracellular localization of the wingless protein and promote signal transduction. J Cell Biol 1996; 135(3):819-827.

(61) Fuerer C, Habib SJ, Nusse R. A study on the interactions between heparan sulfate proteoglycans and Wnt proteins. Dev Dyn 2009.

(62) Komiya Y, Habas R. Wnt signal transduction pathways. Organogenesis 2008; 4(2):68-75.

(63) Fuerer C, Nusse R, Ten BD. Wnt signalling in development and disease. Max Delbruck Center for Molecular Medicine meeting on Wnt signaling in Development and Disease. EMBO Rep 2008; 9(2):134-138.

(64) Winklbauer R, Medina A, Swain RK, Steinbeisser H. Frizzled-7 signalling controls tissue separation during Xenopus gastrulation. Nature 2001; 413(6858):856-860.

(65) Grigoryan T, Wend P, Klaus A, Birchmeier W. Deciphering the function of canonical Wnt signals in development and disease: conditional loss- and gain-of-function mutations of {beta}-catenin in mice. Genes Dev 2008; 22(17):2308-2341.

(66) Yamamoto H, Sakane H, Yamamoto H, Michiue T, Kikuchi A. Wnt3a and Dkk1 regulate distinct internalization pathways of LRP6 to tune the activation of beta-catenin signaling. Dev Cell 2008; 15(1):37-48.

(67) Wharton KA, Jr., Zimmermann G, Rousset R, Scott MP. Vertebrate proteins related to Drosophila Naked Cuticle bind Dishevelled and antagonize Wnt signaling. Dev Biol 2001; 234(1):93-106.

(68) Behrens J, Jerchow BA, Wurtele M, Grimm J, Asbrand C, Wirtz R et al. Functional interaction of an axin homolog, conductin, with beta-catenin, APC, and GSK3beta. Science 1998; 280(5363):596-599.

(69) Tang Y, Liu Z, Zhao L, Clemens TL, Cao X. Smad7 stabilizes beta-catenin binding to E-cadherin complex and promotes cell-cell adhesion. J Biol Chem 2008; 283(35):23956-23963.

(70) Tang Y, Liu Z, Zhao L, Clemens TL, Cao X. Smad7 stabilizes beta-catenin binding to E-cadherin complex and promotes cell-cell adhesion. J Biol Chem 2008; 283(35):23956-23963.

(71) Nelson WJ, Nusse R. Convergence of Wnt, beta-catenin, and cadherin pathways. Science 2004; 303(5663):1483-1487.

(72) Takemaru KI, Moon RT. The transcriptional coactivator CBP interacts with beta-catenin to activate gene expression. J Cell Biol 2000; 149(2):249-254.

(73) Barker N, Hurlstone A, Musisi H, Miles A, Bienz M, Clevers H. The chromatin remodelling factor Brg-1 interacts with beta-catenin to promote target gene activation. EMBO J 2001; 20(17):4935-4943.

(74) Kramps T, Peter O, Brunner E, Nellen D, Froesch B, Chatterjee S et al. Wnt/wingless signaling requires BCL9/legless-mediated recruitment of pygopus to the nuclear beta-catenin-TCF complex. Cell 2002; 109(1):47-60.

(75) Chen G, Fernandez J, Mische S, Courey AJ. A functional interaction between the histone deacetylase Rpd3 and the corepressor groucho in Drosophila development. Genes Dev 1999; 13(17):2218-2230.

(76) Takemaru K, Yamaguchi S, Lee YS, Zhang Y, Carthew RW, Moon RT. Chibby, a nuclear beta-catenin-associated antagonist of the Wnt/Wingless pathway. Nature 2003; 422(6934):905-909.

(77) Daniels DL, Weis WI. ICAT inhibits beta-catenin binding to Tcf/Lef-family transcription factors and the general coactivator p300 using independent structural modules. Mol Cell 2002; 10(3):573-584.

(78) Ishitani T, Ninomiya-Tsuji J, Nagai S, Nishita M, Meneghini M, Barker N et al. The TAK1-NLK-MAPK-related pathway antagonizes signalling between beta-catenin and transcription factor TCF. Nature 1999; 399(6738):798-802.

(79) Spater D, Hill TP, Gruber M, Hartmann C. Role of canonical Wnt-signalling in joint formation. Eur Cell Mater 2006; 12:71-80.

(80) Stark K, Vainio S, Vassileva G, McMahon AP. Epithelial transformation of metanephric mesenchyme in the developing kidney regulated by Wnt-4. Nature 1994; 372(6507):679-683.

(81) James IE, Kumar S, Barnes MR, Gress CJ, Hand AT, Dodds RA et al. FrzB-2: a human secreted frizzled-related protein with a potential role in chondrocyte apoptosis. Osteoarthritis Cartilage 2000; 8(6):452-463.

(82) Nakamura Y, Nawata M, Wakitani S. Expression profiles and functional analyses of Wnt-related genes in human joint disorders. Am J Pathol 2005; 167(1):97-105.

(83) Blom AB, Brockbank SM, van Lent PL, van Beuningen HM, Geurts J, Takahashi N et al. Involvement of the Wnt signaling pathway in experimental and human osteoarthritis: prominent role of Wnt-induced signaling protein 1. Arthritis Rheum 2009; 60(2):501-512.

(84) Geyer M, Grassel S, Straub RH, Schett G, Dinser R, Grifka J et al. Differential transcriptome analysis of intraarticular lesional vs intact cartilage reveals new candidate genes in osteoarthritis pathophysiology. Osteoarthritis Cartilage 2009; 17(3):328-335.

(85) Hopwood B, Tsykin A, Findlay DM, Fazzalari NL. Microarray gene expression profiling of osteoarthritic bone suggests altered bone remodelling,

WNT and transforming growth factor-beta/bone morphogenic protein signalling. Arthritis Res Ther 2007; 9(5):R100.

(86) Loughlin J, Dowling B, Chapman K, Marcelline L, Mustafa Z, Southam L et al. Functional variants within the secreted frizzled-related protein 3 gene are associated with hip osteoarthritis in females. Proc Natl Acad Sci U S A 2004; 101(26):9757-9762.

(87) Lopez-Rios J, Esteve P, Ruiz JM, Bovolenta P. The Netrin-related domain of Sfrp1 interacts with Wnt ligands and antagonizes their activity in the anterior neural plate. Neural Dev 2008; 3:19.

(88) Lories RJ, Peeters J, Bakker A, Tylzanowski P, Derese I, Schrooten J et al. Articular cartilage and biomechanical properties of the long bones in Frzb-knockout mice. Arthritis Rheum 2007; 56(12):4095-4103.

(89) Urano T, Shiraki M, Narusawa K, Usui T, Sasaki N, Hosoi T et al. Q89R polymorphism in the LDL receptor-related protein 5 gene is associated with spinal osteoarthritis in postmenopausal Japanese women. Spine 2007; 32(1):25-29.

(90) Urano T, Narusawa K, Shiraki M, Usui T, Sasaki N, Hosoi T et al. Association of a single nucleotide polymorphism in the WISP1 gene with spinal osteoarthritis in postmenopausal Japanese women. J Bone Miner Metab 2007; 25(4):253-258.

(91) Yuasa T, Otani T, Koike T, Iwamoto M, Enomoto-Iwamoto M. Wnt/beta-catenin signaling stimulates matrix catabolic genes and activity in articular chondrocytes: its possible role in joint degeneration. Lab Invest 2008; 88(3):264-274.

(92) Hwang SG, Ryu JH, Kim IC, Jho EH, Jung HC, Kim K et al. Wnt-7a causes loss of differentiated phenotype and inhibits apoptosis of articular chondrocytes via different mechanisms. J Biol Chem 2004; 279(25):26597-26604.

(93) Hwang SG, Yu SS, Lee SW, Chun JS. Wnt-3a regulates chondrocyte differentiation via c-Jun/AP-1 pathway. FEBS Lett 2005; 579(21):4837-4842.

(94) Diarra D, Stolina M, Polzer K, Zwerina J, Ominsky MS, Dwyer D et al. Dickkopf-1 is a master regulator of joint remodeling. Nat Med 2007; 13(2):156-163.

(95) Zhu M, Tang D, Wu Q, Hao S, Chen M, Xie C et al. Activation of beta-Catenin Signaling in Articular Chondrocytes Leads to Osteoarthritis-Like Phenotype in Adult beta-Catenin Conditional Activation Mice. J Bone Miner Res 2008.

(96) Zhu M, Chen M, Zuscik M, Wu Q, Wang YJ, Rosier RN et al. Inhibition of beta-catenin signaling in articular chondrocytes results in articular cartilage destruction. Arthritis Rheum 2008; 58(7):2053-2064.

(97) Lories RJ, Luyten FP. Bone morphogenetic protein signaling in joint homeostasis and disease. Cytokine Growth Factor Rev 2005; 16(3):287-298.

(98) Matthews SJ. Biological activity of bone morphogenetic proteins (BMP's). Injury 2005; 36 Suppl 3:S34-S37.

(99) Xiao YT, Xiang LX, Shao JZ. Bone morphogenetic protein. Biochem Biophys Res Commun 2007; 362(3):550-553.

(100) Miyazono K, Maeda S, Imamura T. BMP receptor signaling: transcriptional targets, regulation of signals, and signaling cross-talk. Cytokine Growth Factor Rev 2005; 16(3):251-263.

(101) Thomas JT, Kilpatrick MW, Lin K, Erlacher L, Lembessis P, Costa T et al. Disruption of human limb morphogenesis by a dominant negative mutation in CDMP1. Nat Genet 1997; 17(1):58-64.

(102) Duprez D, Bell EJ, Richardson MK, Archer CW, Wolpert L, Brickell PM et al. Overexpression of BMP-2 and BMP-4 alters the size and shape of developing skeletal elements in the chick limb. Mech Dev 1996; 57(2):145-157.

(103) Pathi S, Rutenberg JB, Johnson RL, Vortkamp A. Interaction of Ihh and BMP/Noggin signaling during cartilage differentiation. Dev Biol 1999; 209(2):239-253.

(104) Storm EE, Huynh TV, Copeland NG, Jenkins NA, Kingsley DM, Lee SJ. Limb alterations in brachypodism mice due to mutations in a new member of the TGF beta-superfamily. Nature 1994; 368(6472):639-643.

(105) Polinkovsky A, Robin NH, Thomas JT, Irons M, Lynn A, Goodman FR et al. Mutations in CDMP1 cause autosomal dominant brachydactyly type C. Nat Genet 1997; 17(1):18-19.

(106) Storm EE, Kingsley DM. GDF5 coordinates bone and joint formation during digit development. Dev Biol 1999; 209(1):11-27.

(107) Settle SH, Jr., Rountree RB, Sinha A, Thacker A, Higgins K, Kingsley DM. Multiple joint and skeletal patterning defects caused by single and double mutations in the mouse Gdf6 and Gdf5 genes. Dev Biol 2003; 254(1):116-130.

(108) Zou H, Niswander L. Requirement for BMP signaling in interdigital apoptosis and scale formation. Science 1996; 272(5262):738-741.

(109) Nishida Y, Knudson CB, Eger W, Kuettner KE, Knudson W. Osteogenic protein 1 stimulates cells-associated matrix assembly by normal human articular chondrocytes: up-regulation of hyaluronan synthase, CD44, and aggrecan. Arthritis Rheum 2000; 43(1):206-214.

(110) Gong Y, Krakow D, Marcelino J, Wilkin D, Chitayat D, Babul-Hirji R et al. Heterozygous mutations in the gene encoding noggin affect human joint morphogenesis. Nat Genet 1999; 21(3):302-304.

(111) Dixon ME, Armstrong P, Stevens DB, Bamshad M. Identical mutations in NOG can cause either tarsal/carpal coalition syndrome or proximal symphalangism. Genet Med 2001; 3(5):349-353.

(112) Stottmann RW, Anderson RM, Klingensmith J. The BMP antagonists Chordin and Noggin have essential but redundant roles in mouse mandibular outgrowth. Dev Biol 2001; 240(2):457-473.

(113) Blaney Davidson EN, Vitters EL, van der Kraan PM, van den Berg WB. Expression of transforming growth factor-beta (TGFbeta) and the TGFbeta signalling molecule SMAD-2P in spontaneous and instability-induced osteoarthritis: role in cartilage degradation, chondrogenesis and osteophyte formation. Ann Rheum Dis 2006; 65(11):1414-1421.

(114) Nakase T, Miyaji T, Tomita T, Kaneko M, Kuriyama K, Myoui A et al. Localization of bone morphogenetic protein-2 in human osteoarthritic cartilage and osteophyte. Osteoarthritis Cartilage 2003; 11(4):278-284.

(115) Chubinskaya S, Kumar B, Merrihew C, Heretis K, Rueger DC, Kuettner KE. Age-related changes in cartilage endogenous osteogenic protein-1 (OP-1). Biochim Biophys Acta 2002; 1588(2):126-134.

(116) Erlacher L, Ng CK, Ullrich R, Krieger S, Luyten FP. Presence of cartilage-derived morphogenetic proteins in articular cartilage and enhancement of matrix replacement in vitro. Arthritis Rheum 1998; 41(2):263-273.

(117) Tardif G, Hum D, Pelletier JP, Boileau C, Ranger P, Martel-Pelletier J. Differential gene expression and regulation of the bone morphogenetic protein antagonists follistatin and gremlin in normal and osteoarthritic human chondrocytes and synovial fibroblasts. Arthritis Rheum 2004; 50(8):2521-2530.

(118) Nakayama N, Han CY, Cam L, Lee JI, Pretorius J, Fisher S et al. A novel chordin-like BMP inhibitor, CHL2, expressed preferentially in chondrocytes of developing cartilage and osteoarthritic joint cartilage. Development 2004; 131(1):229-240.

(119) Luyten FP, Yu YM, Yanagishita M, Vukicevic S, Hammonds RG, Reddi AH. Natural bovine osteogenin and recombinant human bone morphogenetic

protein-2B are equipotent in the maintenance of proteoglycans in bovine articular cartilage explant cultures. J Biol Chem 1992; 267(6):3691-3695.

(120) Chubinskaya S, Hakimiyan A, Pacione C, Yanke A, Rappoport L, Aigner T et al. Synergistic effect of IGF-1 and OP-1 on matrix formation by normal and OA chondrocytes cultured in alginate beads. Osteoarthritis Cartilage 2006.

(121) Miyamoto Y, Mabuchi A, Shi D, Kubo T, Takatori Y, Saito S et al. A functional polymorphism in the 5' UTR of GDF5 is associated with susceptibility to osteoarthritis. Nat Genet 2007; 39(4):529-533.

(122) Valdes AM, Hart DJ, Jones KA, Surdulescu G, Swarbrick P, Doyle DV et al. Association study of candidate genes for the prevalence and progression of knee osteoarthritis. Arthritis Rheum 2004; 50(8):2497-2507.

(123) Glansbeek HL, van Beuningen HM, Vitters EL, Morris EA, van der Kraan PM, van den Berg WB. Bone morphogenetic protein 2 stimulates articular cartilage proteoglycan synthesis in vivo but does not counteract interleukin-1alpha effects on proteoglycan synthesis and content. Arthritis Rheum 1997; 40(6):1020-1028.

(124) Blaney Davidson EN, Vitters EL, van Lent PL, van de Loo FA, van den Berg WB, van der Kraan PM. Elevated extracellular matrix production and degradation upon bone morphogenetic protein-2 (BMP-2) stimulation point toward a role for BMP-2 in cartilage repair and remodeling. Arthritis Res Ther 2007; 9(5):R102.

(125) van Beuningen HM, Glansbeek HL, van der Kraan PM, van den Berg WB. Differential effects of local application of BMP-2 or TGF-beta 1 on both articular cartilage composition and osteophyte formation. Osteoarthritis Cartilage 1998; 6(5):306-317.

(126) Badlani N, Inoue A, Healey R, Coutts R, Amiel D. The protective effect of OP-1 on articular cartilage in the development of osteoarthritis. Osteoarthritis Cartilage 2008; 16(5):600-606.

(127) Sekiya I, Tang T, Hayashi M, Morito T, Ju YJ, Mochizuki T et al. Periodic knee injections of BMP-7 delay cartilage degeneration induced by excessive running in rats. J Orthop Res 2009; 27(8):1088-1092.

(128) Rountree RB, Schoor M, Chen H, Marks ME, Harley V, Mishina Y et al. BMP receptor signaling is required for postnatal maintenance of articular cartilage. PLoS Biol 2004; 2(11):e355.

(129) Lories RJ, Daans M, Derese I, Matthys P, Kasran A, Tylzanowski P et al. Noggin haploinsufficiency differentially affects tissue responses in destructive and remodeling arthritis. Arthritis Rheum 2006; 54(6):1736-1746.

(130) Curl WW, Krome J, Gordon ES, Rushing J, Smith BP, Poehling GG. Cartilage injuries: a review of 31,516 knee arthroscopies. Arthroscopy 1997; 13(4):456-460.

(131) Hjelle K, Solheim E, Strand T, Muri R, Brittberg M. Articular cartilage defects in 1,000 knee arthroscopies. Arthroscopy 2002; 18(7):730-734.

(132) Widuchowski W, Widuchowski J, Trzaska T. Articular cartilage defects: study of 25,124 knee arthroscopies. Knee 2007; 14(3):177-182.

(133) Widuchowski W, Kusz D, Widuchowski J, Faltus R, Szyluk K. [Analysis of articular cartilage lesions in 5114 knee arthroscopies]. Chir Narzadow Ruchu Ortop Pol 2006; 71(2):117-121.

(134) Brittberg M, Peterson L, Sjogren-Jansson E, Tallheden T, Lindahl A. Articular cartilage engineering with autologous chondrocyte transplantation. A review of recent developments. J Bone Joint Surg Am 2003; 85-A Suppl 3:109-115.

(135) Buckwalter JA, Brown TD. Joint injury, repair, and remodeling: roles in post-traumatic osteoarthritis. Clin Orthop Relat Res 2004;(423):7-16.

(136) Gelber AC, Hochberg MC, Mead LA, Wang NY, Wigley FM, Klag MJ. Joint injury in young adults and risk for subsequent knee and hip osteoarthritis. Ann Intern Med 2000; 133(5):321-328.

(137) Ding C, Cicuttini F, Jones G. Tibial subchondral bone size and knee cartilage defects: relevance to knee osteoarthritis. Osteoarthritis Cartilage 2007; 15(5):479-486.

(138) Wluka AE, Ding C, Jones G, Cicuttini FM. The clinical correlates of articular cartilage defects in symptomatic knee osteoarthritis: a prospective study. Rheumatology (Oxford) 2005; 44(10):1311-1316.

(139) Qvist P, Bay-Jensen AC, Christiansen C, Dam EB, Pastoureau P, Karsdal MA. The disease modifying osteoarthritis drug (DMOAD): Is it in the horizon? Pharmacol Res 2008; 58(1):1-7.

(140) Hunter W. Of the structure and disease of articulating cartilages. 1743. Clin Orthop Relat Res 1995;(317):3-6.

(141) Messner K, Maletius W. The long-term prognosis for severe damage to weight-bearing cartilage in the knee: a 14-year clinical and radiographic follow-up in 28 young athletes. Acta Orthop Scand 1996; 67(2):165-168.

(142) Shelbourne KD, Jari S, Gray T. Outcome of untreated traumatic articular cartilage defects of the knee: a natural history study. J Bone Joint Surg Am 2003; 85-A Suppl 2:8-16.

(143) Ding C, Cicuttini F, Scott F, Cooley H, Boon C, Jones G. Natural history of knee cartilage defects and factors affecting change. Arch Intern Med 2006; 166(6):651-658.

(144) Davies-Tuck ML, Wluka AE, Wang Y, Teichtahl AJ, Jones G, Ding C et al. The natural history of cartilage defects in people with knee osteoarthritis. Osteoarthritis Cartilage 2008; 16(3):337-342.

(145) Buckwalter JA, Roughley PJ, Rosenberg LC. Age-related changes in cartilage proteoglycans: quantitative electron microscopic studies. Microsc Res Tech 1994; 28(5):398-408.

(146) Martin JA, Buckwalter JA. Roles of articular cartilage aging and chondrocyte senescence in the pathogenesis of osteoarthritis. Iowa Orthop J 2001; 21:1-7.

(147) Volpin G, Dowd GS, Stein H, Bentley G. Degenerative arthritis after intra-articular fractures of the knee. Long-term results. J Bone Joint Surg Br 1990; 72(4):634-638.

(148) Wei X, Gao J, Messner K. Maturation-dependent repair of untreated osteochondral defects in the rabbit knee joint. J Biomed Mater Res 1997; 34(1):63-72.

(149) Buckwalter JA. Articular cartilage injuries. Clin Orthop Relat Res 2002;(402):21-37.

(150) Jackson DW, Lalor PA, Aberman HM, Simon TM. Spontaneous repair of full-thickness defects of articular cartilage in a goat model. A preliminary study. J Bone Joint Surg Am 2001; 83-A(1):53-64.

(151) Convery FR, Akeson WH, Keown GH. The repair of large osteochondral defects. An experimental study in horses. Clin Orthop Relat Res 1972; 82:253-262.

(152) Hunziker EB. Articular cartilage repair: basic science and clinical progress. A review of the current status and prospects. Osteoarthritis Cartilage 2002; 10(6):432-463.

(153) Shapiro F, Koide S, Glimcher MJ. Cell origin and differentiation in the repair of full-thickness defects of articular cartilage. J Bone Joint Surg Am 1993; 75(4):532-553.

(154) Smith GD, Knutsen G, Richardson JB. A clinical review of cartilage repair techniques. J Bone Joint Surg Br 2005; 87(4):445-449.

(155) Martin JA, Buckwalter JA. Post-traumatic osteoarthritis: The role of stress induced chondrocyte damage. Biorheology 2006; 43(3-4):517-521.

(156) Guilak F, Fermor B, Keefe FJ, Kraus VB, Olson SA, Pisetsky DS et al. The role of biomechanics and inflammation in cartilage injury and repair. Clin Orthop Relat Res 2004;(423):17-26.

(157) Appleton CT, McErlain DD, Henry JL, Holdsworth DW, Beier F. Molecular and histological analysis of a new rat model of experimental knee osteoarthritis. Ann N Y Acad Sci 2007; 1117:165-174.

(158) Glasson SS, Blanchet TJ, Morris EA. The surgical destabilization of the medial meniscus (DMM) model of osteoarthritis in the 129/SvEv mouse. Osteoarthritis Cartilage 2007; 15(9):1061-1069.

(159) Lovasz G, Park SH, Ebramzadeh E, Benya PD, Llinas A, Bellyei A et al. Characteristics of degeneration in an unstable knee with a coronal surface step-off. J Bone Joint Surg Br 2001; 83(3):428-436.

(160) Lohmander LS, Englund PM, Dahl LL, Roos EM. The long-term consequence of anterior cruciate ligament and meniscus injuries: osteoarthritis. Am J Sports Med 2007; 35(10):1756-1769.

(161) Knutsen G, Engebretsen L, Ludvigsen TC, Drogset JO, Grontvedt T, Solheim E et al. Autologous chondrocyte implantation compared with microfracture in the knee. A randomized trial. J Bone Joint Surg Am 2004; 86-A(3):455-464.

(162) Steadman JR, Briggs KK, Rodrigo JJ, Kocher MS, Gill TJ, Rodkey WG. Outcomes of microfracture for traumatic chondral defects of the knee: average 11-year follow-up. Arthroscopy 2003; 19(5):477-484.

(163) Kreuz PC, Erggelet C, Steinwachs MR, Krause SJ, Lahm A, Niemeyer P et al. Is microfracture of chondral defects in the knee associated with different results in patients aged 40 years or younger? Arthroscopy 2006; 22(11):1180-1186.

(164) Knutsen G, Drogset JO, Engebretsen L, Grontvedt T, Isaksen V, Ludvigsen TC et al. A randomized trial comparing autologous chondrocyte implantation with microfracture. Findings at five years. J Bone Joint Surg Am 2007; 89(10):2105-2112.

(165) Hangody L, Kish G, Karpati Z, Szerb I, Udvarhelyi I. Arthroscopic autogenous osteochondral mosaicplasty for the treatment of femoral condylar articular defects. A preliminary report. Knee Surg Sports Traumatol Arthrosc 1997; 5(4):262-267.

(166) Hangody L, Vasarhelyi G, Hangody LR, Sukosd Z, Tibay G, Bartha L et al. Autologous osteochondral grafting--technique and long-term results. Injury 2008; 39 Suppl 1:S32-S39.

(167) Evans PJ, Miniaci A, Hurtig MB. Manual punch versus power harvesting of osteochondral grafts. Arthroscopy 2004; 20(3):306-310.

(168) Redman SN, Oldfield SF, Archer CW. Current strategies for articular cartilage repair. Eur Cell Mater 2005; 9:23-32.

(169) Alford JW, Cole BJ. Cartilage restoration, part 1: basic science, historical perspective, patient evaluation, and treatment options. Am J Sports Med 2005; 33(2):295-306.

(170) Ahmad CS, Guiney WB, Drinkwater CJ. Evaluation of donor site intrinsic healing response in autologous osteochondral grafting of the knee. Arthroscopy 2002; 18(1):95-98.

(171) Brittberg M, Lindahl A, Nilsson A, Ohlsson C, Isaksson O, Peterson L. Treatment of deep cartilage defects in the knee with autologous chondrocyte transplantation. N Engl J Med 1994; 331(14):889-895.

(172) Peterson L, Minas T, Brittberg M, Nilsson A, Sjogren-Jansson E, Lindahl A. Two- to 9-year outcome after autologous chondrocyte transplantation of the knee. Clin Orthop Relat Res 2000;(374):212-234.

(173) Brittberg M. Autologous chondrocyte implantation--technique and long-term follow-up. Injury 2008; 39 Suppl 1:S40-S49.

(174) Dell'accio F, Vanlauwe J, Bellemans J, Neys J, De BC, Luyten FP. Expanded phenotypically stable chondrocytes persist in the repair tissue and contribute to cartilage matrix formation and structural integration in a goat model of autologous chondrocyte implantation. J Orthop Res 2003; 21(1):123-131.

(175) Benya PD, Shaffer JD. Dedifferentiated chondrocytes reexpress the differentiated collagen phenotype when cultured in agarose gels. Cell 1982; 30(1):215-224.

(176) Dell'accio F, De BC, Luyten FP. Molecular markers predictive of the capacity of expanded human articular chondrocytes to form stable cartilage in vivo. Arthritis Rheum 2001; 44(7):1608-1619.

(177) Saris DB, Vanlauwe J, Victor J, Haspl M, Bohnsack M, Fortems Y et al. Characterized chondrocyte implantation results in better structural repair when treating symptomatic cartilage defects of the knee in a randomized controlled trial versus microfracture. Am J Sports Med 2008; 36(2):235-246.

(178) Saris DB, Vanlauwe J, Victor J, Almqvist KF, Verdonk R, Bellemans J et al. Treatment of symptomatic cartilage defects of the knee: characterized chondrocyte implantation results in better clinical outcome at 36 months in a randomized trial compared to microfracture. Am J Sports Med 2009; 37 Suppl 1:10S-19S.

(179) Bentley G, Biant LC, Carrington RW, Akmal M, Goldberg A, Williams AM et al. A prospective, randomised comparison of autologous chondrocyte implantation versus mosaicplasty for osteochondral defects in the knee. J Bone Joint Surg Br 2003; 85(2):223-230.

(180) Saris DB, Vanlauwe J, Victor J, Haspl M, Bohnsack M, Fortems Y et al. Characterized chondrocyte implantation results in better structural repair when treating symptomatic cartilage defects of the knee in a randomized controlled trial versus microfracture. Am J Sports Med 2008; 36(2):235-246.

(181) Caplan AI, Bruder SP. Mesenchymal stem cells: building blocks for molecular medicine in the 21st century. Trends Mol Med 2001; 7(6):259-264.

(182) De'Bari C., Dell'accio F, Luyten FP. Human periosteum-derived cells maintain phenotypic stability and chondrogenic potential throughout expansion regardless of donor age. Arthritis Rheum 2001; 44(1):85-95.

(183) De'Bari C., Dell'accio F, Tylzanowski P, Luyten FP. Multipotent mesenchymal stem cells from adult human synovial membrane. Arthritis Rheum 2001; 44(8):1928-1942.

(184) Dowthwaite GP, Bishop JC, Redman SN, Khan IM, Rooney P, Evans DJ et al. The surface of articular cartilage contains a progenitor cell population. J Cell Sci 2004; 117(Pt 6):889-897.

(185) Pittenger MF, Mackay AM, Beck SC, Jaiswal RK, Douglas R, Mosca JD et al. Multilineage potential of adult human mesenchymal stem cells. Science 1999; 284(5411):143-147.

(186) De'Bari C., Dell'accio F. Mesenchymal stem cells in rheumatology: a regenerative approach to joint repair. Clin Sci (Lond) 2007; 113(8):339-348.

(187) Chen FH, Tuan RS. Mesenchymal stem cells in arthritic diseases. Arthritis Res Ther 2008; 10(5):223.

(188) Wakitani S, Goto T, Pineda SJ, Young RG, Mansour JM, Caplan AI et al. Mesenchymal cell-based repair of large, full-thickness defects of articular cartilage. J Bone Joint Surg Am 1994; 76(4):579-592.

(189) Yan H, Yu C. Repair of full-thickness cartilage defects with cells of different origin in a rabbit model. Arthroscopy 2007; 23(2):178-187.

(190) Butnariu-Ephrat M, Robinson D, Mendes DG, Halperin N, Nevo Z. Resurfacing of goat articular cartilage by chondrocytes derived from bone marrow. Clin Orthop Relat Res 1996;(330):234-243.

(191) Qiu YS, Shahgaldi BF, Revell WJ, Heatley FW. Observations of subchondral plate advancement during osteochondral repair: a histomorphometric and

mechanical study in the rabbit femoral condyle. Osteoarthritis Cartilage 2003; 11(11):810-820.

(192) Wakitani S, Yamamoto T. Response of the donor and recipient cells in mesenchymal cell transplantation to cartilage defect. Microsc Res Tech 2002; 58(1):14-18.

(193) Muraglia A, Cancedda R, Quarto R. Clonal mesenchymal progenitors from human bone marrow differentiate in vitro according to a hierarchical model. J Cell Sci 2000; 113 (Pt 7):1161-1166.

(194) Csaki C, Schneider PR, Shakibaei M. Mesenchymal stem cells as a potential pool for cartilage tissue engineering. Ann Anat 2008; 190(5):395-412.

(195) De'Bari C., Dell'accio F, Luyten FP. Failure of in vitro-differentiated mesenchymal stem cells from the synovial membrane to form ectopic stable cartilage in vivo. Arthritis Rheum 2004; 50(1):142-150.

(196) Johnstone B, Hering TM, Caplan AI, Goldberg VM, Yoo JU. In vitro chondrogenesis of bone marrow-derived mesenchymal progenitor cells. Exp Cell Res 1998; 238(1):265-272.

(197) Zhang Z, McCaffery JM, Spencer RG, Francomano CA. Hyaline cartilage engineered by chondrocytes in pellet culture: histological, immunohistochemical and ultrastructural analysis in comparison with cartilage explants. J Anat 2004; 205(3):229-237.

(198) Wakitani S, Imoto K, Yamamoto T, Saito M, Murata N, Yoneda M. Human autologous culture expanded bone marrow mesenchymal cell transplantation for repair of cartilage defects in osteoarthritic knees. Osteoarthritis Cartilage 2002; 10(3):199-206.

(199) Wakitani S, Mitsuoka T, Nakamura N, Toritsuka Y, Nakamura Y, Horibe S. Autologous bone marrow stromal cell transplantation for repair of full-thickness articular cartilage defects in human patellae: two case reports. Cell Transplant 2004; 13(5):595-600.

(200) Wakitani S, Nawata M, Tensho K, Okabe T, Machida H, Ohgushi H. Repair of articular cartilage defects in the patello-femoral joint with autologous bone marrow mesenchymal cell transplantation: three case reports involving nine defects in five knees. J Tissue Eng Regen Med 2007; 1(1):74-79.

(201) Kuroda R, Ishida K, Matsumoto T, Akisue T, Fujioka H, Mizuno K et al. Treatment of a full-thickness articular cartilage defect in the femoral condyle of an athlete with autologous bone-marrow stromal cells. Osteoarthritis Cartilage 2007; 15(2):226-231.

(202) Silva GA, Ducheyne P, Reis RL. Materials in particulate form for tissue engineering. 1. Basic concepts. J Tissue Eng Regen Med 2007; 1(1):4-24.

(203) Frenkel SR, Di Cesare PE. Scaffolds for articular cartilage repair. Ann Biomed Eng 2004; 32(1):26-34.

(204) Ng KW, Wang CC, Mauck RL, Kelly TA, Chahine NO, Costa KD et al. A layered agarose approach to fabricate depth-dependent inhomogeneity in chondrocyte-seeded constructs. J Orthop Res 2005; 23(1):134-141.

(205) Schek RM, Taboas JM, Segvich SJ, Hollister SJ, Krebsbach PH. Engineered osteochondral grafts using biphasic composite solid free-form fabricated scaffolds. Tissue Eng 2004; 10(9-10):1376-1385.

(206) Raghunath J, Salacinski HJ, Sales KM, Butler PE, Seifalian AM. Advancing cartilage tissue engineering: the application of stem cell technology. Curr Opin Biotechnol 2005; 16(5):503-509.

(207) Silva GA, Czeisler C, Niece KL, Beniash E, Harrington DA, Kessler JA et al. Selective differentiation of neural progenitor cells by high-epitope density nanofibers. Science 2004; 303(5662):1352-1355.

(208) Lutolf MP, Weber FE, Schmoekel HG, Schense JC, Kohler T, Muller R et al. Repair of bone defects using synthetic mimetics of collagenous extracellular matrices. Nat Biotechnol 2003; 21(5):513-518.

(209) Gaissmaier C, Koh JL, Weise K. Growth and differentiation factors for cartilage healing and repair. Injury 2008; 39 Suppl 1:S88-S96.

(210) Hunziker EB, Driesang IM, Morris EA. Chondrogenesis in cartilage repair is induced by members of the transforming growth factor-beta superfamily. Clin Orthop Relat Res 2001;(391 Suppl):S171-S181.

(211) Gelse K, von der MK, Aigner T, Park J, Schneider H. Articular cartilage repair by gene therapy using growth factor-producing mesenchymal cells. Arthritis Rheum 2003; 48(2):430-441.

(212) Kuroda R, Usas A, Kubo S, Corsi K, Peng H, Rose T et al. Cartilage repair using bone morphogenetic protein 4 and muscle-derived stem cells. Arthritis Rheum 2006; 54(2):433-442.

(213) Mason JM, Breitbart AS, Barcia M, Porti D, Pergolizzi RG, Grande DA. Cartilage and bone regeneration using gene-enhanced tissue engineering. Clin Orthop Relat Res 2000;(379 Suppl):S171-S178.

(214) Hunziker EB, Driesang IM, Morris EA. Chondrogenesis in cartilage repair is induced by members of the transforming growth factor-beta superfamily. Clin Orthop Relat Res 2001;(391 Suppl):S171-S181.

(215) Gelse K, von der MK, Aigner T, Park J, Schneider H. Articular cartilage repair by gene therapy using growth factor-producing mesenchymal cells. Arthritis Rheum 2003; 48(2):430-441.

(216) Vincent T, Hermansson M, Bolton M, Wait R, Saklatvala J. Basic FGF mediates an immediate response of articular cartilage to mechanical injury. Proc Natl Acad Sci U S A 2002; 99(12):8259-8264.

(217) Kurz B, Lemke AK, Fay J, Pufe T, Grodzinsky AJ, Schunke M. Pathomechanisms of cartilage destruction by mechanical injury. Ann Anat 2005; 187(5-6):473-485.

(218) Chen CT, Burton-Wurster N, Borden C, Hueffer K, Bloom SE, Lust G. Chondrocyte necrosis and apoptosis in impact damaged articular cartilage. J Orthop Res 2001; 19(4):703-711.

(219) Redman SN, Khan IM, Tew SR, Archer CW. In situ detection of cell death in articular cartilage. Methods Mol Med 2007; 135:183-199.

(220) Tew SR, Kwan AP, Hann A, Thomson BM, Archer CW. The reactions of articular cartilage to experimental wounding: role of apoptosis. Arthritis Rheum 2000; 43(1):215-225.

(221) D'Lima DD, Hashimoto S, Chen PC, Lotz MK, Colwell CW, Jr. Cartilage injury induces chondrocyte apoptosis. J Bone Joint Surg Am 2001; 83-A Suppl 2(Pt 1):19-21.

(222) Furman BD, Olson SA, Guilak F. The development of posttraumatic arthritis after articular fracture. J Orthop Trauma 2006; 20(10):719-725.

(223) Redman SN, Dowthwaite GP, Thomson BM, Archer CW. The cellular responses of articular cartilage to sharp and blunt trauma. Osteoarthritis Cartilage 2004; 12(2):106-116.

(224) Mobasheri A, Carter SD, Martin-Vasallo P, Shakibaei M. Integrins and stretch activated ion channels; putative components of functional cell surface mechanoreceptors in articular chondrocytes. Cell Biol Int 2002; 26(1):1-18.

(225) Henson FM, Bowe EA, Davies ME. Promotion of the intrinsic damage-repair response in articular cartilage by fibroblastic growth factor-2. Osteoarthritis Cartilage 2005; 13(6):537-544.

(226) Dimicco MA, Patwari P, Siparsky PN, Kumar S, Pratta MA, Lark MW et al. Mechanisms and kinetics of glycosaminoglycan release following in vitro cartilage injury. Arthritis Rheum 2004; 50(3):840-848.

(227) Lee JH, Fitzgerald JB, Dimicco MA, Grodzinsky AJ. Mechanical injury of cartilage explants causes specific time-dependent changes in chondrocyte gene expression. Arthritis Rheum 2005; 52(8):2386-2395.

(228) Kim YJ, Sah RL, Grodzinsky AJ, Plaas AH, Sandy JD. Mechanical regulation of cartilage biosynthetic behavior: physical stimuli. Arch Biochem Biophys 1994; 311(1):1-12.

(229) Steinmeyer J, Knue S. The proteoglycan metabolism of mature bovine articular cartilage explants superimposed to continuously applied cyclic mechanical loading. Biochem Biophys Res Commun 1997; 240(1):216-221.

(230) Gruber J, Vincent TL, Hermansson M, Bolton M, Wait R, Saklatvala J. Induction of interleukin-1 in articular cartilage by explantation and cutting. Arthritis Rheum 2004; 50(8):2539-2546.

(231) Vincent TL, Hermansson MA, Hansen UN, Amis AA, Saklatvala J. Basic fibroblast growth factor mediates transduction of mechanical signals when articular cartilage is loaded. Arthritis Rheum 2004; 50(2):526-533.

(232) Chuma H, Mizuta H, Kudo S, Takagi K, Hiraki Y. One day exposure to FGF-2 was sufficient for the regenerative repair of full-thickness defects of articular cartilage in rabbits. Osteoarthritis Cartilage 2004; 12(10):834-842.

(233) Sawaji Y, Hynes J, Vincent T, Saklatvala J. Fibroblast growth factor 2 inhibits induction of aggrecanase activity in human articular cartilage. Arthritis Rheum 2008; 58(11):3498-3509.

(234) Reinholz GG, Lu L, Saris DB, Yaszemski MJ, O'Driscoll SW. Animal models for cartilage reconstruction. Biomaterials 2004; 25(9):1511-1521.

(235) Anraku Y, Mizuta H, Sei A, Kudo S, Nakamura E, Senba K et al. The chondrogenic repair response of undifferentiated mesenchymal cells in rat full-thickness articular cartilage defects. Osteoarthritis Cartilage 2008; 16(8):961-964.

(236) Breinan HA, Hsu HP, Spector M. Chondral defects in animal models: effects of selected repair procedures in canines. Clin Orthop Relat Res 2001;(391 Suppl):S219-S230.

(237) Anraku Y, Mizuta H, Sei A, Kudo S, Nakamura E, Senba K et al. Analyses of early events during chondrogenic repair in rat full-thickness articular cartilage defects. J Bone Miner Metab 2009; 27(3):272-286.

(238) Mankin HJ, Dorfman H, Lippiello L, Zarins A. Biochemical and metabolic abnormalities in articular cartilage from osteo-arthritic human hips. II. Correlation of morphology with biochemical and metabolic data. J Bone Joint Surg Am 1971; 53(3):523-537.

(239) van der Sluijs JA, Geesink RG, van der Linden AJ, Bulstra SK, Kuyer R, Drukker J. The reliability of the Mankin score for osteoarthritis. J Orthop Res 1992; 10(1):58-61.

(240) Chambers MG, Cox L, Chong L, Suri N, Cover P, Bayliss MT et al. Matrix metalloproteinases and aggrecanases cleave aggrecan in different zones of normal cartilage but colocalize in the development of osteoarthritic lesions in STR/ort mice. Arthritis Rheum 2001; 44(6):1455-1465.

(241) Dell'accio F, De BC, Eltawil NM, Vanhummelen P, Pitzalis C. Identification of the molecular response of articular cartilage to injury, by microarray screening: Wnt-16 expression and signaling after injury and in osteoarthritis. Arthritis Rheum 2008; 58(5):1410-1421.

(242) Nelson WJ, Nusse R. Convergence of Wnt, beta-catenin, and cadherin pathways. Science 2004; 303(5663):1483-1487.

(243) Sellers RS, Zhang R, Glasson SS, Kim HD, Peluso D, D'Augusta DA et al. Repair of articular cartilage defects one year after treatment with recombinant human bone morphogenetic protein-2 (rhBMP-2). J Bone Joint Surg Am 2000; 82(2):151-160.

(244) Polesskaya A, Seale P, Rudnicki MA. Wnt signaling induces the myogenic specification of resident CD45+ adult stem cells during muscle regeneration. Cell 2003; 113(7):841-852.

(245) Surendran K, Simon TC. CNP gene expression is activated by Wnt signaling and correlates with Wnt4 expression during renal injury. Am J Physiol Renal Physiol 2003; 284(4):F653-F662.

(246) Monga SP, Pediaditakis P, Mule K, Stolz DB, Michalopoulos GK. Changes in WNT/beta-catenin pathway during regulated growth in rat liver regeneration. Hepatology 2001; 33(5):1098-1109.

(247) Kleber M, Sommer L. Wnt signaling and the regulation of stem cell function. Curr Opin Cell Biol 2004; 16(6):681-687.

(248) Luyten FP, Tylzanowski P, Lories RJ. Wnt signaling and osteoarthritis. Bone 2009; 44(4):522-527.

(249) Imai K, Morikawa M, D'Armiento J, Matsumoto H, Komiya K, Okada Y. Differential expression of WNTs and FRPs in the synovium of rheumatoid arthritis and osteoarthritis. Biochem Biophys Res Commun 2006; 345(4):1615-1620.

(250) Tylzanowski P, Mebis L, Luyten FP. The Noggin null mouse phenotype is strain dependent and haploinsufficiency leads to skeletal defects. Dev Dyn 2006; 235(6):1599-1607.

(251) Wang Y, Ding C, Wluka AE, Davis S, Ebeling PR, Jones G et al. Factors affecting progression of knee cartilage defects in normal subjects over 2 years. Rheumatology (Oxford) 2006; 45(1):79-84.

(252) Peister A, Mellad JA, Larson BL, Hall BM, Gibson LF, Prockop DJ. Adult stem cells from bone marrow (MSCs) isolated from different strains of inbred mice vary in surface epitopes, rates of proliferation, and differentiation potential. Blood 2004; 103(5):1662-1668.

(253) Fukui N, Purple CR, Sandell LJ. Cell biology of osteoarthritis: the chondrocyte's response to injury. Curr Rheumatol Rep 2001; 3(6):496-505.

(254) Mistry D, Oue Y, Chambers MG, Kayser MV, Mason RM. Chondrocyte death during murine osteoarthritis. Osteoarthritis Cartilage 2004; 12(2):131-141.

(255) Kim HA, Blanco FJ. Cell death and apoptosis in osteoarthritic cartilage. Curr Drug Targets 2007; 8(2):333-345.

(256) Nowak SJ, Corces VG. Phosphorylation of histone H3: a balancing act between chromosome condensation and transcriptional activation. Trends Genet 2004; 20(4):214-220.

(257) Wong BJ, Pandhoh N, Truong MT, Diaz S, Chao K, Hou S et al. Identification of chondrocyte proliferation following laser irradiation, thermal injury, and mechanical trauma. Lasers Surg Med 2005; 37(1):89-96.

(258) Krenn V, Morawietz L, Burmester GR, Kinne RW, Mueller-Ladner U, Muller B et al. Synovitis score: discrimination between chronic low-grade and high-grade synovitis. Histopathology 2006; 49(4):358-364.

(259) Hunziker EB, Rosenberg LC. Repair of partial-thickness defects in articular cartilage: cell recruitment from the synovial membrane. J Bone Joint Surg Am 1996; 78(5):721-733.

(260) Ballantyne GH. The experimental basis of intestinal suturing. Effect of surgical technique, inflammation, and infection on enteric wound healing. Dis Colon Rectum 1984; 27(1):61-71.

(261) Wang XJ, Han G, Owens P, Siddiqui Y, Li AG. Role of TGF beta-mediated inflammation in cutaneous wound healing. J Investig Dermatol Symp Proc 2006; 11(1):112-117.

(262) Lee ER, Smith CE, Poole R. Ultrastructural localization of the C-propeptide released from type II procollagen in fetal bovine growth plate cartilage. J Histochem Cytochem 1996; 44(5):433-443.

(263) Hembree WC, Ward BD, Furman BD, Zura RD, Nichols LA, Guilak F et al. Viability and apoptosis of human chondrocytes in osteochondral fragments following joint trauma. J Bone Joint Surg Br 2007; 89(10):1388-1395.

(264) Palumbo R, Galvez BG, Pusterla T, De MF, Cossu G, Marcu KB et al. Cells migrating to sites of tissue damage in response to the danger signal HMGB1 require NF-kappaB activation. J Cell Biol 2007; 179(1):33-40.

(265) Loeser RF. Molecular mechanisms of cartilage destruction: mechanics, inflammatory mediators, and aging collide. Arthritis Rheum 2006; 54(5):1357-1360.

(266) Aurich M, Mwale F, Reiner A, Mollenhauer JA, Anders JO, Fuhrmann RA et al. Collagen and proteoglycan turnover in focally damaged human ankle cartilage: evidence for a generalized response and active matrix remodeling across the entire joint surface. Arthritis Rheum 2006; 54(1):244-252.

(267) Nelson F, Dahlberg L, Laverty S, Reiner A, Pidoux I, Ionescu M et al. Evidence for altered synthesis of type II collagen in patients with osteoarthritis. J Clin Invest 1998; 102(12):2115-2125.

(268) Embry Flory JJ, Fosang AJ, Knudson W. The accumulation of intracellular ITEGE and DIPEN neoepitopes in bovine articular chondrocytes is mediated by CD44 internalization of hyaluronan. Arthritis Rheum 2006; 54(2):443-454.

(269) Ruppert R, Hoffmann E, Sebald W. Human bone morphogenetic protein 2 contains a heparin-binding site which modifies its biological activity. Eur J Biochem 1996; 237(1):295-302.

(270) Emans PJ, Spaapen F, Surtel DA, Reilly KM, Cremers A, van Rhijn LW et al. A novel in vivo model to study endochondral bone formation; HIF-1alpha activation and BMP expression. Bone 2006.

(271) Jho EH, Zhang T, Domon C, Joo CK, Freund JN, Costantini F. Wnt/beta-catenin/Tcf signaling induces the transcription of Axin2, a negative regulator of the signaling pathway. Mol Cell Biol 2002; 22(4):1172-1183.

(272) Glass DA, Bialek P, Ahn JD, Starbuck M, Patel MS, Clevers H et al. Canonical Wnt signaling in differentiated osteoblasts controls osteoclast differentiation. Dev Cell 2005; 8(5):751-764.

(273) Dell'accio F, De BC, El Tawil NM, Barone F, Mitsiadis TA, O'Dowd J et al. Activation of WNT and BMP signaling in adult human articular cartilage following mechanical injury. Arthritis Res Ther 2006; 8(5):R139.

(274) Ryu JH, Kim SJ, Kim SH, Oh CD, Hwang SG, Chun CH et al. Regulation of the chondrocyte phenotype by beta-catenin. Development 2002; 129(23):5541-5550.

(275) Maretto S, Cordenonsi M, Dupont S, Braghetta P, Broccoli V, Hassan AB et al. Mapping Wnt/beta-catenin signaling during mouse development and in colorectal tumors. Proc Natl Acad Sci U S A 2003; 100(6):3299-3304.

(276) Cheon SS, Wei Q, Gurung A, Youn A, Bright T, Poon R et al. Beta-catenin regulates wound size and mediates the effect of TGF-beta in cutaneous healing. FASEB J 2006; 20(6):692-701.

(277) Otto A, Schmidt C, Luke G, Allen S, Valasek P, Muntoni F et al. Canonical Wnt signalling induces satellite-cell proliferation during adult skeletal muscle regeneration. J Cell Sci 2008; 121(Pt 17):2939-2950.

(278) Goldring SR, Goldring MB. Eating bone or adding it: the Wnt pathway decides. Nat Med 2007; 13(2):133-134.

(279) Yu HM, Jerchow B, Sheu TJ, Liu B, Costantini F, Puzas JE et al. The role of Axin2 in calvarial morphogenesis and craniosynostosis. Development 2005; 132(8):1995-2005.

(280) Day TF, Guo X, Garrett-Beal L, Yang Y. Wnt/beta-catenin signaling in mesenchymal progenitors controls osteoblast and chondrocyte differentiation during vertebrate skeletogenesis. Dev Cell 2005; 8(5):739-750.

(281) Zhou S, Eid K, Glowacki J. Cooperation between TGF-beta and Wnt pathways during chondrocyte and adipocyte differentiation of human marrow stromal cells. J Bone Miner Res 2004; 19(3):463-470.

(282) Yano F, Kugimiya F, Ohba S, Ikeda T, Chikuda H, Ogasawara T et al. The canonical Wnt signaling pathway promotes chondrocyte differentiation in a Sox9-dependent manner. Biochem Biophys Res Commun 2005; 333(4):1300-1308.

(283) Dessimoz J, Bonnard C, Huelsken J, Grapin-Botton A. Pancreas-specific deletion of beta-catenin reveals Wnt-dependent and Wnt-independent functions during development. Curr Biol 2005; 15(18):1677-1683.

(284) Fathke C, Wilson L, Shah K, Kim B, Hocking A, Moon R et al. Wnt signaling induces epithelial differentiation during cutaneous wound healing. BMC Cell Biol 2006; 7:4.

(285) Filali M, Cheng N, Abbott D, Leontiev V, Engelhardt JF. Wnt-3A/beta-catenin signaling induces transcription from the LEF-1 promoter. J Biol Chem 2002; 277(36):33398-33410.

(286) Labbe E, Letamendia A, Attisano L. Association of Smads with lymphoid enhancer binding factor 1/T cell-specific factor mediates cooperative signaling by the transforming growth factor-beta and wnt pathways. Proc Natl Acad Sci U S A 2000; 97(15):8358-8363.

(287) Brantjes H, Roose J, van De WM, Clevers H. All Tcf HMG box transcription factors interact with Groucho-related co-repressors. Nucleic Acids Res 2001; 29(7):1410-1419.

(288) Barolo S. Transgenic Wnt/TCF pathway reporters: all you need is Lef? Oncogene 2006; 25(57):7505-7511.

(289) Zeng X, Huang H, Tamai K, Zhang X, Harada Y, Yokota C et al. Initiation of Wnt signaling: control of Wnt coreceptor Lrp6 phosphorylation/activation via frizzled, dishevelled and axin functions. Development 2008; 135(2):367-375.

(290) Srikanth VK, Fryer JL, Zhai G, Winzenberg TM, Hosmer D, Jones G. A meta-analysis of sex differences prevalence, incidence and severity of osteoarthritis. Osteoarthritis Cartilage 2005; 13(9):769-781.

(291) Ma HL, Blanchet TJ, Peluso D, Hopkins B, Morris EA, Glasson SS. Osteoarthritis severity is sex dependent in a surgical mouse model. Osteoarthritis Cartilage 2007; 15(6):695-700.

(292) Spater D, Hill TP, O'sullivan RJ, Gruber M, Conner DA, Hartmann C. Wnt9a signaling is required for joint integrity and regulation of Ihh during chondrogenesis. Development 2006.

(293) Beris AE, Lykissas MG, Papageorgiou CD, Georgoulis AD. Advances in articular cartilage repair. Injury 2005; 36 Suppl 4:S14-S23.

(294) Dave M, Attur M, Palmer G, Al-Mussawir HE, Kennish L, Patel J et al. The antioxidant resveratrol protects against chondrocyte apoptosis via effects on mitochondrial polarization and ATP production. Arthritis Rheum 2008; 58(9):2786-2797.

(295) Huser CA, Peacock M, Davies ME. Inhibition of caspase-9 reduces chondrocyte apoptosis and proteoglycan loss following mechanical trauma. Osteoarthritis Cartilage 2006; 14(10):1002-1010.

(296) Murphy G, Nagase H. Reappraising metalloproteinases in rheumatoid arthritis and osteoarthritis: destruction or repair? Nat Clin Pract Rheumatol 2008.

(297) Wilhelmi G, Faust R. Suitability of the C57 black mouse as an experimental animal for the study of skeletal changes due to ageing, with special reference to osteo-arthrosis and its response to tribenoside. Pharmacology 1976; 14(4):289-296.

(298) Wooley PH, Luthra HS, Stuart JM, David CS. Type II collagen-induced arthritis in mice. I. Major histocompatibility complex (I region) linkage and antibody correlates. J Exp Med 1981; 154(3):688-700.

(299) Chia SL, Sawaji Y, Burleigh A, McLean C, Inglis J, Saklatvala J et al. Fibroblast growth factor 2 is an intrinsic chondroprotective agent that suppresses ADAMTS-5 and delays cartilage degradation in murine osteoarthritis. Arthritis Rheum 2009; 60(7):2019-2027.

(300) Lories RJ, Luyten FP. Bone morphogenetic protein signaling and arthritis. Cytokine Growth Factor Rev 2009; 20(5-6):467-473.

(301) Steinert AF, Noth U, Tuan RS. Concepts in gene therapy for cartilage repair. Injury 2008; 39 Suppl 1:S97-113.

(302) Zhang DL, Gu LJ, Liu L, Wang CY, Sun BS, Li Z et al. Effect of Wnt signaling pathway on wound healing. Biochem Biophys Res Commun 2009; 378(2):149-151.

(303) Kawakami Y, Rodriguez EC, Raya M, Kawakami H, Marti M, Dubova I et al. Wnt/beta-catenin signaling regulates vertebrate limb regeneration. Genes Dev 2006; 20(23):3232-3237.

(304) Chien AJ, Moon RT. WNTS and WNT receptors as therapeutic tools and targets in human disease processes. Front Biosci 2007; 12:448-457.

(305) Beachy PA, Karhadkar SS, Berman DM. Tissue repair and stem cell renewal in carcinogenesis. Nature 2004; 432(7015):324-331.

(306) Zhao J, Kim KA, Abo A. Tipping the balance: modulating the Wnt pathway for tissue repair. Trends Biotechnol 2009; 27(3):131-136.